Journal
of
The Franklin Institute
Devoted to Science and the Mechanic Arts

Vol. 252 OCTOBER, 1951 No. 4

RECURRENT MIRAGES AT PUERTO PEÑASCO, SONORA

BY

RONALD L. IVES [1]

ABSTRACT

Mirage behavior at Puerto Peñasco, on the Sonoran shore of the Gulf of California, is not only systematic, but is fully compatible with conditions of atmospheric refraction common in that arid area adjacent to a tropical sea. Images of mountains in Baja California, normally hidden below the visual horizon, are regularly loomed into visibility as the lapse rate in the lower layers of the atmosphere increases; and sink again below the horizon with the onset of nocturnal inversions. False sea horizons, due to refraction, are a standard midday condition; as are inferior mirages over adjacent land areas.

Air stratification is normally accompanied by "paper doll" duplications of distant images; *Fata Morgana* is a common occurrence when cold air drainages from high mountains reach the warm waters of the Gulf of California. Photographic differentiation between mirage lakes and actual bodies of water is sometimes possible by use of deep red filters.

INTRODUCTION

Mirages have been reported from the arid lands bordering on the Gulf of California since before the dawn of written history in that area. In Opata mythology, the abode of *Vatecom Hoatziqui*, the legendary "eater of souls," to whom the spirits of the departed were ferried by the dwarf *Batzu Uri*, was apparently on the far side of the persistent mirage lake over western Sonora and the adjacent waters of the Gulf of California (1)[2]. The more recent legend of "La Reina," the phantom ship of the Gulf of California, also has mirage implications. During the last three decades, with rapid spread of education and the resultant decline in superstition, mirage reports from northern Mexico have come into close agreement with what can be seen there, and in some instances photographed.

The area under consideration (Fig. 1) comprises northwestern Sonora, northeastern Baja California, and the intervening waters of the

[1] Cornell Aeronautical Laboratory, Inc., Buffalo, N. Y.

[2] The boldface numbers in parentheses refer to the references appended to this paper.

(Note—The Franklin Institute is not responsible for the statements and opinions advanced by contributors in the JOURNAL.)

Gulf of California. This area is a southern extension of the basin and range physiographic province (3), and is characterized by block-faulted mountain ranges, broad desert basins, and numerous recent lava flows (5, 9, 10, 11, 12, 14).

Climate is arid, with rainfall deficient at all seasons. Frost is virtually unknown, winters are warm, and summers hot. Coastal winds

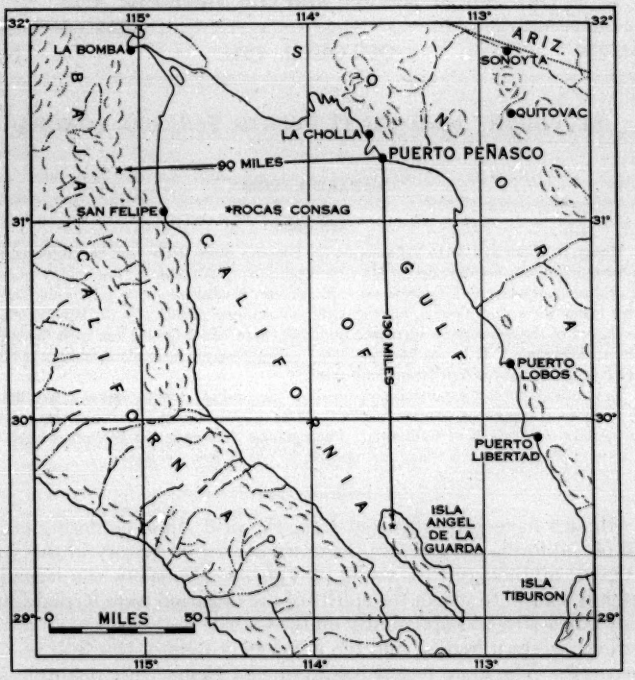

FIG. 1. Summary map of the lands bordering on the northern part of the Gulf of California.

are part of a well-developed land-and-sea breeze circulation. Inland winds, at the surface, are part of the "Sonoran Low" circulation during most of the year. Air drainages are a standard nocturnal occurrence near the desert mountains. Clear skies are the rule at all seasons. Relative humidity is low, and sensible temperatures, in consequence, are very much lower than recorded temperatures (2, 8).

MIRAGES OVER LAND

Most common mirage over Sonoran land areas is the familiar inferior, or "water" mirage (4 (pp. 473–474), 13, 7 (pp. 465–468), 8 (pp. 175–176)), which is observed over the major valley floors near Puerto Peñasco during parts of more than 300 days a year. These mirage lakes normally form in midmorning, and last until late afternoon.

During the very early morning ("false dawn"), when temperature inversions and stratified air are a standard condition, grotesque towers and minarets, similar to the "Guthman's Towers" mirage of the Salt Lake Desert (7, p. 470), are occasionally seen.

Direct observation discloses that Sonoran mirages over land differ in no pertinent feature from those of other deserts in North America, and closely resemble those described and photographed in North Africa, Asia Minor, and Australia. Like "standard" mirages of other areas, Sonoran mirages can be photographed with ordinary cameras and films, demonstrating their physical reality.

FALSE SEA HORIZONS

On hot clear days, which are frequent near the Gulf of California, the sea horizon acquires a peculiar appearance in midmorning, the visible horizon being 10′ to 15′ of arc higher than its sunrise position. This condition persists until very late afternoon, at which time the "upper horizon" dissolves, not always regularly. Onset of this false sea horizon is contemporaneous with the development of a thin warm surface stratum of water. Neither the warm surface stratum nor the false sea horizon develops when the wind speed is much more than 5 mph.

When distant shores are viewed under these weather conditions, inferior mirages commonly develop over flat land areas 15 minutes to two hours before formation of the false sea horizon. On very hot summer afternoons, the inferior mirages over land may merge with the false horizons over water.

Although deceptive to the unaided eye, so that its presence complicates accurate marine navigation, the false sea horizon can be distinguished from the true horizon by use of a deep red viewing filter, such as a Wratten "A" or "F."

When winds of small areal extent blow over the sea surface, they remove the false sea horizon locally and temporarily, in much the same manner that dust devils "eat holes" in inferior mirages on land (6).

In a great majority of observed instances, objects at sea considerably nearer the observer than the apparent horizon have an entirely normal appearance during the middle hours of the day, whether or not a false horizon is present. As these objects recede from the observer, they will cross the horizon and disappear below it in a normal manner if no false horizon is present; but will sail off into the sky, undergo great vertical distortion, or partake of more complicated visual transfigurations when a false sea horizon is present.

MIRAGES AT SEA

The shallow northern part of the Gulf of California, roughly from Latitude 27° north to the mouth of the Colorado River, is noted for its mirages, which, in one form or another, are of almost daily occurrence at all seasons. Most common mirage forms are shown in Fig. 2, a series of sketches of much greater clarity and contrast than any mirages seen by the writer.

A small vessel, travelling away from an observer on the Gulf of California, on almost any clear day, at any season, will usually have an

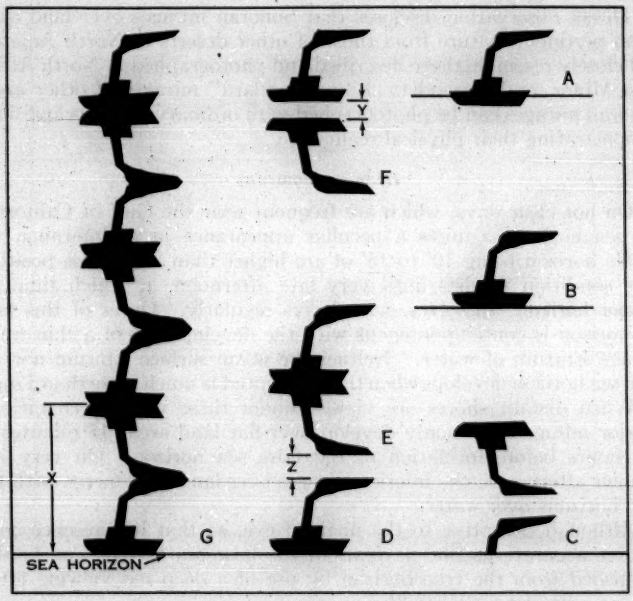

FIG. 2. Mirage types noted on the Gulf of California west of Puerto Peñasco, Sonora, Mexico.

entirely normal appearance, as in A, Fig. 2, while it is quite close to the observer. As it approaches the visible horizon, the vessel will still have a substantially normal appearance, as in B. Fig. 2, although its image may weave and jump considerably as a result of atmospheric turbulence. If mirage conditions do not exist, as is sometimes the case when the sun is from one to three hours high in the morning, when the sky is overcast, or in windy weather, the vessel will gradually fall below the horizon as it recedes, appearing as in the lower part of C, Fig. 2.

If, however, mirage conditions exist, as is usually evidenced by a false horizon at sea, and by inferior mirages over adjacent lands, the appearance of the vessel will not remain normal after it reaches the apparent horizon. Sometimes it will acquire an inverted twin, as in Fig. 2, C (entire sketch). At other times, under similar conditions, it will apparently stay on the horizon, but will be accompanied by "fish-tail" twin images aloft, as in D and E, Fig. 2. These twinned images may be separated from the lower image of the vessel by a clear space (Z in Fig. 2); and the twins may be either adjacent, as in E, or separate, as in F. Dimensions Z and Y usually vary considerably in a short time. Rarely, only the elevated twin images are visible, the lower image being absent. Separated elevated twin images (F in Fig. 2) occasionally have a "water" image between the hulls, filling space Y.

Various and sundry permutations and combinations of the above occur quite frequently. Rapid variations in appearance and vertical spacing of the various images are the rule, rather than the exception. Intensity of the inverted images usually is not the same as that of the upright images; and changes in apparent size, which are continual, are usually not proportional.

Under extreme conditions of air stratification, which are most common between false dawn and about one hour after sunrise, when surface air is much colder than the water, "paper doll" duplications of ship images, as in G, Fig. 2, are occasionally seen. Distance X (Fig. 2, G) appears to be about 10° of arc, but measurement shows that it is commonly less than 30′. Computations, from known distance and object size, indicate that the angular dimension should be about 03′ of arc. These discrepancies indicate that the mirage not only has illusory magnification, which deceives the observer, but also true magnification, so that the arc subtended by the image is very much larger than indicated by trigonometric computations. Under these conditions, also, distance determinations by use of a short-base range finder are not in accord with those made by long-base triangulations, usually being much shorter; and the range-finder determinations "never come out the same twice in a row."

Never reported from Puerto Peñasco, but common in the narrow channels between islands farther south, is the *Fata Morgana*, a weird mélange of diffuse and ever-changing images, perhaps magnified and distorted views of objects on the shore. These annoyances to mariners are most frequent in the Boca del Infiernillo, separating Tiburon Island from the Sonoran mainland; and in the Canal de Ballenas, between Isla Angel de la Guarda and Baja California. They are most commonly seen in the early morning, when the air is very cold relative to the water, and are usually accompanied by steam fogs. These phenomena are usually of small areal extent and short duration, and are not as spectacular as those reported from the Straits of Messina, type area

for this mirage. Similar mirages have been reported to the writer by pearl-divers working out of Loreto, Baja California, but those personally observed between Loreto and Isla Carmen have been of the less spectacular types.

Where study of air conditions has been possible during *Fata Morgana* displays, a thin layer of relatively cold air, in turbulent motion, has been present over the surface of relatively warm water. Above the thin cold air stratum, which usually results from local air drainage, is a layer of much warmer air. Other stratifications aloft are sometimes present.

Observed colors in the main body of the mirage are always degradations of those present in the local environment. Occasionally spectral hues are present, as "rainbow glints," adjacent to steam fogs associated with the *Fata Morgana*.

FIG. 3. Looming of distant mountains.

No "fairy castles" or similar phenomena have been seen, perhaps because adobe or sheet-iron shacks, or Seri reed and driftwood *Jacales*, are still unattractive and unimpressive edifices even when viewed through a multiplicity of natural distorting lenses.

LOOMING OF DISTANT MOUNTAINS

Sometimes classed as a mirage, commonly coexistent with it, and always occurring under similar conditions of atmospheric refraction, is the looming of distant mountains, which are hidden "around the curve of the earth" when mirage conditions do not prevail and which loom into view as the lower part of the atmosphere develops a strong refractional gradient.

The mountains of Baja California, and of Isla Angel de la Guarda (Fig. 1), respectively 90 and 130 miles distant from Puerto Peñasco, are not visible from that point according to ordinary curvature formulae. Likewise, they cannot be seen during the early part of the day, being,

both theoretically and actually, below the horizon, or "around the curve of the earth."

As the day progresses, both mountain groups become visible, in a rather systematic and predictable manner, reaching their greatest apparent height near sunset. This phenomenon is illustrated in the sketches of Fig. 3.

The eastern outlier of the Sierra San Pedro Martir, sometimes called the Sierra San Felipe, with a maximum height of about 4,000 feet, is about 90 miles distant from Puerto Peñasco, and hence, under average conditions of refraction, is invisible from the port. On any ordinary clear day, when air temperatures are substantially normal for the season, and wind speed is below about 15 miles per hour, dim shapes, that might be distant mountains shrouded in desert haze, appear on the western horizon at about noon (Fig. 3, 1). These retain the indefinite outline until about an hour before sunset, at which time they grow rapidly and the images sharpen, until there is no doubt that they are mountains. A few minutes before sunset, the images tower and sharpen still more, and change color from an indefinite dark gray to the dull reds, browns, and greens of typical desert mountains. Outlines at this time are so sharp that they can be clearly identified as the Sierra San Felipe, and other members of the San Pedro Martir massif, at greater distances, are dimly visible (Fig. 3, 2). This image lasts for about half an hour, until very shortly after sunset, at which time it darkens, and rapidly falls below the horizon.

After an abnormally hot still day, the image towers to a much greater height, and the sea appears to have a concave surface from the observer to the base of the range, with "embayments" of mirage extending up valleys in the distant mountains. In extreme developments, a "fishtail" twin image forms below the loomed image of the mountains (Fig. 3, 3). At other times, the entire range, with its eastern pediments, "floats free" above the sea horizon.

Although these loomed images tower until they apparently "fill half the sky," their actual angular height, as measured, is quite small. When the entire Sierra San Felipe is visible, from base up, the angular elevation of the summit, measured at Puerto Peñasco, is about 40′ of arc. At this time, which is maximum normal development, the curvature of the line of sight approximates the curvature of the earth.

Greatest angular elevation of the summit of the range is noted when its base either "floats free," or is supported by a "fishtail" twin, as in Fig. 3, 3. Largest angle measured was about 3° of arc, although residents of Puerto Peñasco state emphatically that it is sometimes much greater. Such an elevation, without the interposition of abnormally refractive air, would require that the Sierra San Felipe have the dimensions of the Everest massif!

Even at extreme developments of loomed images of the Sierra San

Pedro Martir and its outliers, no mirage effects attributable to the nearer Consag Rocks ("Rocas Consag," Fig. 1) were noted, perhaps because of the small dimensions of these semi-submerged crags.

Occasionally, in the early evening, a cluster of lights is seen on the far side of the Gulf, or floating in the sky. These have the azimuth of the small seaport of San Felipe, but are too indefinite in arrangement, even when viewed through a telescope, for certain identification.

Loomed images of the mountains of Isla Angel de la Guarda (Fig. 1) are not usually visible from sea level near Puerto Peñasco, but can be seen regularly from the summit of Rocky Point (Elev. 250′ MSL). These, light yellow in color, like the barren peaks of the island, are visible under conditions similar to those already described, and are sketched in Fig. 3. Earliest view, occurring in midmorning or later, is shown in Fig. 3, 4. These, when first seen, have an angular elevation of about 01′ of arc, apparently "snapping into view" when they first appear. The images slowly rise as the day progresses, so that the isolated points join, forming, later in the day, an almost complete image of the island, as in Fig. 3, 5.

Under abnormal conditions, multiple partial images appear above the vertically-expanded image of the island, appearing as in Fig. 3, 6. The upper, supernumerary, images are darker than the lower image, and usually appear to be twinned about a horizontal plane. It is sometimes stated locally that multiple images of Isla Angel are indications of a tropical cyclone to come ("Cordonazo"), and such has been the case whenever they have been seen by the writer.

Appearance of the upper images changes with each minor change in the position of the observer, and the actual changes in appearance with changes in the height of the observer's eye above sea level are disproportionate to the change of elevation. Attempts to photograph the loomed images of Isla Angel are partially successful, producing a faint image on the negative, near the limits of resolution of the emulsion. Supernumerary images disappear completely when a red filter is used, but the main image remains.

Magnitudes of the loomed images of Isla Angel are about the same as those of the Sierra San Pedro Martir, but the images tend to be much steadier, perhaps a result of the elevation of the point of observation, which is above the local zone of extreme shimmer.

Rarely, vague images of supposed objects more distant than Isla Angel can be seen. These may be loomed images of the Sierra de Calmalli, in Baja California, but their dimensions are so small, and their contrast so weak, that certain identification is not possible.

METEOROLOGICAL CONCORDANCE

Mirages, and related optical phenomena, occur with great regularity in the area bordering on the northern part of the Gulf of California,

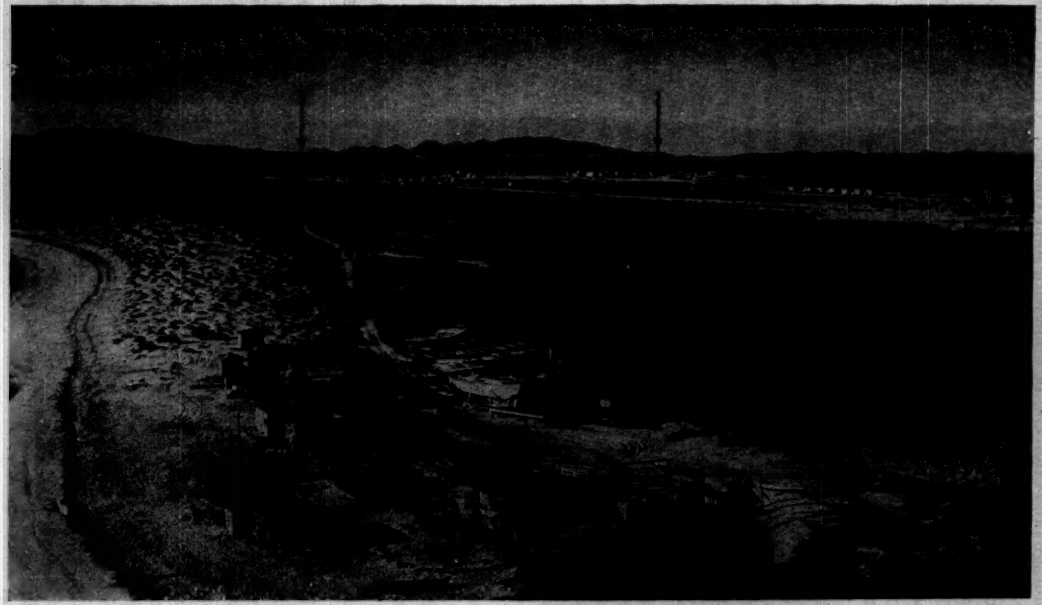

FIG. 4. View northeastward across the tidal basin at Puerto Peñasco, showing mirage strip at base of Sierra Blanca (between arrows). Pinacate Volcano, at extreme left, has a similar mirage strip, above which is a white line, the crest line of the "Great Sand Dunes" that line the Sonoran shore in this area.

and are accompanied by fairly characteristic meteorological conditions, so that mirage prediction can be done with some confidence from a good weather forecast.

Inferior mirages on land, "false horizons" at sea, and single inverted images of vessels at sea, occur most commonly when there is a very steep lapse in the lower part of the atmosphere, are almost invariably absent under isothermal conditions, and can be explained entirely on the basis of refractive conditions accompanying steep lapse rates.

Multiple inverted and twinned images occur most commonly when the air is stratified, and the number of "twinned" images seems to approximate the number of atmospheric strata in the vertical range under consideration. Because of a smaller number of observations, and the greater difficulty of determining temperature gradients at moderate elevations, this concordance is given with less confidence than the first.

Looming and towering of distant mountains are most commonly observed when the lapse through a considerable vertical range is steep. Lapses of from 0.5 to 1.5° F. per foot, from the sea surface to 20 feet (or more) above it, are commonly measured over the Gulf of California; and lapses exceeding (an average of) 4° F. per foot, in the lower 10 feet of the atmosphere, are common in summer over adjacent land areas. Refractive effects of such lapse rates are more than enough to produce the looming and towering observed in this area.

SUMMARY

Mirages at and near Puerto Peñasco, Sonora, are of standard types, similar to those observed by the writer in all of the major desert areas of North America, and resemble quite closely those described in other large deserts in other parts of the world.

Wherever mirages of a given general type are observed, the meteorological and terrain conditions are similar. Prediction methods that succeed in one area are generally successful in any other.

In all areas where instrumental measurements have been made by the writer, the apparent size of mirage images has far exceeded the measured dimensions, which commonly approach the lower size limit for dependable observation. In most instances also, the measured dimensions of the mirage images are considerably larger than the computed dimensions.

These discrepancies apparently indicate that a part of almost any mirage is subjective, and that magnification is a standard occurrence, along with bending of the line of sight. In addition, it seems that the writer has been singularly unfortunate in his choice of times for observation, for in no area studied have the observed mirages been as large, as continuous, or as complicated as those described to him by local residents!

MAP REFERENCE

South America, 1/1,000,000, Sheet NH-12, *Baja California, Norte*, American Geographical Society of New York, 1928.

REFERENCES

(1) CRISTOBAL DE CAÑAS (supposed author), see R. L. IVES, "The Sonoran Census of 1730," *Records Amer. Cath. Hist. Soc.*, Vol. 59, No. 4, p. 321 (1948).

(2) A. CONTRERAS ARIAS, "Mapa de las Provincias Climatológicas de la República Mexicana," México, D. F., 1942.

(3) N. M. FENNEMAN, "Physiography of the Western United States," New York, McGraw-Hill, 1931, pp. 326–395.

(4) W. J. HUMPHREYS, "Physics of the Air," New York, McGraw-Hill, 1940.

(5) R. L. IVES, "Recent Volcanism in Northwestern Mexico," *Pan-American Geologist*, Vol. 63, pp. 335–338 (1934).

(6) R. L. IVES, "Behavior of Dust Devils," *Bull. Amer. Met. Soc.*, Vol. 28, pp. 168–175 (1947).

(7) R. L. IVES, "Meteorological Conditions Accompanying Mirages in the Salt Lake Desert," JOUR. FRANKLIN INST., Vol. 245, pp. 457–475 (1948).

(8) R. L. IVES, "Climate of the Sonoran Desert Region," *Annals Amer. Assn. Geog.*, Vol. 39, pp. 143–187 (1949).

(9) R. L. IVES, "Puerto Peñasco, Sonora," *Jour. Geog.*, Vol. 49, pp. 239–261 (1950).

(10) E. F. KINO, "Favores Celestiales" (unpublished ms. ca. 1710); see H. E. BOLTON, "Kino's Historical Memoir of Pimeria Alta," Cleveland, Arthur H. Clark Co., 1919, and Berkeley, Univ. of Calif. Press, 1948.

(11) CARL LUMHOLTZ, "New Trails in Mexico," New York, Scribner, 1912.

(12) J. M. MANJE, "Luz de Tierra Incognita" (ms. ca. 1721) Mexico, D. F. several printed versions ca. 1850, best in *Documentos Para la Historia de México*, ser. IV, tomo 1, undated.

(13) SIR N. SHAW, "Manual of Meteorology," Vol. III, Cambridge, 1942, pp. 53–68.

(14) GODFREY SYKES, "The Colorado Delta," Carnegie Inst. of Washington, Special Pub. 480, 1937.

Beta-Ray Gage.—In the first installation of its kind, a General Electric beta-ray gage is being used at the Antioch, Calif., plant of the Fibreboard Products Corporation to help maintain accurate and uniform weight of milk carton paperboard.

The gage, mounted on one of the company's 136-in. paperboard machines, records the varying amounts of beta-rays absorbed by the board as it passes through the gage head of the non-contacting device. The amount of beta-rays absorbed varies with the weight of the board, thus allowing a constant check to be maintained. Variations as slight as one per cent from the desired weight per unit area of the board are automatically indicated and recorded.

Operators are able to make adjustments of the processing machinery as needed to produce paperboard of uniform weight. This is particularly important in the case of milk carton board and similar material that is run through folding machines which operate on extremely close tolerances.

According to E. H. Entricken, in charge of instruments at the Fibreboard plant, the G-E beta-ray gage is "more than a watchdog to prevent bad runs—it also aids in setting up new runs more quickly."

The gage, which is not affected by the speed, consistency, or temperature of the material being measured, may also be applied to plastics, rubber, metals, and special sheet materials where a continuous indication is desired. Since no part of the gage is in actual contact with the material being measured, it leaves no mark or scratch.

Pre-service tests of helicopter blades and rotors are now being conducted on actual equipment instead of scale models. Wright Air Development Center at Dayton does the job in two "whirley-bird cages" where all new and experimental rotors are tested for aerodynamic calibration for power and thrust, strain on various parts of the blades, and endurance. The larger cage is enclosed by six layers of chain link fence 75 ft. high and 100 ft. in diameter, uses a 4000 hp. electric motor to whirl rotors up to 90 ft. in diameter at speeds of 450 rpm. Floodlights permit night operation and overhead cranes lift rotors to the 50 ft. stand.

A flexible exhaust tailpipe for jet fighter engines developed by the Power Plant Laboratory, Wright-Patterson AF Base features a simple bellows fabricated from high-temperature, corrosion-resistant steel. Planes in high-G dives meet with forces resulting in after-fuselage deflection of as much as three inches which poses no problem for piston engine craft, but may buckle tailcones or damage turbine blades in jet engines. Units in use with F-80, F-84 and F-94 jets have been built by Solar Aircraft and Republic Aviation.

A new red blood cell counter developed at Cornell U. as part of a Naval Research study of the electrostatic forces in the blood, and their relation to coagulation, permits three technicians to perform from 40 to 60 blood counts per hour as compared to the present rate of 12 to 18 an hour. Errors in visual blood counting methods now used are avoided in the new instrument, since there is no dilution of blood and the quantity used is not critical.

THE SLOW NEUTRON-INDUCED RADIOACTIVITIES OF NUCLEAR EXPLOSIONS

BY

C. E. MANDEVILLE[1]

ABSTRACT

The slow neutron-induced radioactivities of nuclear explosions have been evaluated for infinite media of filtered Schuylkill water and the earth's crust. The magnitudes of these effects are compared with the activity of the fission fragments, and the conditions under which they may be of importance are considered.

It has been assumed that a gram-molecule of neutrons is liberated in the blast.

I. INTRODUCTION

The physical, thermal, and radioactive properties of nuclear explosions have been outlined in detail.[2] Although at least fifteen references are made to slow neutron-induced radioactivities of the nuclear blast,[3] it appears that no quantitative estimates of the total induced radioactivity are available. Difficulties are encountered in making such evaluations because of the various special conditions surrounding each burst. However, the general question of the order of magnitude of the induced radioactivity has persisted. It has been usually assumed, and correctly so, that radioactive intensities induced by the slow neutrons are small in comparison with the total activity of the fission fragments. However, it is also known that for certain specific types of bursts, the fission fragments proceed skyward to the upper atmosphere, leaving only the slow neutron-induced radioactivities. Thus, the question immediately arises as to what radioactivities must be dealt with and what maximum intensities might be present. For all of these reasons, it has been decided to evaluate as simply as possible the extent of the slow neutron-induced radioactivity. The calculations have been limited to underwater and underground bursts. In the first case, the explosion is assumed to occur in an infinite medium of impure water; in the second, in an infinite medium of the earth's crust. Results obtained under these circumstances may then be employed to give the total induced activity resulting from a nuclear explosion in various combinations of the two media. The underwater explosion has been applied specifically to filtered Schuylkill water.

---

[1] Deputy Chief, Radiological Branch of the Technical Division, Philadelphia District Civil Defense Council; and, Physicist, Bartol Research Foundation of The Franklin Institute, Swarthmore, Pa.

[2] "The Effects of Atomic Weapons," U. S. Government Printing Office, Washington, D. C.

[3] Footnote 2, pp. 35, 221, 222, 254, 255, 256, 268, 269, 270, 274, 276, 287, 312, 320, and 394.

II. THE UNDERWATER BURST

Should a nuclear explosion occur in inland water, it would be necessary to consider three possible sources of residual radioactivity. These are:

1. Radioactive fission fragments remaining in the water after the explosion.
2. Presence of unexploded plutonium, a residue resulting from the inefficiency of the fission process.
3. Neutron-induced activities resulting from the absorption of slow neutrons released in the blast, the absorption occurring in the water itself and in the impurities contained therein.

General experience with the fission process has led to the conclusion that the first two of the above-listed factors are dominant in rendering the water contaminated with radioactive isotopes. However, as stated in the introduction of this paper, the exact role of part 3 above has not been evaluated. It has seemed advisable to compute the contribution of the slow neutron-induced activities of the impurities to the general radioactivity of the water for the following specific reasons:

1. The tolerance values of radioactivity in microcuries per cubic centimeter are very small for human consumption.
2. The fission fragments settled to the floor of Bikini Lagoon.[4] This could also occur in an inland explosion. However, the slow neutron-induced activities of soluble impurities will remain uniformly distributed throughout a body of water.
3. The radioactive decay of the fission fragments is relatively rapid. Should the slow neutron-induced activities of the soluble impurities decay less rapidly, at a time considerably removed from the moment of the explosion, their contribution to the general over-all residual radioactivity might become comparable with that of the fission fragments.
4. The quantity of fission fragments present might be reduced if, in the case of a shallow explosion in a reservoir of small surface area, the fragments are carried upward in the water column and spread overland in the "base surge." The relative importance of the remaining slow neutron-induced activities might thus be enhanced. It is probable that the slow neutron-induced activity of the earthen floor of the reservoir would be the major contributor. This activity will be computed in a later section of this paper.

Most of the neutrons emitted under water are ineffective in inducing radioactivity, because they are absorbed in the hydrogen of the water to form stable deuterium. The nuclear reaction in which this absorption occurs is

$$_1H^1 + {}_0n^1 \rightarrow {}_1H^2 + 2.23 \text{ Mev.}$$

Of the neutrons liberated in the nuclear explosion, the greater fraction

[4] Footnote 2, p. 283.

participates in this reaction, because there is such a large number of hydrogen atoms in each cubic centimeter of H_2O and because the nuclear cross-section, the so-called slow neutron capture cross-section (0.3 barn*) for the reaction, is appreciable. It is this heavy absorption of the neutrons in hydrogen which introduces such a great difference between the intensities of the slow neutron-induced activities of a ground or low air burst and an underwater explosion. It is this same heavy absorption arising from the presence of an abundance of hydrogen, however, which tremendously simplifies the mathematical calculations; that is, the concentration of slow neutrons at any point in the water is determined almost entirely by the absorption in hydrogen. The oxygen content of the water contributes little to slow neutron absorption, because the cross-section for the process is < 9 millibarns (0.009 barn). This cross-section is obviously small relative to that of hydrogen.

Although, as previously stated, hydrogen is the dominant absorbing nucleus, the slow neutron-induced activities of small quantities of impurities may be quite appreciable in the absolute sense, if the total number of neutrons released is very great, as in the case of the nuclear explosions which occurred at Hiroshima and Nagasaki.

III. CALCULATIONS RELATING TO THE UNDERWATER BURST

The explosion is considered to occur in an infinite continuous medium of water; that is, the reservoir is assumed to extend to infinity in all directions. This is a good assumption, even for relatively shallow explosions, because, although the neutrons initially emitted are fast, they are quickly thermalized in a "random walk" resulting from scattering collisions with hydrogen and oxygen in the infinite medium. The now slow neutrons are assumed to diffuse outward on the surface of an expanding sphere with center at the point of the explosion.[5]

Some symbols must be defined:

n = number of atoms of hydrogen per cubic centimeter of H_2O.
n' = number of atoms of a particular impurity per cubic centimeter of H_2O.
σ = slow neutron capture cross-section of hydrogen.
σ' = slow neutron capture cross-section for production of a given isotope of the particular impurity.[6]

* One barn is a cross-section of 10^{-24} cm^2. This term has its origin in the phrase "as big as a barn," as explained by M. G. Holloway and C. P. Baker, LAMS-523 (1944).

[5] It is desired to obtain only the total number of radioactive atoms formed in the explosion, which is regarded as a single burst of neutrons from a point source. There has been no thought of computing the neutron density or the number of radioactive atoms at any particular distance from the source at any particular time after the explosion. The effects of slow neutron scattering and the complications of diffusion theory have been omitted.

[6] The quantity, σ', is the "natural atom cross-section" or "atomic cross-section." This cross-section is the "isotopic cross-section" of the absorbing isotope of a particular element, weighted by the isotopic abundance of the target nucleus.

TABLE II.

Target Element	Al	Ba	B	Cu	Cr	F	Pb	Ni	Mn
Micrograms of Impurity/cc. of H_2O	0.3	0.1	0.02	0.02	0.01	0.01	0.02	0.01	0.3
Radioactive Element Produced	Al^{28}	$Ba^{131,133m,133,135m,137m,139}$	B^{12}	$Cu^{64,66}$	$Cr^{51,55}$	F^{20}	Pb^{209}	$Ni^{59,63,65}$	Mn^{56}
Half-Period of the Slow Neutron Induced Activity	2.4 M.	12 D. 38 Hr. 20 Yr. 28.7 Hr. 2.63 M. 84 M.	0.027 S.	12.8 Hr. 5 M.	2.65 D. 1.3 Hr.	10.4 S.	3.32 Hr.	2×10^{5} Yr. 85 Yr. 2.6 Hr.	2.59 Hr.
Slow Neutron Capture Cross-Section σ Barns	0.21	2.4×10^{-2} 0.058 0.058 0.19 0.60 0.35	0.04	2.0 0.56	0.5 1.4×10	9.4×10^{-3}	0.5	2.9 0.44 1.7×10^{-2}	10.7×10^{-26}
No. of Atoms of Impurity per cc. n'	7×10^{15}	4.2×10^{14}	1.1×10^{15}	1.1×10^{15}	10^{14}	3×10^{14}	6×10^{13}	1.7×10^{13}	6×10^{14}
$n'\sigma'$	1.5×10^{-3}	10^{-14} 2.5×10^{-11} 2.5×10^{-11} 8.0×10^{-11} 2.5×10^{-10} 1.4×10^{-10}	4.4×10^{-11}	2.2×10^{-3} 6.0×10^{-16}	5.0×10^{-12} 1.4×10^{-14}	2.8×10^{-12}	5.6×10^{-11}	5×10^{-11} 8×10^{-12} 3×10^{-12}	6.4×10^{-3}
$\frac{N_{sn'\sigma'}}{n\sigma}$	4.4×10^{16}	3.0×10^{11} 7.5×10^{14} 7.5×10^{14} 2.4×10^{15} 7.4×10^{15} 4.2×10^{16}	1.3×10^{15}	6.6×10^{16} 1.8×10^{16}	1.5×10^{15} 4×10^{11}	8.4×10^{13}	1.7×10^{15}	1.5×10^{15} 2.4×10^{14} 8.6×10^{12}	2×10^{17}
Disintegrations/sec. at Time Zero	2×10^{14}	2.0×10^{9} 3.8×10^{9} 8.0×10^{8} 1.7×10^{10} 3.4×10^{10} 6.0×10^{11}	3.4×10^{10}	1×10^{12} 4×10^{12}	1×10^{10} 6×10^{7}	6×10^{12}	1×10^{11}	160 6×10^{4} 6×10^{8}	1.4×10^{12}
Total No. of Curies at Time Zero $\Sigma C\sim1.4\times10^{4}$ Curies	5400	6×10^{-6} 0.10 2×10^{-3} 0.46 920.0 160.0	1×10^{6}	28 1080	0.28 0.002	160	2.56	4×10^{-9} 2×10^{-6} 0.016	380
Total No. of Curies at $T=1$ Hour $\Sigma C\sim500$ Curies	2.2×10^{-3}	6×10^{-6} 0.10 2×10^{-5} 0.46 0.0092 60.0	—	26.0 0.26	0.28 0.001	—	1.82	4×10^{-9} 2×10^{-6} 0.0096	246
Total No. of Curies at $T=24$ Hr. $\Sigma C\sim60$ Curies	5×10^{-177}	6×10^{-6} 0.04 9×10^{-6} 0.20 — 6×10^{-6}	—	8.0 —	0.27 —	—	0.026	4×10^{-9} 2×10^{-6} 8×10^{-6}	1.6

Total Activity at T = 168 Hr. (one Week)—$\Sigma C < 0.4$ Curie

TABLE II.—*Continued.*

Target Element	K	Na	Ag	Sr	Sn	Zn	V	Sb	Mo	O
Micrograms of Impurity/cc. of H_2O	0.06	6.0	0.03	1.5	0.01	0.03	0.02	0.04	Trace	
Radioactive Element Produced	K^{42}	Na^{24}	$Ag^{106,110m,110}$	$Sr^{87m,89}$	$Sn^{113-126}$	$Zn^{65,69m,69}$	V^{52}	$Sb^{122,124}$	$Mo^{99,101,?}$	O^{19}
Half-Period of the Slow Neutron Induced Activity	12.4 Hr.	15 Hr.	2.3 M. 22 S. 225 D.	2.7 Hr. 55 D.	105 D. 9 M. 40 M. 26 Hr. 10 D. 400 D.	250 D. 57 M. 13.8 Hr.	3.9 M.	2.8 D. 60 D.	67 Hr. 19 M. 7 Hr.	31 S.
Slow Neutron Capture Cross-Section σ Barns	6.7×10^{-2}	0.63	23.0 46.6 1.1	0.128 4×10^{-3}	0.012 0.039 0.014 0.072 0.009 0.018	0.26 0.19 0.054	4.5	3.8 1.1	0.10 0.044 0.001	
No. of Atoms of Impurity per cc. n'	1.4×10^{24}	25×10^{24}	3×10^{23}	1.7×10^{23}	10^{23}	5×10^{23}	4×10^{23}	3×10^{23}	10^{23}	3.3×10^{22}
$n'\sigma'$	9.4×10^{-12}	1.5×10^{-2}	6.9×10^{-10} 1.4×10^{-9} 3.0×10^{-11}	2.0×10^{-10} 7.0×10	1.2×10^{-12} 3.9×10^{-13} 1.4×10^{-13} 7.2×10^{-13} 9.0×10^{-14} 1.8×10^{-13}	1.3×10^{-11} 1.0×10^{-11} 2.7×10^{-12}	2×10^{-10}	1.1×10^{-10} 3.3×10^{-11}	1×10^{-13} 4×10^{-14} 1×10^{-15}	1.3×10^{-2}
$\frac{Nn'\sigma'}{n\sigma}$	2.8×10^{24}	4.6×10^{27}	1.9×10^{26} 6.2×10^{26} 9.0×10^{24}	6×10^{25} 2×10^{24}	3.6×10^{22} 1.2×10^{22} 4.2×10^{22} 2.2×10^{22} 2.6×10^{22} 5.4×10^{22}	4×10^{24} 3×10^{24} 8×10^{23}	5×10^{25}	3.4×10^{25} 1.0×10^{25}	3.0×10^{22} 1.4×10^{21} 3.0×10^{20}	4×10^{27}
Disintegrations/sec. at Time Zero	4×10^{19}	6×10^{22}	1×10^{22} 2×10^{25} 3×10^{7}	4×10^{21} 3×10^{7}	2.8×10^{8} 1.4×10^{10} 1.2×10^{8} 1.4×10^{8} 2.4×10^{8} 3.2×10^{8}	1.2×10^{7} 6.0×10^{10} 4.6×10^{7}	1.6×10^{23}	1.0×10^{8} 1.4×10^{8}	8×10^{6} 8×10^{7} 8×10^{6}	1×10^{18}
Total No. of Curies at Time Zero $\Sigma C\sim1.4\times10^{5}$ Curies	1.08	160	280 5.4×10^{4} 8.0×10^{-4}	10.8 8×10^{-4}	8.0×10^{-6} 0.4 3.2×10^{-2} 3.8×10^{-3} 6.4×10^{-6} 8.6×10^{-6}	3.2×10^{-4} 1.6 1.3×10^{-2}	420	0.028 0.004	2.2×10^{-4} 2.2×10^{-2} 2.2×10^{-6}	2.6×10^{5}
Total No. of Curies at $T=1$ Hour $\Sigma C\sim500$ Curies	1.0	152	2.8×10^{-2} — 8.0×10^{-4}	8 8×10^{-4}	8.0×10^{-6} 6.0×10^{-2} 2.0×10^{-2} 3.7×10^{-3} 6.4×10^{-6} 8.6×10^{-6}	3.2×10^{-4} 0.8 3.4×10^{-4}	0.014	0.026 0.004	2×10^{-4} 3×10^{-4} 2×10^{-6}	—
Total No. of Curies at $T=24$ Hr. $\Sigma C\sim60$ Curies	0.26	54	— — 8×10^{-4}	0.032 8×10^{-4}	8.0×10^{-6} — 1.8×10^{-2} 5.8×10^{-6} 8.6×10^{-6}	3.2×10^{-4} 1.6×10^{-2} 3.2×10^{-4}	—	0.022 0.004	2×10^{-4} — 3×10^{-4}	—

Total Activity at $T=168$ Hr. (One Week)—$\Sigma C<0.4$ Curie

N_0 = total number of neutrons released in the blast.
N_0' = total number of radioactive atoms of a given isotope of a particular impurity present at time zero.
N' = total number of radioactive atoms of an isotope of a particular impurity present at any subsequent time.

It can be easily shown that the total number of radioactive atoms of a radio-isotope of a particular impurity produced throughout the infinite medium would be

$$N_0' = \frac{N_0 n' \sigma'}{n\sigma}. \tag{1}$$

Thus, from Eq. 1, N_0', the total number of nuclei of a particular radio-isotope formed throughout the medium at time zero, may be calculated. The number of disintegrations per second at time zero arising from the radio-element of the impurity would be given by

$$\left.\frac{dN'}{dt}\right|_{t=0} = -\lambda N_0'. \tag{2}$$

The number of curies of activity present at time zero is, then,

$$C_0 = -\frac{\lambda N_0'}{3.7 \times 10^{10}}. \tag{3}$$

From Eq. 3, the number of curies[7] of a particular activity present at any subsequent time may be calculated.[8]

IV. THE INDUCED ACTIVITY OF SCHUYLKILL WATER

The calculations of the preceding section have been applied to an analysis of the slow neutron activation of Schuylkill water at time zero, one hour afterwards, twenty-four hours later, and one week thereafter. The disintegration rates are shown in Table I.[9]

[7] The curie is taken to be 3.7×10^{10} nuclear disintegrations per second.

[8] N_0' is obtained from Eq. 1, where $N_0/n\sigma$ is 3×10^{25}, if a gram-molecule of neutrons is assumed liberated. N_0 is 6.02×10^{23}, Avogadro's number, for the nominal, or Hiroshima, type explosion (footnote 2, pp. 243, 244).

[9] Table I is a condensation of Table II, which is self-explanatory. The data of Table II are based upon a spectrographic analysis of H_2O filtered from the Schuylkill. From the analysis, the number of micrograms per cubic centimeter of the chemical impurities were derived. The radio-isotopes formed and their various half-periods were taken from Seaborg and Perlman, *Rev. Mod. Phys.*, Vol. 20, p. 585 (1948). The slow neutron activation cross-sections were taken from Seren, Friedlander and Turkel, *Phys. Rev.*, Vol. 72, p. 888 (1947) and from *Nuclear Data*, Circular of the National Bureau of Standards, 499, 1950. Difficulties were encountered in determining the contributions made to the total activity by radio-barium, because the cross-sections for production of Ba^{135m} and Ba^{137m} were not known when Table II was compiled in the spring of 1951. Since the cross-sections for the formation of the other isotopes of barium are known, these were subtracted from the total "atomic cross-section" of barium, and the remainder was divided according to the relative isotopic abundance of Ba^{134} and Ba^{138}, to give the cross-sections for production of Ba^{135m} and Ba^{137m}.

Because of incompleteness of data, several omissions occur in Table II. Approximate calculations show that the short-lived isomers of antimony, Sb^{122m} (3.5 min.), Sb^{124m} (21 min.)

TABLE I.

Total Activity (curies)	Time after Explosion
1.4×10^6	zero
500	one hour
60	24 hours
<0.4	one week

The high activity at time zero arises chiefly from the presence of the 31-second O^{19} and the 0.027-second B^{12}. It will be noted that the effects of oxygen in the H_2O are included in Table II along with those of the spectrographically identified impurities. By "time zero" is meant a time which is short as compared with the half-period of B^{12}.

The East Park Reservoir of the Philadelphia water supply contains approximately 3×10^{12} cc. of H_2O. The specific activities of the water at various times subsequent to the explosion are shown in Table III, calculated from Table I.

TABLE III.

Time	Activity in microcuries/cc.
zero	0.46
1 hour	1.7×10^{-4}
24 hours	2×10^{-5}
1 week	$<1.3 \times 10^{-7}$

If the tolerance level of the beta-gamma activity is taken to be 4×10^{-6} microcurie/cc.,[10] it is clear that, were the slow neutron-induced activities alone present in the reservoir, the water would be usable within a time less than a week. Emergency values of the tolerance activity are considerably more than that given above.[11]

The gamma ray activity of the fission fragments is given as a function of time in Table IV.[12]

---

and Sb^{134m} (1.3 min.), contribute ~300 curies of activity at time zero and ~1.5 curies of activity one hour later. The writer has recently been informed that the 9-minute and 10-day tin activities are isomers of Sn^{125}, both growing the 2.7 year Sb^{125}. [*Note added in proof:* The isomeric relation and characteristic radiations of the tin activities have been discussed by Lee and Pool, *Phys. Rev.*, Vol. 76, p. 606 (1949).] A calculation has shown that the contribution of Sb^{125} to the total activity never exceeds 2 microcuries.

It is evident that any errors in computing the contributions of barium and antimony would not influence the results in the practical sense.

When the total intensities of the short-lived activities have become less than a millimicrocurie, negligibly small, at time long after the explosion, their values have been left blank in Tables II and VII.

[10] Footnote 2, p. 332.

[11] Acceptable emergency levels of the beta-gamma activity are 9×10^{-2} microcurie/cc. if the water is to be consumed over a period of 10 days and 3×10^{-2} microcurie/cc. for use during a time of 30 days.

[12] Footnote 2, p. 251.

TABLE IV.

Time	Activity in curies
1 minute	8.2×10^{11}
1 hour	6×10^{9}
24 hours	1.3×10^{8}
1 week	1.3×10^{7}
1 year	1.1×10^{5}

Clearly, from Table IV, if all the fission fragments remain in the reservoir and uniformly distributed throughout it, they would, as a hazard, dominate the effects of the slow neutron-induced activities. Assuming a uniform distribution, the gamma ray activity per cubic centimeter is given in Table V for the particular case of the East Park Reservoir of Philadelphia.

TABLE V.

Time	Activity in microcuries/cc.
1 minute	2.7×10^{5}
1 hour	2×10^{3}
24 hours	40
1 week	4
1 year	4×10^{-2}

According to Table V, the water would be unusable for almost any length of time, even after the elapse of a period of one year.[13] Tables IV and V give the curies of gamma ray activity present at the specified times. In the case of drinking water, however, it is the number of nuclear disintegrations per second which is of importance, because the effects of beta rays must be considered. The activities of Tables IV and V should actually be increased by a factor of two, because roughly two beta rays are emitted for each gamma ray in the disintegration of the fission fragments.[14]

Before leaving the problem of water contamination it should be pointed out for the sake of completeness that should the explosion involve 100 Kg. of plutonium,[15] a contamination activity of 1.8×10^{-3} microcurie/cc. would be present in the East Park Reservoir. This is to be compared with the normally accepted tolerance level[16] of 1.2

[13] The values of all the activities of all the tables of this paper have been computed without taking into account dilution of the radioactivity by precipitation and evaporation. Moreover, the radioactivity may be further reduced by such factors as adsorption, etc., which the writer does not know how to evaluate quantitatively (see footnote 2, pp. 283, 330). The values of contamination given in the various tables then represent the extreme contamination to be expected in a nominal explosion (one gram of neutrons emitted in the blast).

[14] Footnote 2, p. 251.

[15] Footnote 2, p. 257.

[16] Footnote 2, p. 396.

$\times 10^{-6}$ microcurie/cc. Emergency levels of alpha activity are quoted as 5×10^{-3} microcurie/cc. if the water is to be used for a ten day period and 1.7×10^{-3} microcurie/cc. for use over a time of thirty days.

V. THE UNDERGROUND BURST

The explosion is assumed to occur in an infinite medium of the earth's crust with an assumed continental density of 2.67 g./cm^3. The induced radioactivity of the eighteen most abundant elements has been calculated. The number of nuclei of a particular radioisotope of a given element formed by slow neutron capture is

$$N_0' = \frac{N_0 n_i \sigma_{r_i}}{\sum_1^m n_j \sigma_{r_j} + \sum_1^{m'} n_k \sigma_{s_k}} = \frac{N_0 n_i \sigma_{r_i}}{\sum_{l=1}^{18} (n_T \sigma_T)_l}. \tag{4}$$

In Eq. 4, the subscript r refers to the formation of a radioactive nucleus by slow neutron capture, and the subscript s refers to the formation of a stable nucleus. n_T is the total number of nuclei including all isotopes present per cc. for a given element and σ_T is the total atomic cross-section for the element.

The total slow neutron-induced radioactivity of the earth's crust is given as a function of time in Table VI.

TABLE VI.

Time	Total Activity (curies)
zero	2.8×10^9
1 hour	1.2×10^8
24 hours	2.84×10^6
1 week	4000

Table VI is a condensation of Table VII where the calculations are given in detail. The data of Tables I and VI may be combined to treat explosions at the boundary of the two media, Schuylkill water and the earth's crust. This circumstance would simulate the explosion of a nuclear bomb lying on the floor of a reservoir.

VI. CONCLUSION

The slow neutron-induced activities of nuclear explosions in infinite media of Schuylkill water and the earth's crust have been quantitatively evaluated. Fast neutron-induced radioactivities have been neglected. The data show that the total activity of the fission fragments exceeds the slow neutron-induced activity of the water by a factor of $\sim 10^6$ and the slow neutron-induced radioactivity of the earth's crust by a factor of $\sim 10^9$. Conditions have been cited in which the slow neutron-induced activities could be of importance.

TABLE VII.

Target Element	O	Si	Al	Fe	Ca	Na	K	Mg	Ti
g/cm²	1.24	0.74	0.21	0.13	0.10	0.075	0.07	0.06	0.02
Radioactive Element Produced	O^{19}	Si^{31}	Al^{28}	Fe^{59}	$Ca^{45,49,49m}$	Na^{24}	K^{42}	Mg^{27}	Ti^{51}
No. of Atoms/cc.	4.8×10^{22}	1.6×10^{22}	4.8×10^{21}	1.4×10^{21}	1.5×10^{21}	2×10^{21}	1.1×10^{21}	1.5×10^{21}	2.5×10^{20}
Half-Period of the Slow Neutron Induced Activity	31 S.	170 M.	2.4 M.	46.3 D.	152 D. 2.5 Hr. 30 M.	15 Hr.	12.4 Hr.	10.2 M.	6 M.
Capture Cross-Section For Production of the Radio Element σ_r (Barns)	4×10^{-7}	4.9×10^{-3}	0.21	10^{-3}	0.013 3.9×10^{-4} 10^{-3}	0.63	0.067	5.4×10^{-3}	7.5×10^{-3}
Total Capture Cross-Section, σ_T (Barns)	9×10^{-4}	0.135	0.21	2.425	0.42	0.63	2.05	0.06	5.85
$n_r\sigma_r$	1.9×10^{-6}	7.8×10^{-4}	10^{-3}	1.9×10^{-6}	2.0×10^{-5} 5.9×10^{-7} 1.5×10^{-6}	1.3×10^{-3}	7.2×10^{-6}	8.1×10^{-6}	1.9×10^{-6}
$n_T\sigma_T$	4.3×10^{-5}	0.022	10^{-3}	3.3×10^{-3}	6.3×10^{-4}	1.3×10^{-2}	2.2×10^{-2}	9×10^{-5}	1.4×10^{-2}
$\frac{N_a n_i \sigma_{ri}}{\sum_1^m n_j\sigma_{rj}+\sum_1^{m'} n_k\sigma_{rk}}$	3.8×10^{17}	1.5×10^{22}	2×10^{22}	2.8×10^{19}	4.0×10^{20} 1.2×10^{19} 3.0×10^{19}	2.5×10^{22}	1.5×10^{21}	1.8×10^{21}	3.8×10^{19}
Disintegrations/sec. at Time Zero	7.6×10^{15}	1.1×10^{16}	10^{20}	4.9×10^{12}	2.0×10^{12} 9.0×10^{14} 1.2×10^{16}	3.2×10^{17}	2×10^{16}	2×10^{16}	7.4×10^{16}
Total No. of Curies at Time Zero $\Sigma C\sim2.8\times10^9$ Curies	2.1×10^5	2.9×10^7	2.7×10^9	140	540 2.4×10^4 3.2×10^5	8.6×10^6	5.4×10^5	5.4×10^7	2×10^6
Total No. of Curies at $T=1$ Hour $\Sigma C\sim1.2\times10^9$ Curies	—	2.2×10^7	4.6	140	540 1.8×10^4 8.0×10^4	8.2×10^6	5×10^5	8×10^5	2×10^5
Total No. of Curies at $T=24$ Hr. $\Sigma C\sim2.84\times10^6$ Curies	—	5.8×10^4	—	138	538 24 —	2.6×10^6	1.4×10^5	—	—

Total Activity at $T=168$ Hr. (One Week)—$\Sigma C\sim4000$ Curies

TABLE VII.—*Continued*

Target Element	P	H	Mn	F	Cl	S	Ba	C	Sr
g/cm³	0.003	0.003	0.002	0.002	0.001	0.001	0.001	0.0007	0.0005
Radioactive Element Produced	P^{32}		Mn^{56}	F^{20}	$Cl^{36,38}$	$S^{35,37}$	$Ba^{131,133,133m,135m,137m,139}$	C^{14}	$Sr^{87m,89}$
No. of Atoms/cc.	6×10^{19}		2.4×10^{19}	6×10^{19}	1.8×10^{19}	1.8×10^{19}	4.2×10^{18}	3.6×10^{19}	3×10^{18}
Half-Period of the Slow Neutron Induced Activity	14.3 D.		2.6 Hr.	10.4 S.	2×10^{6} Yr. 38.5 M.	87.1 D. 5.0 M.	12 D. 38 Hr. 20 Yr. 28.7 Hr. 2.6 M. 84 M.	5100 Yr.	2.7 Hr. 53 D.
Capture Cross-Section For Production of the Radio Element σ_r (Barns)	0.23		10.7	9.4×10^{-3}	31.9 0.137	0.011 1.4×10^{-5}	2.4×10^{-6} 0.058 0.058 0.19 0.60 0.35	10^{-3}	0.128 4×10^{-3}
Total Capture Cross-Section, σ_T (Barns)	0.23	0.3	10.7	9.4×10^{-3}	32	0.5	1.10	4.7×10^{-3}	1.35
$n_r\sigma_r$	1.4×10^{-6}		2.8×10^{-6}	5.6×10^{-7}	5.7×10^{-4} 2.5×10^{-6}	2.0×10^{-7} 2.5×10^{-10}	10^{10} 2.4×10^{-9} 2.4×10^{-9} 8.0×10^{-7} 2.5×10^{-6} 1.5×10^{-6}	1.7×10^{-7}	3.8×10^{-7} 1.2×10^{-6}
$n_T\sigma_T$	2×10^{-6}	5.4×10^{-4}	2.6×10^{-6}	5.6×10^{-7}	5.8×10^{-4}	9×10^{-8}	4.6×10^{-6}	1.7×10^{-7}	4.1×10^{-6}
$\frac{N_0 n_i \sigma_{r_i}}{\sum_1^m n_j\sigma_{r_j}+\sum_1^{m'} n_k\sigma_{t_k}}$	2.8×10^{20}		5.2×10^{19}	1.1×10^{19}	1.1×10^{22} 5.0×10^{19}	4×10^{18} 5×10^{16}	2.0×10^{18} 4.8×10^{16} 4.8×10^{16} 1.6×10^{19} 5.0×10^{19} 3.0×10^{19}	3.4×10^{18}	7.7×10^{18} 2.4×10^{17}
Disintegrations/sec. at Time Zero	1.6×10^{14}		4×10^{18}	7×10^{17}	1.4×10^{18} 1.5×10^{16}	4.0×10^{11} 1.2×10^{13}	1.4×10^{9} 2.5×10^{11} 6.0×10^{9} 1.1×10^{14} 2.2×10^{17} 4.0×10^{15}	1.5×10^{8}	6.0×10^{14} 3.4×10^{16}
Total No. of Curies at Time Zero $\Sigma C\sim2.8\times10^{8}$ Curies	4.4×10^{3}		1.1×10^{8}	1.9×10^{7}	3.6×10^{-2} 4.0×10^{3}	10.8 310	3.8×10^{-2} 6.6 1.6×10^{-4} 3.0×10^{8} 6.0×10^{8} 1.1×10^{8}	4×10^{-6}	1.6×10^{4} 0.92
Total No. of Curies at $T=1$ Hour $\Sigma C\sim1.2\times10^{8}$ Curies	4.4×10^{3}		9.1×10^{7}	—	3.6×10^{-2} 1.4×10^{3}	10.8 7.8×10^{-3}	3.8×10^{-2} 6.46 1.6×10^{-4} 2.9×10^{8} 0.108 4.3×10^{4}	4×10^{-6}	1.2×10^{4} 0.92
Total No. of Curies at $T=24$ Hr. $\Sigma C\sim2.84\times10^{8}$ Curies	4.1×10^{3}		1×10^{6}	—	3.6×10^{-2} 4.0×10^{-7}	10.72 —	3.5×10^{-2} 3.6 1.6×10^{-4} 1.4×10^{8} — 1.08	4×10^{-6}	32.0 0.84

Total Activity at $T=168$ Hr. (One Week)—$\Sigma C\sim4000$ Curies

It is evident that the data of Table II can be readily extended to include waters of differing composition, for example, salt water. Since the computations are based upon emission of one gram of neutrons ($N_0 = 6.02 \times 10^{23}$), they can be immediately extended to larger explosions.

Perhaps it should be emphasized that the neutron-induced activities of the underwater explosion given in Table I hold only for the spectrographic analysis shown in Table II. Thus, the underwater burst is more correctly one in an infinite medium of water filtered for consumption by the populace. Not taken into account are the effects of sulfur, iron, chlorine, silicon, etc., which are sometimes found in "raw" Schuylkill river water. Not considered also is the fact that the water may be chlorinated twenty-four to forty-eight hours before use. Should the explosion occur after chlorination, appreciable quantities of the 37-minute Cl^{38} would be present. Organic matter is not considered in Table II. However, it certainly should not contribute more than the C^{14} activity of Table VII, which does not exceed four micrograms.

Taking into account all of the above-mentioned points, the total activity of "raw" Schuylkill river water should not exceed the values of Table I by more than a factor of ten, this increase being apparent at most for a period of only a few hours after time zero.[17]

[17] Were chlorides present in raw river water to such an extent that chlorine would reach a concentration of 10 micrograms/cc., the activity arising from Cl^{38} would be 1.3×10^{6} curies at time zero, accounting for an increase of a factor of two.

SUPERPOSITION OR MIXTURE OF SIMPLE QUANTIC CHARACTERISTIC CURVES OF PHOTOGRAPHIC EMULSION LAYERS. THE CORRESPONDING RELATIVE CONTRAST

BY

L. SILBERSTEIN [1]

The need of a superposition of two (or more) simple quantic expressions for the photographic density as function of exposure has originally arisen through the necessity of reducing the quotient γ/D_m (relative contrast) below the lowest theoretical value of the relative contrast which belongs to an exponential emulsion, under the one-quantic hypothesis,[2] namely,

$$\gamma/D_m = 0.682.$$

Now, experimentally, much lower relative contrasts have been measured for a great variety of emulsions, not only the commercial but also the experimental ones, as will be seen later on.

The only way of providing for such low values of γ/D_m, without having recourse to any further special hypotheses, was the superposition (addition) of two, or if necessary, of more quantic expressions found.

It will suffice to consider a superposition of *two* such expressions or a *binary* mixture of simple quantic terms which will, conceptually, correspond to a mixture of two emulsions (not necessarily a deliberate mixture of two ingredients prepared separately).

For an emulsion of an exponential size-frequency distribution, with sensitivity ϵ common to all grains, the quantic density formulas for $r = 1, 2, 3$ are, respectively:

$$\begin{aligned} \frac{D}{D_m} &= \frac{y(2+y)}{(1+y)^2} \equiv E(y), \\ \frac{D}{D_m} &= \frac{y^2(3+y)}{(1+y)^3} \equiv F(y), \\ \frac{D}{D_m} &= \frac{y^3(4+y)}{(1+y)^4} \equiv G(y), \end{aligned} \tag{0}$$

where $y = n\bar{a}\epsilon$ (n exposure in quanta, $\bar{a}$ mean grain size).

Some experimental characteristic curves are well covered by a single term of this type. More frequently, however, a binary combination of

[1] Deceased; formerly, Research Consultant, Rochester, N. Y.

[2] For a uniform emulsion, the lowest value of γ/D_m (for $r = 1$) was much higher, *viz.* 0.847. Also the one-quantic γ/D_m for the steepest Gaussian emulsion is higher than 0.682.

such terms, for example,

$$\frac{D}{D_m} = \alpha E(y) + \beta E(my), \qquad \alpha + \beta = 1,$$

is required for a close representation of the observed curve, as if a fraction (α) of all grains of the emulsion had one value of $\bar{a}\epsilon$ and the remainder, m times that value. (Without loss to generality, we may take $m < 1$.) In particular, for the case of *equipartition* ($\alpha = \beta$),

$$\frac{D}{D_m} = \tfrac{1}{2}\{E(y) + E(my)\} \qquad (r = 1)$$

or

$$\frac{D}{D_m} = \tfrac{1}{2}\{F(y) + F(my)\} \qquad (r = 2)$$

or

$$\frac{D}{D_m} = \tfrac{1}{2}\{G(y) + G(my)\}. \qquad (r = 3)$$

The most expedient method of adapting any of these binary expressions to the observed curve consists in requiring the theoretical *relative contrast* γ/D_m to coincide (nearly enough) with the observed one, and in determining accordingly the value of the parameter m.

If $y = \bar{y}$ be the inflection point of the $D/\log y$ curve, then the relative contrast is:

$$\gamma/D_m = \frac{\bar{y}}{M}\frac{D'(y)}{D_m}, \qquad M = \log e, \qquad (1)$$

and thus implies the knowledge of the numerical value of $\bar{y}$. For a single term, $\bar{y}$ is the root of a linear equation, to wit, $\bar{y} = r/2$ for any quantum number r and thus, for the three cases mentioned, $\bar{y} = 1/2$, 1, and 3/2. For a binary combination, even in the case of equipartition ($\alpha = \beta$) as above, the inflection point $\bar{y}$ is a root of a quintic, sextic, and septic, for $r = 1$, 2, 3, respectively.

TWO-QUANTIC

The two-quantic case, $D/D_m = 1/2\{F(y) + F(my)\}$, will be treated first.

If y be our independent variable, proportional to the exposure, the most general form of a binary mixture may be written

$$D = \alpha X(y) + \beta Y\frac{(y)}{m}, \qquad (2)$$

where α, β are constant coefficients and X and Y simple quantic functions of their argument, either of the same or different forms, satisfying

the conditions so that

$$X(0) = Y(0) = 0, \qquad X(\infty) = Y(\infty) = 1, \qquad \alpha + \beta = D_m.$$

The second term in (2) contains m, a constant or parameter which is positive, of course. Without loss to generality, we may forthwith assume

$$m > 1.*$$

The graphical meaning, or interpretation, of the parameter m or of its logarithm is obvious. The characteristic curve $D/\log y$, corresponding to (2), is, manifestly, constructed by adding the ordinates $D_1 = \alpha X(y)$ to the ordinates of the curve $D_2 = \beta Y(y)$ shifted rigidly forward through $\log m$. Such is the case also if the second component is of the same form as the first, when our formula becomes

$$D = \alpha X(y) + \beta X\frac{(y)}{m}. \tag{2a}$$

The resultant is, in this case, the superposition of a curve with the same curve after a rigid shift $\log m$ along the axis of abscissae and a magnification of all its ordinates in the ratio $\beta:\alpha$.

Even without computation one can see that gamma or the maximum slope of the resultant curve, divided by $D_m = \alpha + \beta$, may be made smaller than the relative contrast of either of the two component curves by shifting them apart, that is to say, by choosing high values of the parameter m.

In our practical applications of the quantum theory of exposure the only quantic terms to appear as components of the superposition or "mixture" will be the *one-*, *two-*, and *three*-quantic functions of the exposure corresponding, moreover, to a simple exponential form of the size-frequency distribution. Thus, in our previous notation, X and Y in the general formula (2) will stand for either E or F or G, as defined by Eqs. 0. We shall frequently write $D_1(y)$ for the first and $D_2(y)$ for the second term of (2), so that the resultant density D will be $D_1 + D_2$.

As we saw before, the only symmetrical characteristic curve expressed by a single quantic term is $D = D_m F(y)$, the functions $E(y)$ and $G(y)$ being perceptibly asymmetrical.

To see the effect of superposition on the resulting relative contrast, γ/D_m, it will suffice to consider in some detail the "mixture" or sum of two *two-quantic* terms, that is,

$$D = \alpha F(y) + \beta F\frac{(y)}{m}, \qquad \alpha + \beta = D_m, \qquad m > 1. \tag{3}$$

* For the alternative, $m < 1$, would imply only an interchange of the roles of X and Y as the first and second component.

Although each component curve of this binary mixture is symmetrical, the resultant curve, $D/\log y$, will in general be asymmetrical. In fact, it is not difficult to see that such will always be the case whenever $\alpha \neq \beta$. The resultant curve will be rigorously symmetrical when (and only when)

$$\alpha = \beta = \tfrac{1}{2}D_m,$$

that is,

$$D = \tfrac{1}{2}D_m\left\{F(y) + F\frac{(y)}{m}\right\}. \tag{3a}$$

The center of (rational) symmetry of the corresponding $D/\log y$ curve and, at the same time, its inflection point, will be seen presently to be located at

$$y = \bar{y} = \sqrt{m}.$$

If we denote by y^*, $D = D(y^*)$, the point into which a point y, $D = D(y)$ of the resultant curve is carried by a rigid rotation of the curve through 180° about its center, then $yy^* = \bar{y}^2 = m$ or

$$y^* = \frac{m}{y}.$$

Now, by (3a)

$$D(y^*) = \tfrac{1}{2}D_m\left\{F\frac{(m)}{y} + F\frac{(1)}{y}\right\};$$

hence

$$D(y) + D(y^*) = \tfrac{1}{2}D_m\left\{\left[F(y) + F\frac{(1)}{y}\right] + \left[F\frac{(y)}{m} + \frac{m}{y}\right]\right\}$$
$$= \tfrac{1}{2}D_m\{1 + 1\} = D_m,$$

which proves the symmetry of the resultant curve about $y = \sqrt{m}$ as its center. That this is also its inflection point (one of a possible plurality of such points) will be seen presently.

Returning to the most general superposition, (3), of two two-quantic components, we have the first derivative of D,

$$D'(y) = \alpha F'(y) + \frac{\beta}{m}F'\frac{(y)}{m},$$

and, similarly, the second derivative,

$$D''(y) = \alpha F''(y) + \frac{\beta}{m^2}F''\frac{(y)}{m},$$

whence the equation, $D'(y) + yD''(y) = 0$, of *the inflection point*

$$\alpha F'(y) + \frac{\beta}{m}F'\frac{(y)}{m} + y\left[\alpha F''(y) + \frac{\beta}{m^2}F''\frac{(y)}{m}\right] = 0.$$

Since

$$F(y) = \frac{y^3 + 3y^2}{(1 + y)^3},$$

we have

$$F'(y) = \frac{6y}{(1+y)^4}, \qquad F''(y) = \frac{6(1-3y)}{(1+y)^5},$$

so that the equation expressing the necessary condition for an inflection point of the resultant curve becomes

$$\frac{\alpha}{(1+y)^4} + \frac{\frac{\beta}{m^2}}{\left(\frac{1+y}{m}\right)^4} + \frac{2(1-3y)}{(1+y)^5} + \frac{\frac{\beta(1-3y)}{m}}{m^2\left(\frac{1+y}{m}\right)^5} = 0. \qquad (4)$$

This holds for any binary mixture of two-quantic terms.

It will suffice to analyze this complicated equation for the case of *equipartition*, that is to say, for

$$\alpha = \beta = \tfrac{1}{2}D_m.$$

We then have

$$\frac{1-y}{(1+y)^5} + \frac{m^2(m-y)}{(m+y)^5} = 0, \qquad (4a)$$

a *sextic* equation for y. That one of its roots is $y = \sqrt{m}$, the center of the resultant curve, is readily verified. Another root, negative and thus of no physical interest, is $y = -\sqrt{m}$, as the reader may verify directly.

Such being the case, the polynomial of sixth degree,

$$\phi(y) \equiv (1-y)(m+y)^5 + m^2(m-y)(1+y)^5,$$

should be divisible by $(y-\sqrt{m})(y+\sqrt{m}) = y^2 - m$. And so it is. The quotient, $\phi(y) \div (m-y^2)$, equated to zero gives, after simple reductions, the *quantic* equation

$$\chi(y) \equiv (1+m^2)y^4 - (1-5m-5m^2+m^3)y^3 - 4m(1-5m+m^2)y^2 - m(1-5m-5m^2+m^3)y + m^2(1+m^2) = 0. \qquad (5a)$$

Now, if y is a root of this equation, so must be $y^* = m/y$. Hence, the four roots of this quartic must be of the form

$$y_1, \quad \frac{m}{y_1}, \quad y_2, \quad \frac{m}{y_2}$$

and

$$\chi(y) = (1+m^2)(y-y_1)\frac{y-m}{y_1}(y-y_2)\frac{y-m}{y_2}$$

or, if we put

$$\chi_i = y_i + \frac{m}{y_i}, \qquad i = 1, 2,$$

$\chi(y) = (1+m^2)\{y^4 - (x_1+x_2)y^3 + (2m + x_1x_2)y^2 - m(x_1+x_2)y + m^2\}$. This polynomial, then, must be identical with (5a). In fact, the coefficients of y^3 and of my are here equal, just as in (5a). Comparing the coefficients of y^3 and y^2 in the two forms, we now have

$$x_1 + x_2 = \frac{1 - 5m - 5m^2 + m^3}{1 + m^2} = A, \qquad \text{say}$$

and

$$x_1x_2 = -\frac{2m(3 - 10m + 3m^2)}{1 + m^2} = B, \qquad \text{say}$$

the sum and the product of the unknown x_1 and x_2, whence

$$\begin{aligned} x_1 &\equiv y_1 + \frac{m}{y_1} = \tfrac{1}{2}A + \tfrac{1}{2}\sqrt{A^2 + 4B} \\ x_2 &\equiv y_2 + \frac{m}{y_2} = \tfrac{1}{2}A - \tfrac{1}{2}\sqrt{A^2 + 4B}, \end{aligned} \qquad (6a)$$

a quadratic for y, and another quadratic for y_2. (The two roots of the first quadratic are, of course, y_1 and m/y_1, and similarly for the second quadratic.) Thus the sextic (4a) is completely solved. Its roots are

$$\pm\sqrt{m} \qquad \text{and} \qquad y_1,\ m/y_1,\ y_2,\ m/y_2,$$

the last two pairs being determined by the quadratics (6a), where A and B are known functions of m, the "separation" of the two component curves.

The first of these six roots, $\sqrt{m}$, gives the main, central inflection point; the second, being negative, need not be considered. The remaining two pairs of roots or, at least, one of these pairs may be real and positive if the separation m is large enough.

To form a good idea of these relations, let us consider a few numerical examples.

Let $m = 4$, or $\log m = 0.602$. Then $A = -35/17$, $B = -88/17$.

$$y_1 + \frac{4}{y_1} = \frac{1}{34}\{\sqrt{35^2 - 352.17} - 35\},$$

and

$$y_2 + \frac{4}{y_2} = \frac{1}{34}\{\sqrt{\text{idem}} + 35\}.$$

Both expressions are manifestly complex. Such, therefore, are also the two pairs of roots.

Let $m = 20$ or $\log m = 1.301$. Then

$$A = \frac{5901}{401}, \qquad B = \frac{40120}{401},$$

and $A^2 + 4B$ is again negative, so that both pairs of roots are complex.

Take a much greater separation, $\log m = 2$ or $m = 100$. Then closely enough,

$$A = 95, \qquad B = -290,$$

$$A^2 + 4B = +7864,$$

$$y_1 + \frac{100}{y_1} = 47.5 + 44.35 = 91.85,$$

$$y_2 + \frac{100}{y_2} = 47.5 - 44.35 = 3.15,$$

whence

$$y_1 = 90.89, \qquad y_1^* = 1.10$$

and

$$y_2 = 1.58 + \sqrt{2.50 - 100}, \quad \text{complex.}$$

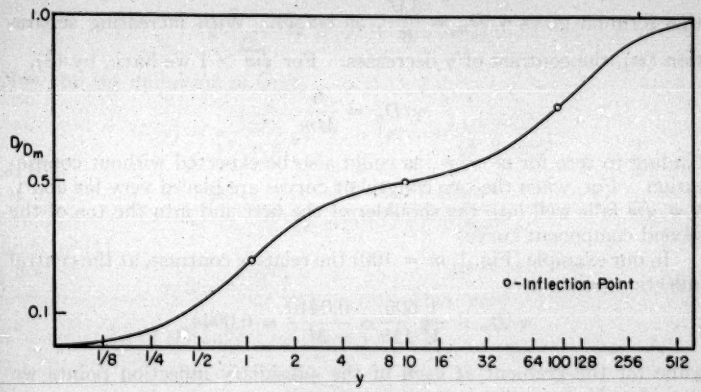

FIG. 1.

Thus, the resultant characteristic curve,

$$D/D_m = \frac{1}{2}\left\{F(y) + F\left(\frac{y}{100}\right)\right\},$$

plotted against $\log y$, has the central inflection point

$$\bar{y} = \sqrt{100} = 10$$

and the pair of inflection points

$$y_1 = 91.85, \qquad y_1^* = \frac{100}{91.85} = 1.09$$

placed symmetrically about the central one ($\log y_1 = 1 + 0.963$, $\log y_1^* = 1 - 0.963$). See Fig. 1.

The gradient, $g(y) = \frac{y}{M} D'(y)$, of the characteristic curve corresponding to the density formula (3*a*), with any value of the parameter m, is, at any point of the curve.

$$\frac{g(y)}{D_m} = \frac{3y^2}{M}\left\{\frac{1}{(1+y)^4} + \frac{m^2}{(m+y)^4}\right\}, \tag{7}$$

and thus, at its central inflection point $\bar{y} = \sqrt{m}$

$$\gamma/D_m = \frac{6m}{M(1+\sqrt{m})^4}. \tag{8}$$

For $m = 1$, when the two component curves coalesce into $D = D_m F(y)$, this formula gives $\gamma/D_m = \frac{3M}{8}$, as before. With increasing separation (m), the contrast of γ decreases. For $\sqrt{m} > 1$ we have, by (8),

$$\gamma/D_m = \frac{6}{Mm},$$

tending to zero for $m \to \infty$, as could also be expected without computation. For, when the two congruent curves are placed very far apart, $\bar{y} = \sqrt{m}$ falls well into the shoulder of the first and into the toe of the second component curve.

In our example (Fig. 1, $m = 100$) the relative contrast, at the central inflection point, is

$$\gamma/D_m = \frac{1}{M}\frac{600}{11^4} = \frac{0.0410}{M} = 0.0944,$$

while for the gradient at each of the subsidiary inflection points we have, by (7),

$$\frac{g(y_1)}{D_m} = \frac{g(y_1^*)}{D_m} = \frac{0.187}{M} = 0.430.$$

The central gamma, $0.0944\, D_m$, is thus about $4\frac{1}{2}$ times smaller than each of these subsidiary maxima of the gradient, which is seen also at a glance from our drawing (Fig. 1).

Such is the case for $m = 100$. For smaller m, the two subsidiary inflection points are closer to the central one and, finally, coalesce with it, three roots of the general sextic becoming equal. For still smaller separations m, the pair of roots become complex, leaving but one real root, $y = \sqrt{m}$, coinciding with the center of symmetry of the resultant curve. Thus, the vigorous determination of $\bar{y}$, for any m, offers no difficulty in the two-quantic case.

This is not the case for $r = 1$ or $r = 3$. The functions of $E(y)$ and

$G(y)$, unlike $F(y)$, are *not* rotationally symmetrical, and thus it is that the corresponding equations, of the fifth and the seventh degree, are not reducible to lower ones, and can, therefore, be solved only approximately by trial and error or by successive approximations for any given m, and thence to determine γ/D_m by (1).

It is the purpose now to deal in such a manner with the outstanding two cases of binary combinations: $r = 1$ and $r = 3$. We shall begin with the latter, which is slightly more complicated than the former.

THREE-QUANTIC

The doubled relative density is

$$2\frac{D(y)}{D_m} = G(y) + G(my),$$

whence

$$2\frac{D'(y)}{D_m} = G'(y) + mG'(my).$$

Now, by the definition of $G(y)$,

$$G'(y) = \frac{12y^2}{(1+y)^5}, \qquad G'(my) = \frac{12m^2y^2}{(1+my)^5},$$

so that

$$\frac{1}{6}\frac{D'(y)}{D_m} = \frac{y^2}{(1+y)^5} + \frac{m^3n^2}{(1+my)^5}$$

and, by (1),

$$\gamma/D_m = \frac{6\bar{y}^3}{M}\left\{\frac{1}{(1+y)^5} + \frac{m^3}{(1+my)^5}\right\}. \tag{9}$$

The equation of the inflection point $y = \bar{y}$ is

$$\frac{d}{dy}(yD') = 0$$

or

$$D'(y) + yD''(y) = 0,$$

where $D'(y)$ is as above. Ultimately, therefore, after removal of a common factor y^2, the question for the inflection point becomes

$$\frac{3-2y}{(1+y)^6} + m^3\frac{3-2my}{(1+my)^6} = 0 \tag{10}$$

which, as announced, is of the *seventh* degree in y. It is even of the sixth degree in m, so that neither y in terms of m nor m in terms of y can be expressed rigorously in a round form.

For $m = 1$ (when the two component curves coalesce into one), the only root of (3) is $y = \bar{y} = 3/2$, as we already know. With decreasing m the two curves are shifted apart and $\bar{y}$ can be expected to increase.

It seems natural, therefore, to develop $\bar{y}$ into a power series of $m - 1$,

$$\bar{y} = \tfrac{3}{2} + y_1'(m-1) + y_1''\frac{(m-1)^2}{2!} + y_1'''\frac{(m-1)^3}{3!} + \cdots,$$

where y_1', y_1'', etc. are the derivatives of y with respect to m, taken for $m = 1$, to be determined by successive differentiations of (3). With the abbreviation $f(y) = (3 - 2y)/(1 + y)^6$, this equation may be written

$$f(y) + m^3 f(my) = 0 \qquad (10a)$$

whence

$$f'(y)y' + 3m^2 f(my) + m^3 f'(my)\cdot(y + my') = 0. \qquad (10')$$

For $m = 1$, $y = 3/2$, $f(3/2) = 0$, $f'(3/2) = -2(2/5)^6 \neq 0$, and we are left with $y_1' + 3/2 + y_1' = 0$, whence $y_1' = -3/4$.

The next derivative equation (already rather unwieldy) is

$$f''(y)y'^2 + f'(y)y'' + 6mf(my) + 6m^2 f'(my)\cdot(y + my') + m^3 f''(my)\cdot(y + my')^2 + m^3 f'(my)\cdot(2my' + my'') = 0,$$

whence for $m = 1$, after simple reductions,

$$y_1'' = -\frac{9}{16}\frac{f''(3/2)}{f'(3/2)} - \frac{3}{2},$$

and since $f'(3/2) = -2(2/5)^6$ and $f''(3/2) = 60(2/5)^8$, we have

$$y_1'' = \frac{9}{16}\cdot\frac{24}{5} - \frac{3}{2} = \frac{6}{5}.$$

So far, then, our expansion is

$$\bar{y} = \frac{3}{2} - \frac{3}{4}(m-1) + \frac{6}{5}\frac{(m-1)^2}{2} + \cdots$$

or

$$\bar{y} = \tfrac{3}{2} + \tfrac{3}{4}(1-m) + \tfrac{3}{5}(1-m)^2 + \cdots.$$

The third derivative of (10) or (10a) consists of 12 terms and will not be rewritten here, and the fourth derivative equation is well-nigh prohibitively complicated. Under these circumstances it has turned out to be more convenient to substitute into the original Eq. 10 the power series

$$y = \tfrac{3}{2} + c_1 x + c_2 x^2 + c_3 x^3 + c_4 x^4 + \cdots, \qquad x = 1 - m,$$

and to determine the c's by comparing the coefficients of equal powers of x. This has given $c_1 = 3/4$, $c_2 = 3/5$, confirming the previous results, and (with considerable labor)

$$c_3 = \frac{3\cdot 7}{5\cdot 8} = \frac{21}{40}, \qquad c_4 = \frac{3^5}{4\times 5^3} = \frac{243}{500}.$$

Thus, up to the fifth power of the fraction $(1 - m)$, we have

$$\bar{y} = \frac{3}{2} + \frac{3}{4}(1 - m) + \frac{3}{5}(1 - m)^2 + \frac{21}{40}(1 - m)^3 + \frac{243}{500}(1 - m)^4 + \cdots. \quad (11)$$

To guess from $\frac{3}{5}, \frac{3 \cdot 7}{5 \cdot 8}, \frac{3 \cdot 81}{5 \cdot 100}$ at the structure of c_5, c_6, and so on, would be a hopeless task. But if the coefficients are written in decimal form,

$$0.750, \quad 0.600, \quad 0.525, \quad 0.486,$$

we see that their differences,

$$0.150, \quad 0.075, \quad 0.039,$$

decrease regularly, almost geometrically, as if tending to a limit not much lower than 1/2. Tentatively, we may take, as a possible approximation,

$$\bar{y} \doteqdot \tfrac{3}{2} + \tfrac{3}{4}(1 - m) + \tfrac{3}{8}(1 - m^2) + \tfrac{1}{2}\{(1 - m)^3 + (1 - m)^4 + \cdots\}$$

or, since the bracketed series amounts to $\frac{(1 - m)^3}{1 - (1 - m)} = \frac{(1 - m)^3}{m}$,

$$\bar{y} \doteqdot \tfrac{3}{2} + \tfrac{3}{4}(1 - m) + \tfrac{3}{8}(1 - m)^2 + \frac{(1 - m)^3}{2m}. \quad (11a)$$

This formula turns out to give close approximations even for m-values considerably smaller than one. Thus, for example, for $m = 1/2$, $\bar{y} = 2.15$ and $m\bar{y} = 1.075$. The rigorous equation is

$$\frac{-m^3 f(my)}{f(y)} = 1.$$

Now, to five figures,

$$-\frac{1}{8}\frac{f(1.075)}{f(2.15)} = \frac{1.3295}{1.3306} \doteqdot 0.9992.$$

For $m = 1/4$, (11a) gives $\bar{y} = 3.244$, $m\bar{y} = 0.811$, and the said quotient approaches unity almost as closely. In fine, the formula (11a) holds very accurately from $m = 1$ down to $m = 1/4$, at least. For $m = 1/5$ it gives $\bar{y} = 3.764$ and $\frac{-m^3 f(my)}{f(y)} = 1.066$, not close enough to unity. The application of formula (11a) can thus be extended a little, but not much, below $m = 1/4$.

For smaller m (or greater separations of the two component curves) we have to solve the equation $f(y) + m^3 f(my) = 0$, approximately by "trial and error."

Let us rewrite it, conveniently,

$$\phi(y) \equiv \frac{-m^3 f(my)}{f(y)} = 1,$$

and consider the case of $m = 1/8$, when

$$\phi(y) = \frac{1}{512} \cdot \frac{f\frac{(y)}{8}}{f(y)}.$$

Now, recalling the meaning of $f(y)$, we find

$$\phi(4) = 1.072 \quad \text{and} \quad \phi(3.5) = 0.976,$$

whence we see that $3.5 < \bar{y} < 4.0$. Next $\phi(3.8) = 1.032_8$, so that the range is narrowed down to $3.5 < \bar{y} < 3.8$. This suggests the mean value,

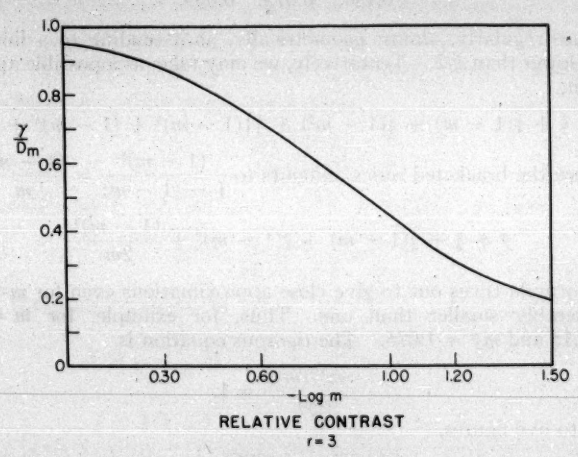

FIG. 2.

3.65, which gives $\phi(3.65) = 1.004_6$, close enough to one. Thus we have

$$\bar{y} = 3.65 \quad \text{or} \quad m = 1/8.$$

In much the same way we find, for $m = 1/4$, $\bar{y} = 3.30_8$ which shows a slight correction to the previous approximation, for $m = 1/16$, $\bar{y} = 5.81$, and a few more values of $\bar{y}$ which may be of practical interest. All these $\bar{y}$-values, together with those of the corresponding relative contrast, which is easily determined by formula (9), are collected in the following table:

$m =$	1	1/2	1/4	1/8	1/10	1/16	1/20	1/32
$\bar{y} =$	1.50	2.15	3.30_8	3.65	4.33	5.81	6.60	8.63
$\gamma/D_m =$	0.955	0.888	0.721	0.522	0.448	0.297	0.260	0.189.

These values of the relative contrast are represented graphically in Fig. 2 with $-\log m$ as abscissa (which is the separation of the two component curves along the $\log E$ axis). From the smooth curve of this figure the "separation" corresponding to any given (observed) relative contrast, between 0.96 and 0.19, can be read off with sufficient accuracy.

We may mention that the curve $\bar{y}/\log m$ has a peculiar saddle-shaped portion around an m-value for which $y' = dy/dm$ vanishes. This particular "separation," at which $\bar{y}$ becomes stationary and beyond which it continues to increase, is determined by Eq. 10′ with $y' = 0$, that is to say, by

$$3f(x) + xf'(x) = 0, \qquad \text{where } x = my.$$

Now,

$$f(x) = \frac{3 - 2x}{(1 + x)^6}, \qquad f'(x) = \frac{10(x - 2)}{(1 + x)^7},$$

so that the equation becomes

$$3(3 - 2x)(1 + x) + 10x(x - 2) = 0$$

or

$$x^2 - \frac{17x}{4} + \frac{9}{4} = 0,$$

a quadratic for $x = my$. Its two roots are

$$x = \tfrac{1}{8}\{17 \pm \sqrt{145}\} = 0.619_4 \text{ and } 3.63.$$

The second root, which gives a negative $f(x)$ and thus cannot satisfy the original septic, is ruled out, and the first root corresponds to the saddle or stationary point shown by our drawing at about $m = \dfrac{1}{4\sqrt{2}}$, where $\bar{y} = 3.5$. In fact, $\dfrac{3.5}{4\sqrt{2}} = 0.619$, close enough to that root.

ONE-QUANTIC

From

$$\frac{D(y)}{D_m} = \tfrac{1}{2}\{E(y) + E(my)\}$$

follows

$$\frac{2D'(y)}{D_m} = E'(y) + mE'(my).$$

Now,

$$E(y) = 1 - \frac{1}{(1 + y)^2}, \qquad E'(y) = \frac{2}{(1 + y)^3},$$

so that

$$\frac{D'(y)}{D_m} = \frac{1}{(1 + y)^3} + \frac{m}{(1 + my)^3},$$

and, by (8),

$$\gamma/D_m = \frac{\bar{y}}{M}\left\{\frac{1}{(1+\bar{y})^3} + \frac{m}{(1+m\bar{y})^3}\right\}. \qquad (12)$$

The equation for the inflection point $y = \bar{y}$ is

$$D'(y) + yD''(y) = 0,$$

and therefore, after simple reductions,

$$f(y) + mf(my) \equiv \frac{1-2y}{(1+y)^4} + m\,\frac{1-2my}{(1+my)^4} = 0, \qquad (13)$$

a quintic for y in terms of m.

For $m = 1$ (no separation) the inflection point is placed at $y = 1/2$. With decreasing m, $\bar{y}$ can be expected, initially at least, to increase. For small values of $(1 - m)$, the inflection exposure can be developed into a power series of $(1 - m)$, as in the preceding case. The derivative of the function $f(y) = \dfrac{1-2y}{(1+y)^4}$ with respect to its argument is

$$f'(y) = \frac{6(y-1)}{(1+y)^5}.$$

For the derivative $y' = dy/dm$ we have, by Eq. 13,

$$f'(y)y' + f(my) + mf'(my)\cdot(y + my') = 0,$$

that is,

$$6\left\{\frac{y-1}{(1+y)^5} + \frac{m^2(my-1)}{(1+my)^5}\right\}y' + \frac{1-7my+4m^2y^2}{(1+my)^5} = 0. \qquad (14)$$

Whence, for $m = 1$ (and $y = 1/2$), $y' = -1/4$, so that, for small $(1 - m)$,

$$\bar{y} = \tfrac{1}{2} - \tfrac{1}{4}(m-1) \quad \text{or} \quad \bar{y} = \tfrac{1}{2} + \tfrac{1}{4}(1-m). \qquad (15a)$$

With decreasing m (increasing separation of the two component curves) $\bar{y}$ increases, initially, as expected. Unlike the three-quantic case, however, $\bar{y}$ increases now only up to a certain maximum, of a moderate value, and then decreases steadily, so tending towards its original value 1/2. Let us determine this maximum or the extreme position of the inflection point under discussion.[3] Its first, necessary, condition is the vanishing of the derivative y'. Now, by (14), we have $y' = 0$ when

$$m^2y^2 - \tfrac{7}{4}my + \tfrac{1}{4} = 0,$$

[3] For small m (large separation) there is a second inflection point, distant from that discussed above (and of no practical interest). Its position is determined approximately by $m\bar{y} = 1/2$; thus, for example, for $m = 1/64$, $\bar{y} = 32$, where the first component $E(y)$ has nearly reached its limiting value 1.

a quadratic for $x \equiv my$. Its two roots are

$$x = \tfrac{1}{8}\{7 \pm \sqrt{33}\}$$

or

$$x \equiv my = 1.593 \text{ and } 0.157.$$

The larger root is ruled out, since it would give, by (13), $yfy = -xf(x) > 0$ and thus $f(y)$ positive, implying $y < \frac{1}{2}$. We are thus left with the smaller root,

$$x = 0.157,$$

which, by (13), gives for the unknown y:

$$\phi(y) \equiv yf(y) = -0.0601,$$

that is, $\dfrac{y(2y-1)}{(1+y)^4} = 0.0601$. Now, $\phi(1) = -0.0625$ and $\phi(0.95) = -0.0591_4$, so that y is contained between 0.95 and 1.00. After two

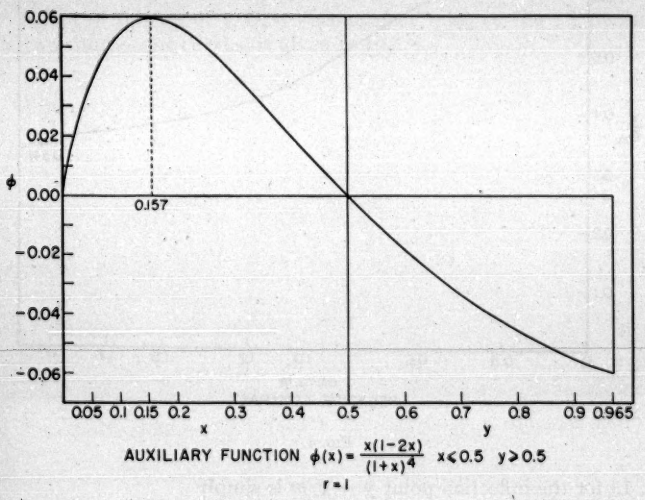

FIG. 3.

more trials we find $\phi(0.965) = -0.0601_7$ which is close enough for the required value. Thus, y' vanishes at $y = 0.965$, and since $x = my = 0.157$, this inflection exposure corresponds to $m = 0.163$. By Eq. 14, moreover, we find that the second derivative, at this y-value and $y' = 0$, is negative, namely, $y'' = -48.9$. Thus, $y = 0.965$ is a genuine *maximum*. With a further decrease of m, below 0.163, the inflection point moves backwards, towards its original position $\bar{y} = 1/2$. The

only interval of practical interest is, then, $y = 0.50$ to 0.965, covered and recovered, and it remains to determine within it a number of pairs of corresponding values m, $\bar{y}$, keeping in mind that to each $\bar{y}$ belong two different m's and thus two different values of the relative contrast γ/D_m of the resultant curve. The following graphical method is most convenient for picking out such pairs of corresponding values with sufficient accuracy:

A graph of the function

$$\phi x = \frac{x(1-2x)}{(1+x)^4},$$

on a sufficiently large scale, is given in Fig. 3. In terms of this function,

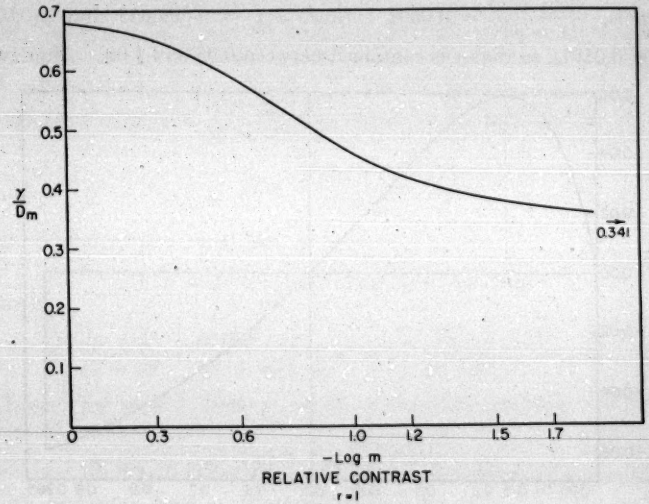

FIG. 4.

Eq. 13 for the inflection point $y = x/m$ is simply

$$\phi(x) + \phi(y) = 0. \qquad (13')$$

Thence, to solve our problem, for any y chosen between 0.5 and 0.965, it is enough to read off the graph the negative ordinate $\phi(y)$ and to read, below 0.5, the two abscissae x of the equal positive ordinates $\phi(x)$. The quotient x/y will then give the required m-values. Thus, for example, for $y = 0.8$ we have $\phi = -0.046$ and $\phi(x) = 0.046$ is attained at $x = 0.074_5$ and $x = 0.275_5$, whence $m = 0.093$ and 0.345. (To $y = 0.965$ corresponds, of course, the *single* ordinate $\phi(x) = 0.0601$,

the maximum of $\phi(x)$, placed at $x = 0.157$, and thus, $m = 0.163$.) In this manner, and with some slight computational retouching, the following table of values, with the corresponding contrasts γ/D_m found directly by (12), has been constructed:

m =	1.000	0.831	0.688	0.564	0.486	0.407	0.350
$\bar{y}$ =	0.500	0.550	0.600	0.650	0.700	0.750	0.800
γ/D_m =	0.682	0.681	0.675	0.658	0.654	0.639	0.623
m =	0.294	0.244	0.184	0.163	0.158	0.117	0.100
$\bar{y}$ =	0.850	0.900	0.950	0.965 (max.)	0.950	0.900	0.850
γ/D_m =	0.604	0.580	0.544	0.527	0.522	0.481	0.462
m =	0.088	0.076	0.061	0.046_2	0.033_3	0.018	0.000
$\bar{y}$ =	0.800	0.750	0.700	0.650	0.600	0.550	0.500
γ/D_m =	0.448	0.433	0.414	0.396	0.381	0.363	0.341

A plot of this set of γ/D_m-values against $-\log m$, the separation of the two component curves, is given in Fig. 4.

Research on Sesame.—Extensive basic and technological data on sesame seed and oil have been reported in ten technical articles since January 1950 by chemists of the Department of Agriculture. This information will be of value to oilseed processors in the Cotton Belt in the event the crop is grown on a large scale as a supplement or alternate raw material for cottonseed.

The data are the result of investigations at the Southern Regional Research Laboratory in New Orleans, Louisiana. The work was part of a broad program of research being conducted by Department agencies and State Agricultural Experiment Stations to develop varieties of sesame better suited to American farming, and to obtain increased knowledge of the chemical composition and characteristics of the seed.

Sesame seed and oil are well-known commodities in international trade and quantities of both are imported into this country. But the seed has not been produced extensively here, mainly because of harvesting difficulties, some of which are being met through the development of nonshattering varieties. Under good cultural practices the crop yields 800 pounds or more of seed per acre and more oil per acre than any other annual oilseed crop—per 100 pounds of seed 47 pounds of an edible oil equal or superior in quality to cottonseed and peanut oils.

Besides being rich in oil, sesame seed yields a meal which is a nutritious stockfeed, containing 45–55 per cent of high quality protein. Also, the seed has superior qualities from the standpoint of the processor—it requires no preparation other than cleaning before milling and it is easily processed in conventional oil milling equipment.

In Southern Laboratory research, oil was recovered from 4 varieties of seed by batch solvent extraction; physical and chemical analyses were made; and each oil was evaluated for use as a salad and cooking oil and for the production of shortening. The crude oil was low in free fatty acids; very light in color; had low refining losses; and bleached well. Hardened to shortening consistency the product showed great stability toward oxidative rancidity. This superior stability was shown to be due to sesamol, a unique component of the seed. A method for determining the free and bound sesamol was developed. Also worked out was a method of determining the amount of sesamin, another unique minor component of sesame oil.

The processing and utilization research on sesame oil at the Southern Regional Research Laboratory is the first systematic chemical investigation of the oil to be recorded. The publications on the work have aroused the interest of vegetable-oil manufacturing firms in almost every part of the world. The series of articles represents more than one-tenth of the technical literature in English on sesame oil.

Reprints of the articles may be obtained by writing the Southern Regional Research Laboratory, 2100 Robert E. Lee Boulevard, New Orleans 19, Louisiana. The publications are entitled: Sesame Oil. I–VII: Properties of a Solvent-Extracted Sesame Oil; Some Chemical and Physical Properties of the Oils from Different Varieties of Sesame Seed; Antioxidant Properties of Sesamol; Determination of Free and Bound Sesamol; The Stability of Sesame Oil; Determination of Sesamin; Optical Rotation; and the Minor Components of Sesame Oil. The Chemical and Physiological Properties of Sesame Oil. Some Physical and Chemical Properties of Sesame Protein. Sesame—A New Oilseed Crop for the South.

CYLINDRICAL AND ROTATIONAL COORDINATE SYSTEMS

BY

PARRY MOON[1] AND DOMINA EBERLE SPENCER[2]

Conformal transformation of the complex plane has been employed in potential theory since the time of Cauchy and Riemann. A rectangular map of uniformly spaced lines in the w-plane may be regarded as the representation of a uniform field, with equipotentials as one family of lines and flow lines as the orthogonal family. A functional transformation yields a z-plane map, which is conformal to the original map and which again (1)[3] represents a solution of Laplace's equation.

Note, however, that this well-known method gives a solution of Laplace's equation only for a plane distribution or for a cylindrical distribution where the potential is independent of the distance along the generators of the cylinders. It does not even apply in the symmetrical rotational case, though it is often assumed to be an approximation in this case. Moreover, it gives the solution only for the Dirichlet problem with constant potentials on the boundaries, and is not directly applicable to arbitrary potential distributions, to Neumann problems, or to mixed boundary conditions.

These limitations are removed to a great extent if one regards the z-plane map as a *new coordinate system*. This plane system is made into a cylindrical or a rotational system by translation or rotation. Solutions of the Laplace, Helmholtz, wave, and diffusion equations are then obtained for any boundary conditions if the coordinate system allows separation of variables. The idea is an obvious one but it seems never to have been properly exploited. The present paper outlines this method of finding new coordinate systems and indicates how it can be employed in solving field problems.

1. PROCEDURE

Let

$$w = u + iv,$$
$$z = x + iy,$$

and transform the families of lines (u = const and v = const) by means of the arbitrary relation,

$$z = \mathfrak{F}(w), \tag{1}$$

where $\mathfrak{F}$ is any analytic function. It may be chosen at random or it may be made to fit a particular shape of boundary by use of the Schwarz-

[1] Massachusetts Institute of Technology, Cambridge, Mass.

[2] University of Connecticut, Storrs, Conn.

[3] The boldface numbers in parentheses refer to the references appended to this paper.

Christoffel method (2). The Cauchy-Riemann equations apply:

$$\frac{\partial x}{\partial u} = \frac{\partial y}{\partial v}, \qquad \frac{\partial x}{\partial v} = -\frac{\partial y}{\partial u},$$

so angles are preserved by the transformation, and squares in the w-plane always map into curvilinear squares in the z-plane.

Separation of Eq. 1 into real and imaginary parts gives two equations,

$$\begin{cases} x = \xi_1(u, v), \\ y = \xi_2(u, v). \end{cases} \tag{2}$$

These equations can be used in plotting the two families of curves, u = const and v = const, which form the orthogonal map in the z-plane.

We now generate coordinate systems in 3-space. *Cylindrical* systems are formed by translating the z-plane map perpendicular to itself, the resulting coordinate system (u^1, u^2, u^3) being specified by

$$\begin{cases} x = \xi_1(u^1, u^2), \\ y = \xi_2(u^1, u^2), \\ z = u^3, \end{cases} \tag{3}$$

where ξ_1 and ξ_2 are the functions of Eq. 2. If the plane map is rotated about what was originally the y-axis, we obtain the *rotational coordinate system* (u^1, u^2, ψ),

$$\begin{cases} x = \xi_1(u^1, u^2) \cdot \cos \psi, \\ y = \xi_1(u^1, u^2) \cdot \sin \psi, \\ z = \xi_2(u^1, u^2). \end{cases} \tag{4}$$

If rotation is about what was originally the x-axis,

$$\begin{cases} x = \xi_2(u^1, u^2) \cdot \cos \psi, \\ y = \xi_2(u^1, u^2) \cdot \sin \psi, \\ z = \xi_1(u^1, u^2). \end{cases} \tag{5}$$

In either case, the rotational axis in 3-space is called the z-axis.

Metric coefficients for any of the three-dimensional coordinate systems are obtained by employing the usual equation,

$$g_{ii} = \left(\frac{\partial x}{\partial u^i}\right)^2 + \left(\frac{\partial y}{\partial u^i}\right)^2 + \left(\frac{\partial z}{\partial u^i}\right)^2, \quad (i = 1, 2, 3). \tag{6}$$

For a cylindrical system, Eq. 3, the application of Eq. 6 gives the very simple result:

$$g_{11} = g_{22} = \left(\frac{\partial \xi_1}{\partial u^1}\right)^2 + \left(\frac{\partial \xi_2}{\partial u^1}\right)^2, \quad g_{33} = 1. \tag{7}$$

For the rotational system of Eq. 4,

$$g_{11} = g_{22} = \left(\frac{\partial \xi_1}{\partial u^1}\right)^2 + \left(\frac{\partial \xi_2}{\partial u^1}\right)^2, \quad g_{33} = [\xi_1(u^1, u^2)]^2; \tag{8}$$

and with the rotational system of Eq. 5,

$$g_{11} = g_{22} = \left(\frac{\partial \xi_1}{\partial u^1}\right)^2 + \left(\frac{\partial \xi_2}{\partial u^1}\right)^2, \quad g_{33} = [\xi_2(u^1, u^2)]^2. \tag{9}$$

Note that g_{11} and g_{22} are always the same, for a given function $\mathfrak{F}$, and are what would be obtained directly from the plane map by application of Eq. 6.

Knowing the metric coefficients, one can apply all the usual equations of curvilinear coordinates. An infinitesimal distance is obtained from

$$(ds)^2 = g_{11}(du^1)^2 + g_{22}(du^2)^2 + g_{33}(du^3)^2.$$

An infinitesimal volume is

$$d\mathcal{V} = \sqrt{g_{11}g_{22}g_{33}}\, du^1du^2du^3 = \sqrt{g}\, du^1du^2du^3.$$

The gradient is

$$\nabla\varphi = \frac{\mathbf{a}_1}{\sqrt{g_{11}}}\frac{\partial\varphi}{\partial u^1} + \frac{\mathbf{a}_2}{\sqrt{g_{22}}}\frac{\partial\varphi}{\partial u^2} + \frac{\mathbf{a}_3}{\sqrt{g_{33}}}\frac{\partial\varphi}{\partial u^3}.$$

The Laplacian is

$$\nabla^2\varphi = \frac{1}{\sqrt{g}}\sum_{i=1}^{3}\frac{\partial}{\partial u^i}\left(\frac{\sqrt{g}}{g_{ii}}\frac{\partial\varphi}{\partial u^i}\right). \tag{10}$$

Thus the Helmholtz equation may be expressed in any of our coordinate systems as

$$\frac{1}{\sqrt{g}}\sum_{i=1}^{3}\frac{\partial}{\partial u^i}\left(\frac{\sqrt{g}}{g_{ii}}\frac{\partial\varphi}{\partial u^i}\right) + (k)^2\varphi = 0, \tag{11}$$

and Laplace's equation results if $k = 0$. If the equation is simply separable, solutions are

$$\varphi = U^1(u^1)\cdot U^2(u^2)\cdot U^3(u^3)$$

and the separated equations corresponding to Eq. 11 can be written immediately (3):

$$\frac{1}{f_i}\frac{d}{du^i}\left(f_i\frac{dU^i}{du^i}\right) + U^i\sum_{j=1}^{3}\alpha_j\Phi_{ij} = 0, \tag{12}$$

where α_j are separation constants, Φ_{ij} are elements of the Stäckel matrix $[S]$, and f_i are obtained from the relation,

$$\frac{\sqrt{g}}{S} = f_1(u^1)\cdot f_2(u^2)\cdot f_3(u^3).$$

If the Laplace equation is R-separable,

$$\varphi = \frac{U^1(u^1)\cdot U^2(u^2)\cdot U^3(u^3)}{R(u^1, u^2, u^3)},$$

and the separated equations are still given by Eq. 12. Separability conditions are discussed in previous papers (3, 4).

2. TRANSFORMATIONS

As an example, take the transformation

$$\bar{z} = c \operatorname{sech} w, \tag{1a}$$

where for convenience the complex conjugate $\bar{z}$ has been used instead of z. Then

$$\begin{aligned} x - iy &= \frac{c}{\cosh u \cos v + i \sinh u \sin v} \\ &= \frac{c[\cosh u \cos v - i \sinh u \sin v]}{\cosh^2 u \cos^2 v + \sinh^2 u \sin^2 v}. \end{aligned}$$

Thus Eq. 2 becomes

$$\begin{cases} x = \dfrac{c \cosh u \cos v}{\cosh^2 u - \sin^2 v}, \\ y = \dfrac{c \sinh u \sin v}{\cosh^2 u - \sin^2 v}. \end{cases} \tag{2a}$$

The appearance of the lines, u = const and v = const, is shown in Fig. 8.

The metric coefficients are obtained from the equation,

$$g_{11} = g_{22} = \left(\frac{\partial x}{\partial u}\right)^2 + \left(\frac{\partial x}{\partial v}\right)^2. \tag{6a}$$

From Eq. 2a,

$$\begin{aligned} \frac{\partial x}{\partial u} &= -\frac{c \sinh u \cos v}{[\cosh^2 u - \sin^2 v]^2}(\cosh^2 u + \sin^2 v), \\ \frac{\partial x}{\partial v} &= -\frac{c \cosh u \sin v}{[\cosh^2 u - \sin^2 v]^2}(\sinh^2 u - \cos^2 v), \end{aligned}$$

and therefore,

$$\begin{aligned} g_{11} = g_{22} &= \frac{c^2}{[\cosh^2 u - \sin^2 v]^4}\{\sinh^2 u \cos^2 v(\cosh^2 u + \sin^2 v)^2 \\ &\qquad + \cosh^2 u \sin^2 v(\sinh^2 u - \cos^2 v)^2\} \\ &= \frac{c^2(\cosh^2 u - \cos^2 v)}{[\cosh^2 u - \sin^2 v]^2}. \end{aligned}$$

TABLE I.—*Transformations.*

No.	Transformation	Coordinate Lines	Inversion of	x	y	g_{11}
1	$\bar{z} = 1/w$	Tangent circles	Rectangular coordinates	$\frac{u}{u^2+v^2}$	$\frac{v}{u^2+v^2}$	$\frac{1}{(u^2+v^2)^2}$
2	$z = \frac{w^2}{2}$	Parabolas	No. 3	$\frac{1}{2}(u^2-v^2)$	uv	u^2+v^2
3	$\bar{z} = \frac{1}{2}w^{-2}$	Cardioids	No. 2	$\frac{1}{2}\frac{u^2-v^2}{(u^2+v^2)^2}$	$\frac{uv}{(u^2+v^2)^2}$	$\frac{1}{(u^2+v^2)^2}$
4	$z = \sqrt{2}w^{\frac{1}{2}}$	Hyperbolas	4-leaf roses	$\frac{\sqrt{\rho+u}}{\text{where } \rho = +\sqrt{u^2+v^2}}$	$\sqrt{\rho-u}$	$\frac{1}{2\sqrt{u^2+v^2}}$
5	$z = e^w$	Circles and radial lines	No. 5	$e^u \cos v$	$e^u \sin v$	e^{2u}
6	$\bar{z} = \frac{c(e^w+1)}{e^w-1}$	Bipolar circles	No. 5	$\frac{c \sinh u}{\cosh u - \cos v}$	$\frac{c \sin v}{\cosh u - \cos v}$	$\frac{c^2}{(\cosh u - \cos v)^2}$
7	$z = c \cosh w$	Ellipses and hyperbolas	No. 8	$c \cosh u \cos v$	$c \sinh u \sin v$	$c^2(\cosh^2 u - \cos^2 v)$
8	$\bar{z} = c \operatorname{sech} w$		No. 7	$\frac{c \cosh u \cos v}{\cosh^2 u - \sin^2 v}$	$\frac{c \sinh u \sin v}{\cosh^2 u - \sin^2 v}$	$\frac{c^2(\cosh^2 u - \cos^2 v)}{(\cosh^2 u - \sin^2 v)^2}$
9	$z = c \operatorname{sn} w$			$\frac{c}{\Lambda}\operatorname{sn}(u,k)\cdot\operatorname{dn}(v,k')$	$\frac{c}{\Lambda}\operatorname{cn}(u,k)\cdot\operatorname{dn}(u,k)\cdot\operatorname{sn}(v,k')\cdot\operatorname{cn}(v,k')$	$\frac{c^2}{\Lambda^2}(1-\operatorname{sn}^2 u\,\operatorname{dn}^2 v)(\operatorname{dn}^2 v - k^2\operatorname{sn}^2 u)$
10	$z = c \operatorname{cn} w$			$\frac{c}{\Lambda}\operatorname{cn}(u,k)\cdot\operatorname{cn}(v,k')$ $\text{where } \Lambda = 1-\operatorname{dn}^2 u \operatorname{sn}^2 v$	$\frac{c}{\Lambda}\operatorname{sn}(u,k)\cdot\operatorname{dn}(u,k)\cdot\operatorname{sn}(v,k')\cdot\operatorname{dn}(v,k')$	$\frac{c^2}{\Lambda^2}(\operatorname{sn}^2 v + \operatorname{sn}^2 u \operatorname{cn}^2 v)(\operatorname{dn}^2 v - k^2\operatorname{sn}^2 u)$

These metric coefficients apply to both cylindrical and rotational coordinate systems obtained from this transformation.

There is no limit to the number of transformations, Eq. 1, nor to the number of coordinate systems obtained from them. To conserve

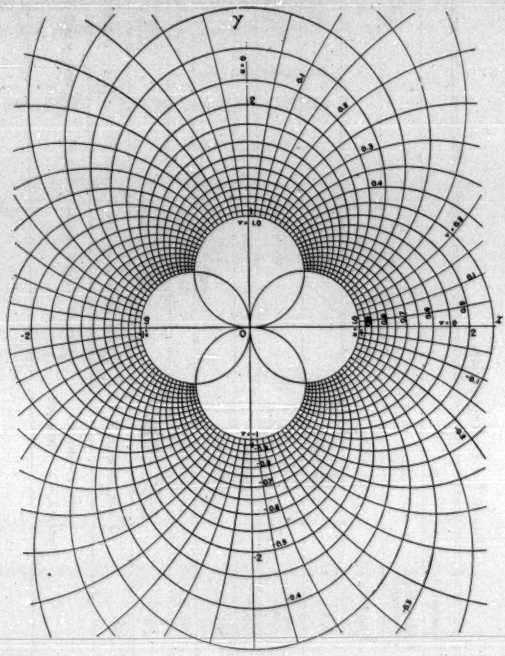

FIG. 1.

space, however, we have limited ourselves in this paper to ten transformations, which are listed in Table I. Corresponding maps are exhibited in Figs. 1 to 10, inclusive.

3. CYLINDRICAL SYSTEMS

The ten transformations of Table I give the ten cylindrical coordinate systems of Table II. To emphasize the fact that the lines of the plane map have become surfaces in 3-space, the u and v of Table I have been replaced by new symbols. The coordinate surfaces are the cylinders $u^1 = \text{const}$ and $u^2 = \text{const}$, plus the family of parallel planes $z = \text{const}$. Cross-sections through the cylinders are given by Figs. 1 to 10.

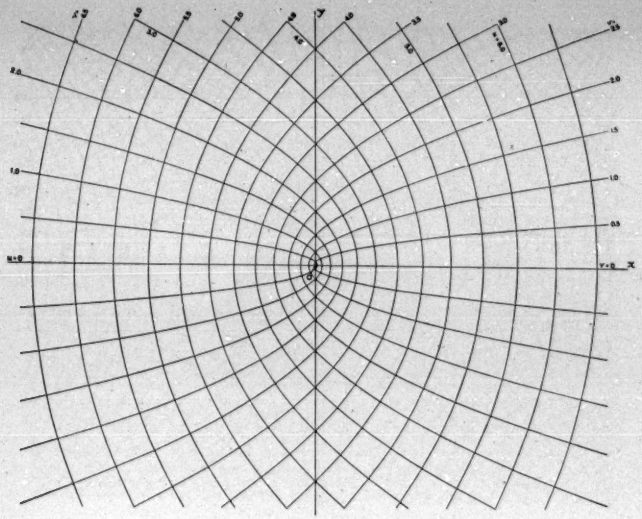

FIG. 2.

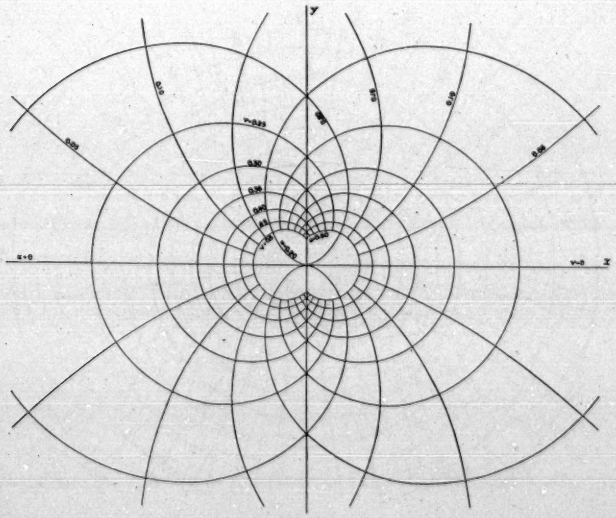

FIG. 3.

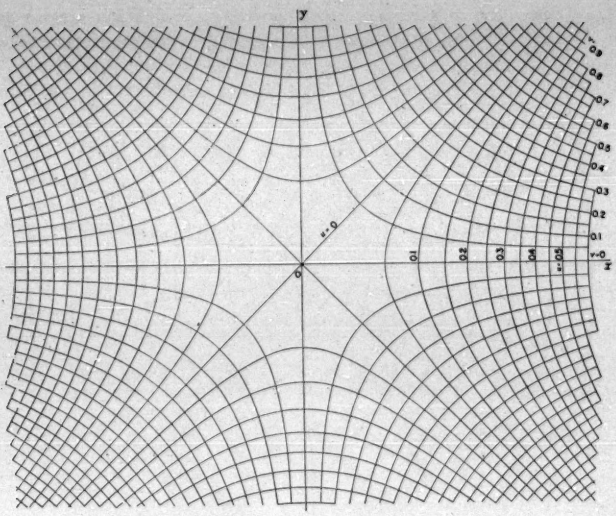

FIG. 4.

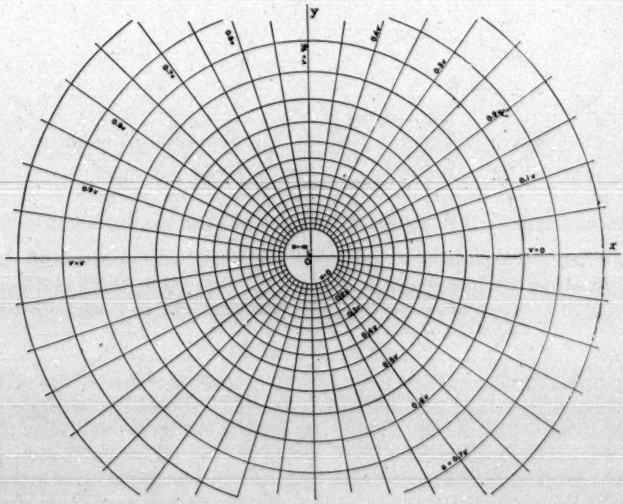

FIG. 5.

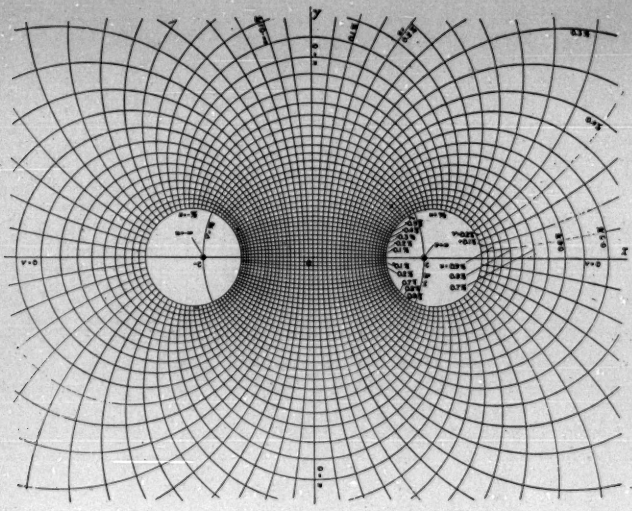

FIG. 6.

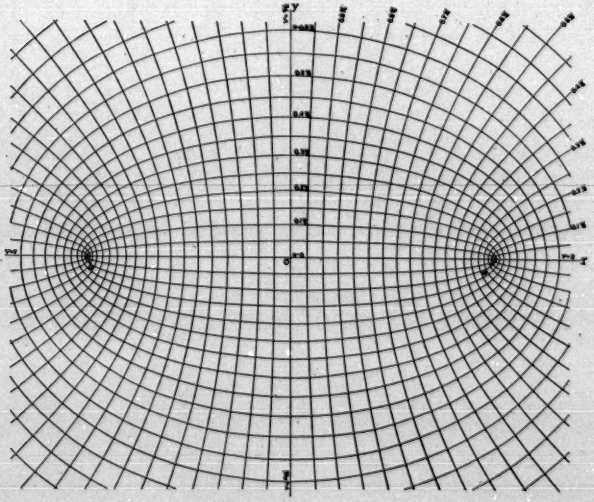

FIG. 7.

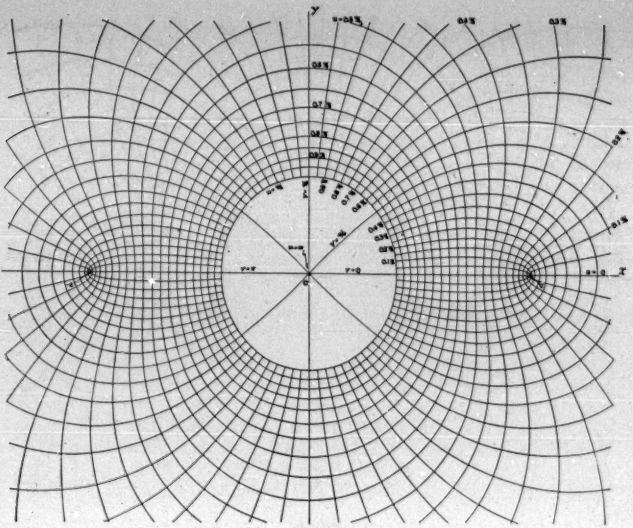

FIG. 8.

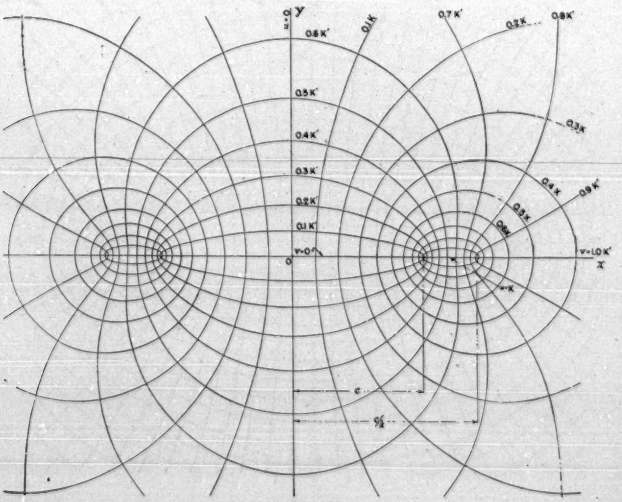

FIG. 9.

The previous criteria (3, 4) for separability have been applied to indicate whether separation is possible in three dimensions,

$$\varphi = \varphi(u^1, u^2, u^3)$$

or in two dimensions,

$$\varphi = \varphi(u^1, u^2).$$

Table II also shows in what coordinate systems a one-dimensional solution is possible:

$$\varphi = \varphi(u^1).$$

Of the 10 cylindrical systems, we note that the Helmholtz equation separates in only 3. The same is true of the Laplace equation with

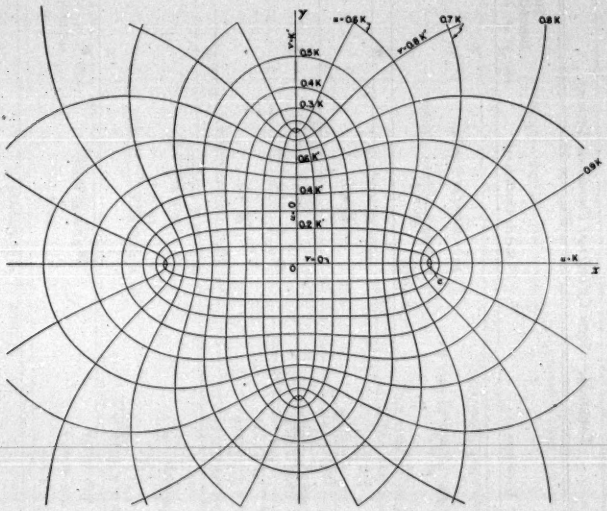

FIG. 10.

$\varphi = \varphi(u^1, u^2, u^3)$. But, as shown in another paper (4), *Laplace's equation separates in every cylindrical coordinate system* obtained from Eq. 1, if $\varphi = \varphi(u^1, u^2)$. An infinite number of cylindrical coordinate systems are therefore possible; in all of which Laplace's equation separates. There is no question of R-separability in Table II, since only simple separability occurs in cylindrical coordinates (3).

4. ROTATIONAL SYSTEMS

We now consider the coordinate systems obtained by rotating the plane maps (Figs. 1 to 10) about an axis. The axis of rotation is called

TABLE II.—*Some Cylindrical Coordinate Systems.*

No.	Name of Coordinate System	Fig. No.	Equations	Metric Coefficients	Simple Separability: Helmholtz $\phi(u^1, u^2, u^3)$	Simple Separability: Helmholtz $\phi(u^1, u^2)$	Simple Separability: Laplace $\phi(u^1, u^2, u^3)$	Simple Separability: Laplace $\phi(u^1, u^2)$	One-dimensional Solution: Helm.	One-dimensional Solution: Lap.
1	Tangent cylinder	1	$x = \frac{\mu}{\mu^2 + \nu^2}$, $y = \frac{\nu}{\mu^2 + \nu^2}$, $z = z$.	$g_{11} = g_{22} = (\mu^2 + \nu^2)^{-2}$, $g_{33} = 1$.	×	×	×	●	×	●
2	Parabolic cylinder	2	$x = \frac{1}{2}(\mu^2 - \nu^2)$, $y = \mu\nu$, $z = z$.	$g_{11} = g_{22} = \mu^2 + \nu^2$, $g_{33} = 1$.	●	●	●	●	×	●
3	Cardioid cylinder	3	$x = \frac{1}{2}\frac{\mu^2 - \nu^2}{(\mu^2 + \nu^2)^2}$, $y = \frac{\mu\nu}{(\mu^2 + \nu^2)^2}$, $z = z$.	$g_{11} = g_{22} = (\mu^2 + \nu^2)^{-2}$, $g_{33} = 1$.	×	×	×	●	×	●
4	Hyperbolic cylinder	4	$x = \sqrt{\rho + \mu}$, $y = \sqrt{\rho - \mu}$, $z = z$, where $\rho = +\sqrt{\mu^2 + \nu^2}$.	$g_{11} = g_{22} = \frac{1}{2\sqrt{\mu^2 + \nu^2}}$, $g_{33} = 1$.	×	×	×	●	×	●
5	Circular cylinder	5	$x = e^{\eta}\cos\psi$, $y = e^{\eta}\sin\psi$, $z = z$.	$g_{11} = g_{22} = e^{2\eta}$, $g_{33} = 1$.	●	●	●	●	●	●

TABLE II.—*Continued.*

No.	Name of Coordinate System	Fig. No.	Equations	Metric Coefficients	Simple Separability: Helmholtz $\phi(u^1, u^2, u^3)$	Simple Separability: Helmholtz $\phi(u^1, u^2)$	Simple Separability: Laplace $\phi(u^1, u^2, u^3)$	Simple Separability: Laplace $\phi(u^1, u^2)$	One-dimensional Solution: Helm.	One-dimensional Solution: Lap.
6	Bipolar cylinder	6	$x = \frac{c \sinh \eta}{\cosh \eta - \cos \theta}$, $y = \frac{c \sin \theta}{\cosh \eta - \cos \theta}$, $z = z$.	$g_{11} = g_{22} = \frac{c^2}{(\cosh \eta - \cos \theta)^2}$, $g_{33} = 1$.	×	×	×	●	×	●
7	Elliptic cylinder	7	$x = c \cosh \eta \cos \theta$, $y = c \sinh \eta \sin \theta$, $z = z$.	$g_{11} = g_{22} = c^2(\cosh^2 \eta - \cos^2 \theta)$, $g_{33} = 1$.	●	●	●	●	×	●
8		8	$x = \frac{c \cosh \eta \cos \theta}{\cosh^2 \eta - \sin^2 \theta}$, $y = \frac{c \sinh \eta \sin \theta}{\cosh^2 \eta - \sin^2 \theta}$, $z = z$.	$g_{11} = g_{22} = \frac{c^2(\cosh^2 \eta - \cos^2 \theta)}{(\cosh^2 \eta - \sin^2 \theta)^2}$, $g_{33} = 1$.	×	×	×	●	×	●
9		9	$x = \frac{c}{\Delta} \operatorname{sn}(\mu, k) \cdot \operatorname{dn}(\nu, k')$, $y = \frac{c}{\Delta} \operatorname{cn}(\mu, k) \cdot \operatorname{dn}(\mu, k) \cdot \operatorname{sn}(\nu, k') \cdot \operatorname{cn}(\nu, k')$, $z = z$, where $\Delta = 1 - \operatorname{dn}^2\mu \operatorname{sn}^2\nu$.	$g_{11} = g_{22} = \frac{c^2}{\Delta^2}(1 - \operatorname{sn}^2\mu \operatorname{dn}^2\nu)(\operatorname{dn}^2\nu - k^2\operatorname{sn}^2\mu)$, $g_{33} = 1$.	×	×	×	●	×	●
10		10	$x = \frac{c}{\Delta} \operatorname{cn}(\mu, k) \cdot \operatorname{cn}(\nu, k')$, $y = \frac{c}{\Delta} \operatorname{sn}(\mu, k) \cdot \operatorname{dn}(\mu, k) \cdot \operatorname{sn}(\nu, k') \cdot \operatorname{dn}(\nu, k')$, $z = z$, where $\Delta = 1 - \operatorname{dn}^2\mu \operatorname{sn}^2\nu$.	$g_{11} = g_{22} = \frac{c^2}{\Delta^2}(\operatorname{sn}^2\nu + \operatorname{sn}^2\mu \operatorname{cn}^2\nu)(\operatorname{dn}^2\nu - k^2\operatorname{sn}^2\mu)$, $g_{33} = 1$.	×	×	×	●	×	●

NOTE—Crosses indicate non-separability, dots indicate separability.

the z-axis in all cases, and the angle about this axis is called ψ. Because a change in the axis of rotation sometimes produces a distinctly new coordinate system, Table III contains 14 instead of 10 systems.

The simplest way of checking separability in a new coordinate system is to begin with the two-dimensional case $\varphi = \varphi(u^1, u^2)$. Separability criteria are so simple in this case that inspection of the metric coefficients shows immediately if separation is possible. If the answer is negative, there is no chance of separation in the more complicated case $\varphi = \varphi(u^1, u^2, u^3)$ and no need to employ the more complicated separability conditions.

With rotational coordinates and φ independent of the angle ψ, Laplace's equation is R-separable (4) if and only if g_{11}/g_{33} is a separable sum:

$$\frac{g_{11}}{g_{33}} = \Omega_1(u^1) + \Omega_2(u^2).$$

For example, in the first rotational system obtained from the transformation $z = c \operatorname{sn} w$ (no. 9a),

$$g_{11} = \frac{c^2}{\Lambda^2}(1 - \operatorname{sn}^2\mu \operatorname{dn}^2\nu)(\operatorname{dn}^2\nu - k^2\operatorname{sn}^2\mu),$$

$$g_{33} = \frac{c^2}{\Lambda^2}\operatorname{sn}^2\mu \operatorname{dn}^2\nu.$$

The ratio is

$$\frac{g_{11}}{g_{33}} = \frac{1}{\operatorname{sn}^2\mu} - \frac{k^2}{\operatorname{dn}^2\nu} - \operatorname{dn}^2\nu + k^2\operatorname{sn}^2\mu,$$

so the axially symmetric case separates. The general three-dimensional case requires also (3) the relation,

$$\frac{1}{f_1}\frac{\partial}{\partial\mu}\left(f_1\frac{\partial R}{\partial\mu}\right) + \frac{1}{f_2}\frac{\partial}{\partial\nu}\left(f_2\frac{\partial R}{\partial\nu}\right) + \alpha_1(\Phi_{11} + \Phi_{21}) = 0.$$

This criterion is also satisfied in this particular coordinate system, and the separation content α_1 is found to be zero.

Table III shows that the Helmholtz equation separates in only 4 of the 14 rotational systems. The Laplace equation, however, allows R-separation in a number of other rotational coordinates. The one completely useless system in Table III is the hyperbolic rotational case, though even that transformation is of value for cylindrical coordinates (Table II).

This hyperbolic case is typical of coordinate systems obtained by the Schwarz-Christoffel transformation: The coordinates are useful in the two-dimensional case of cylindrical coordinates, but most of them do not allow any kind of separation in rotational coordinates.

TABLE III.—*Some Rotational Coordinate Systems.*

No.	Name of Coordinate System	Fig. No.	Equations	Metric Coefficients	Separability: Helmholtz $\phi(u^1, u^2, u^3)$	Separability: Helmholtz $\phi(u^1, u^2)$	Separability: Laplace $\phi(u^1, u^2, u^3)$	Separability: Laplace $\phi(u^1, u^2)$	One-dim. Solution: Helm.	One-dim. Solution: Lap.	α_1
1	Tangent-sphere	1, Rot. about y-axis.	$x = \frac{\mu}{\mu^2 + \nu^2}\cos\psi$, $y = \frac{\mu}{\mu^2 + \nu^2}\sin\psi$, $z = \frac{\nu}{\mu^2 + \nu^2}$.	$g_{11} = g_{22} = (\mu^2 + \nu^2)^{-2}$, $g_{33} = \frac{\mu^2}{(\mu^2 + \nu^2)^2}$.	×	×	R	R	×	×	0
2	Parabolic	2, Rot. about x-axis.	$x = \mu\nu\cos\psi$, $y = \mu\nu\sin\psi$, $z = \frac{1}{2}(\mu^2 - \nu^2)$.	$g_{11} = g_{22} = \mu^2 + \nu^2$, $g_{33} = \mu^2\nu^2$.	S	S	S	S	×	●	0
3	Cardioid	3, Rot. about x-axis.	$x = \frac{\mu\nu}{(\mu^2 + \nu^2)^2}\cos\psi$, $y = \frac{\mu\nu}{(\mu^2 + \nu^2)^2}\sin\psi$, $z = \frac{1}{2}\frac{\mu^2 - \nu^2}{(\mu^2 + \nu^2)^2}$.	$g_{11} = g_{22} = (\mu^2 + \nu^2)^{-2}$, $g_{33} = \frac{\mu^2\nu^2}{(\mu^2 + \nu^2)^4}$.	×	×	R	R	×	×	0
4	Hyperbolic	4, Rot. about y-axis.	$x = \sqrt{\rho + \mu}\cos\psi$, $y = \sqrt{\rho + \mu}\sin\psi$, $z = \sqrt{\rho - \mu}$, where $\rho = +\sqrt{\mu^2 + \nu^2}$.	$g_{11} = g_{22} = \frac{1}{2\sqrt{\mu^2 + \nu^2}}$, $g_{33} = \rho + \mu$.	×	×	×	×	×	×	–
5	Spherical	5, Rot. about x-axis.	$x = e^{\eta}\sin\theta\cos\psi$, $y = e^{\eta}\sin\theta\sin\psi$, $z = e^{\eta}\cos\theta$.	$g_{11} = g_{22} = e^{2\eta}$, $g_{33} = e^{2\eta}\sin^2\theta$.	S	S	S	S	●	●	0

TABLE III.—*Continued.*

No.	Name of Coordinate System	Fig. No.	Equations	Metric Coefficients	Separability: Helmholtz $\phi(u^1, u^2, u^3)$	Separability: Helmholtz $\phi(u^1, u^2)$	Separability: Laplace $\phi(u^1, u^2, u^3)$	Separability: Laplace $\phi(u^1, u^2)$	One-dim. Solution: Helm.	One-dim. Solution: Lap.	α_1
6	Toroidal	6, Rot. about y-axis.	$x = \frac{c \sinh \eta \cos \psi}{\cosh \eta - \cos \theta}$, $y = \frac{c \sinh \eta \sin \psi}{\cosh \eta - \cos \theta}$, $z = \frac{c \sin \theta}{\cosh \eta - \cos \theta}$.	$g_{11} = g_{22} = \frac{c^2}{(\cosh \eta - \cos \theta)^2}$, $g_{33} = \frac{c^2 \sinh^2 \eta}{(\cosh \eta - \cos \theta)^2}$.	×	×	R	R	×	×	¼
7	Bispherical	7, Rot. about x-axis.	$x = \frac{c \sin \theta \cos \psi}{\cosh \eta - \cos \theta}$, $y = \frac{c \sin \theta \sin \psi}{\cosh \eta - \cos \theta}$, $z = \frac{c \sinh \eta}{\cosh \eta - \cos \theta}$.	$g_{11} = g_{22} = \frac{c^2}{(\cosh \eta - \cos \theta)^2}$, $g_{33} = \frac{c^2 \sin^2 \theta}{(\cosh \eta - \cos \theta)^2}$.	×	×	R	R	×	×	−¼
7a	Prolate spheroidal	7, Rot. about x-axis.	$x = c \sinh \eta \sin \theta \cos \psi$, $y = c \sinh \eta \sin \theta \sin \psi$, $z = c \cosh \eta \cos \theta$.	$g_{11} = g_{22} = c^2(\cosh^2 \eta - \cos^2 \theta) = c^2(\sinh^2 \eta + \sin^2 \theta)$, $g_{33} = c^2 \sinh^2 \eta \sin^2 \theta$.	S	S	S	S	×	●	0
7b	Oblate spheroidal	7, Rot. about y-axis.*	$x = c \cosh \eta \sin \theta \cos \psi$, $y = c \cosh \eta \sin \theta \sin \psi$, $z = c \sinh \eta \cos \theta$.	$g_{11} = g_{22} = c^2(\cosh^2 \eta - \sin^2 \theta)$, $g_{33} = c^2 \cosh^2 \eta \sin^2 \theta$.	S	S	S	S	×	●	0
8a	Inversion of prolate spheroidal	8, Rot. about x-axis.	$x = \frac{c \sinh \eta \sin \theta \cos \psi}{\cosh^2 \eta - \sin^2 \theta}$, $y = \frac{c \sinh \eta \sin \theta \sin \psi}{\cosh^2 \eta - \sin^2 \theta}$, $z = \frac{c \cosh \eta \cos \theta}{\cosh^2 \eta - \sin^2 \theta}$.	$g_{11} = g_{22} = \frac{c^2(\sinh^2 \eta + \sin^2 \theta)}{(\cosh^2 \eta - \sin^2 \theta)^2}$, $g_{33} = \frac{c^2 \sinh^2 \eta \sin^2 \theta}{(\cosh^2 \eta - \sin^2 \theta)^2}$.	×	×	R	R	×	×	0

* $\theta = \pi - \pi/2$ in this case, to make the equations agree with usual oblate nomenclature.

TABLE III.—*Continued.*

No.	Name of Coordinate System	Fig. No.	Equations	Metric Coefficients	Separability: Helmholtz $\phi(u^1, u^2, u^3)$	Separability: Helmholtz $\phi(u^1, u^2)$	Separability: Laplace $\phi(u^1, u^2, u^3)$	Separability: Laplace $\phi(u^1 u^2)$	One-dim. Solution: Helm.	One-dim. Solution: Lap.	σ_1
8b	Inversion of oblate spheroidal	8, Rot. about y-axis.*	$x = c\dfrac{\cosh\eta \sin\theta \cos\psi}{\cosh^2\eta - \cos^2\theta}$, $y = c\dfrac{\cosh\eta \sin\theta \sin\psi}{\cosh^2\eta - \cos^2\theta}$, $z = \dfrac{c \sinh\eta \cos\theta}{\cosh^2\eta - \cos^2\theta}$.	$g_{11} = g_{22} = \dfrac{c^2(\cosh^2\eta - \sin^2\theta)}{(\cosh^2\eta - \cos^2\theta)^2}$, $g_{33} = \dfrac{c^2 \cosh^2\eta \sin^2\theta}{(\cosh^2\eta - \cos^2\theta)^2}$.	×	×	R	R	×	×	0
9a		9, Rot. about y-axis.	$x = \dfrac{c}{\Lambda}\,\mathrm{sn}(\mu, k)\cdot\mathrm{dn}(\nu, k')\cos\psi$, $y = \dfrac{c}{\Lambda}\,\mathrm{sn}(\mu, k)\cdot\mathrm{dn}(\nu, k')\sin\psi$, $z = \dfrac{c}{\Lambda}\,\mathrm{cn}(\mu, k)\cdot\mathrm{dn}(\mu, k)\cdot\mathrm{sn}\nu\,\mathrm{cn}\nu$.	$g_{11} = g_{22} = \dfrac{c^2}{\Lambda^2}(1 - \mathrm{sn}^2\mu\,\mathrm{dn}^2\nu)(\mathrm{dn}^2\nu - k^2\mathrm{sn}^2\mu)$, $g_{33} = \dfrac{c^2}{\Lambda^2}\mathrm{sn}^2\mu\,\mathrm{dn}^2\nu$.	×	×	R	R	×	×	0
9b		9, Rot. about x-axis.	$x = \dfrac{c}{\Lambda}\,\mathrm{cn}\mu\,\mathrm{dn}\mu\,\mathrm{sn}\nu\,\mathrm{cn}\nu\cos\psi$, $y = \dfrac{c}{\Lambda}\,\mathrm{cn}\mu\,\mathrm{dn}\mu\,\mathrm{sn}\nu\,\mathrm{cn}\nu\sin\psi$, $z = \dfrac{c}{\Lambda}\,\mathrm{sn}\mu\,\mathrm{dn}\nu$.	$g_{11} = g_{22} = \dfrac{c^2}{\Lambda^2}(1 - \mathrm{sn}^2\mu\,\mathrm{dn}^2\nu)(\mathrm{dn}^2\nu - k^2\mathrm{sn}^2\mu)$, $g_{33} = \dfrac{c^2}{\Lambda^2}\mathrm{cn}^2\mu\,\mathrm{dn}^2\mu\,\mathrm{sn}^2\nu\,\mathrm{cn}^2\nu$.	×	×	R	R	×	×	0
10		10, Rot. about y-axis.	$x = \dfrac{c}{\Lambda}\,\mathrm{cn}\mu\,\mathrm{cn}\nu\cos\psi$, $y = \dfrac{c}{\Lambda}\,\mathrm{cn}\mu\,\mathrm{cn}\nu\sin\psi$, $z = \dfrac{c}{\Lambda}\,\mathrm{sn}\mu\,\mathrm{dn}\mu\,\mathrm{sn}\nu\,\mathrm{dn}\nu$, where $\Lambda = 1 - \mathrm{dn}^2\mu\,\mathrm{sn}^2\nu$.	$g_{11} = g_{22} = \dfrac{c^2}{\Lambda^2}(\mathrm{sn}^2\nu + \mathrm{sn}^2\mu\,\mathrm{cn}^2\nu)(\mathrm{dn}^2\nu - k^2\mathrm{sn}^2\mu)$, $g_{33} = \dfrac{c^2}{\Lambda^2}\mathrm{cn}^2\mu\,\mathrm{cn}^2\nu$.	×	×	R	R	×	×	0

NOTE—Crosses indicate non-separability, S indicates simple separability, R indicates R-separability, σ_1 refers to Laplace's equation.

REFERENCES

(1) R. ROTHE, F. OLLENDORFF, AND K. POHLHAUSEN, "Theory of Functions as Applied to Engineering," Cambridge, Mass., Technology Press, 1933;
F. OLLENDORFF, "Potentialfelder der Elektrotechnik," Berlin, Springer, 1932;
M. WALKER, "Conjugate Functions for Engineers," Cambridge, Oxford Univ. Press, 1933;
L. V. BEWLEY, "Two-dimensional Fields in Electrical Engineering," New York, Macmillan Co., 1948;
E. WEBER, "Electromagnetic Fields," New York, John Wiley & Sons, 1950, Vol. I, Chap. VII.

(2) H. A. SCHWARZ, "Über einige Abbildungsaufgaben," *Crelle's J. f. Math.*, Vol. 70, p. 105 (1869);
E. B. CHRISTOFFEL, "Sul problema della temperature stazionarie e la rappresentazione die una data superficie," *Annali di Mat.*, Vol. 1, p. 89 (1867); "Über die Abbildung einer einfach einblättrigen zusammenhangenden Fläche auf den Kreis," Göttinger Nachrichten, 1870.

(3) P. MOON AND D. E. SPENCER, "Separability Conditions for the Laplace and Helmholtz Equations," to be published.

(4) P. MOON AND D. E. SPENCER, "Separability in a Class of Coordinate Systems," to be published.

NOTES FROM THE NATIONAL BUREAU OF STANDARDS*

A PHOTOGRAPHIC FILM DOSIMETER

A compact film badge has been developed by the National Bureau of Standards for industrial safety programs and for monitoring in civilian defense. The development, under the direction of Margarete Ehrlich of the NBS staff, resulted from investigations of X-ray effects on photographic film emulsions. The studies involved the effects of high-energy X-rays—ranging from those produced by constant exciting potentials of 50 kv. to the radiation from a 10 Mev. betatron—and included a determination of the sensitivity and energy dependence of the photographic emulsions.

Ideally, a film dosimeter should indicate the quantity of radiation or dosage, and, at the same time, be independent of the size of radiation quanta. Considerable effort was therefore expended in devising methods of compensating for the inherent energy dependence of the film. The NBS film badge, based on these considerations, is designed to monitor gamma and X-radiation in the quantum energy range from 120 kev. to about 10 Mev. Although somewhat less accurate than other types of radiation meters, the badge is rugged and inexpensive, thus readily lending itself to large quantity production.

Current advances in the technology of atomic energy for civilian as well as military uses are bringing an increasing number of persons in contact with gamma and X-radiation. Even workers in the television industry—where the trend is toward larger screens and higher accelerating potentials—must be cautious in dealing with X-radiation produced in cathode-ray tubes. As more and more industries use radioactive materials in production, the problem of detecting radiation grows in complexity.

The maximum total dosage to which any part of the human body should be exposed continuously or intermittently in one week is currently set at 0.3 roentgen. The effect of a given dosage of radiation varies with the individual and with the nature of the radiation. Occasional exposure to a dose above the permissible limit may not be harmful. Radiation exposure effects are cumulative, however, and a continuation of slight overexposures can become very dangerous. While Geiger-Mueller counters and similar radiation meters are widely used, they are generally too cumbersome for periodic personnel-type monitoring. Film badges, on the other hand, by virtue of their small, compact size, are suited for this type of monitoring. Badges responding to dosages from 0.1 to 2 or more roentgens are made to be worn by workers

* Communicated by the Director.

in plants as continuous safety checks. At regular intervals the film is developed and the amount of radiation dosage for a given period of time determined. Should there be an indication of dangerous overexposure the wearer is warned, the necessary treatment is prescribed, and a survey is made to determine the source or cause of his overexposure. The NBS film badge, designed as an industrial casualty and civilian defense monitor for radiation intensities from 0.5 to 10,000 roentgens, may be used to obtain a permanent record of the radiation exposures received by structures and individuals in critical areas resulting from industrial accidents or national disasters.

The use of photographic emulsions for X- and gamma-ray dosimetry over wide ranges is complicated by the absorption characteristics of the silver bromide they contain. Because the film response is a maximum at quantum energies near the silver bromide absorption edges, the low-energy radiation—which would show on the film 10 or more times as heavily as the high-energy radiation but is usually no more harmful to man—must be filtered through absorbers enclosing the film. The NBS film badge uses an absorber made of 1.07 mm. of tin and 0.3 mm. of lead placed over a bakelite container 8.25 mm. thick. The layer of bakelite protects the film from secondary electrons which are expected to result from more energetic gamma rays encountered in atomic energy work. A lead strip, approximately 0.78 mm. thick, is wrapped around the periphery of the badge to guard against tangential radiation as well as to cover the badge seam.

Before the NBS film badge could be constructed, two major problems had to be solved. The first of these was to select film emulsions which would detect dosages within the required range. The second was to devise means which would make the response of the emulsions independent of the extraneous electron flux and of the radiation energy.

Sixteen film emulsions were tested, and of this group, four were selected which offered the lowest possible inaccuracies within the dosage range from 0.5 to 10,000 roentgens. The films were all exposed to X-rays with an effective potential of approximately 600 kev. This energy range was used because the response of the emulsions is essentially independent of the quantum energy of the incident radiation. Dupont films 510 and 605 and Eastman 5302 and double-coated 548–0 were chosen as most suitable in the dosage range of greatest biological interest.

In the course of the investigation, absorbers of different materials and thicknesses were exposed to radiation energies of varying potentials. In the final analysis of the resulting data, the tin and lead absorber thicknesses used in the NBS film badge were found to represent the best compromise for all possible variations in radiation energy and film type.

The film badges were calibrated with X-radiation energies from 115 kev. to 10 Mev. The accuracy limits within the ranges from 1 to 50

roentgens and from 500 to 10,000 roentgens are ± 12 per cent. In the center range, from 50 to 500 roentgens, the resulting limits are ± 20 per cent.

CERAMIC COATINGS PREVENT EXHAUST-GAS CORROSION

An investigation of the corrosive effects of lead bromide vapors on various heat-resistant alloys, both with and without protective ceramic coatings, has recently been completed at the National Bureau of Standards. Lead bromide, which is the principal lead compound present in aircraft exhaust gases, has been suspected of contributing significantly to exhaust-system corrosion. Until now, however, available data bearing on this question have been few and inconclusive. The NBS investigation demonstrates that the uncoated alloys corrode fairly rapidly when exposed to lead bromide vapors at high temperatures, but that certain ceramic coatings effectively prevent corrosion under the same conditions. Sponsored by the National Advisory Committee for Aeronautics, the studies were conducted by Dwight G. Moore and Mary A. Mason of the NBS enameled metals laboratory.

Lead bromide is present in the exhaust gases of all engines that use leaded gasoline as a fuel. Aviation gasoline is more heavily leaded than automobile fuel, however, and aircraft exhaust temperatures are higher. For these reasons, corrosion from lead bromide is a greater possibility in aircraft than in automobiles. The fact that lead bromide vapors prove corrosive under certain conditions does not, of course, mean that leaded gasoline is undesirable as a motor fuel.

The lead bromide found in exhaust gases results from the interaction of tetraethyl lead and ethylene dibromide, the active additives of leaded gasoline. The tetraethyl lead is added to improve combustion characteristics, while the ethylene dibromide acts as a scavenging agent. In this capacity the ethylene dibromide converts the lead oxide, which would otherwise be formed during combustion, into lead bromide. Lead bromide has a considerably higher vapor pressure than lead oxide and is therefore more readily passed through the exhaust system as a vapor.

Five heat-resisting alloys were investigated by NBS: Inconel (a high nickel alloy), types 347 and 19–9DL stainless steels, Vitallium, and S–816. The first three alloys are in regular use in exhaust systems. Vitallium and S–816 are turbine blade alloys and, although too expensive for general exhaust system use, could be used for small critical parts. Specimens of each alloy with five different coating conditions were studied: an uncoated specimen, a preoxidized specimen, and three ceramic-coated specimens. The ceramic coatings, all commercially available, were NBS types A–417, A–19, and A–520. Specimens were exposed to lead bromide vapor for periods up to six hours in an air atmosphere at temperatures of 1350°, 1500°, and 1650° F.

In the NBS investigation, a small furnace was first preheated to the desired temperature. After temperature equilibrium had been reached, the lid was removed and a 1-gram charge of chemically pure lead bromide was dropped into the furnace. A second lid, from which eight alloy specimens were suspended, was then quickly put into position. This lid fitted loosely and allowed some air to diffuse into the furnace. Determination of the effectiveness of the ceramic coatings did not require that the lead bromide vapor concentration be kept constant.

Each batch of specimens was heated in the furnace for a total of 6 hr. At 1-hr. intervals, however, the specimens were removed, examined, and then replaced together with a new charge of lead bromide. This hourly examination included cleaning of a limited area of the specimens—which were in the form of flat strips—and measuring the loss in metal thickness from corrosion. Loss in weight was also measured in some instances. At the end of the tests, cross-sections of the specimens were studied microscopically, and both the scale layer and the cleaned alloy surface were examined spectrochemically for lead content.

Large differences in the resistance of the several alloys to attack by lead bromide were found: although all five uncoated alloys suffered corrosion at all test temperatures, the loss of thickness in the full 6-hr. period ranged from 1.2 to 10.1 mils. Alloys S–816, Vitallium, and Inconel were notably more resistant than the 19–9DL and type 347 stainless steels, both of which are high-iron, austenitic-type alloys. Microscopic examination indicated that a selective attack took place with the 19–9DL and 347 steels, leaving a spongy layer near the surface. With the other alloys, however, very little selective penetration was found.

Preoxidation of the surfaces of the alloys tended to retard corrosion for the first hour or two only, after which corrosion proceeded at an undiminished rate. Preoxidation was accomplished by heating specimens in air for 4 hr. at the test temperature.

No consistent relation was found between temperature and rate of corrosion; some but not all of the alloys showed less corrosion at the higher temperatures. Similar results have been reported by other investigators of alloy corrosion and are apparently not unusual. However, it must be remembered that in the NBS test method the lead bromide concentration probably dropped off more rapidly with time at higher temperatures than at lower temperatures. Thus at 1650° F. a 1-gram charge of lead bromide may have left the furnace as vapor in a few minutes, whereas at the lower temperatures a 1-gram charge probably fed vapor into the furnace atmosphere throughout the entire 1-hr. heating period.

NOTE: For information on an earlier related development at NBS, see "High-temperature Ceramic Coatings for Molybdenum," *NBS Tech. News Bull.*, Vol. 32, p. 125 (1948).

COMBUSTION EFFICIENCY OF JET ENGINES

Accurate data on the efficiency of the combustion process in jet engines is provided by a gravimetric method of exhaust-gas analysis recently developed by Fillmer W. Ruegg and Carl Halpern of the National Bureau of Standards. As the NBS procedure[1] also supplies information on the nature of the components of the exhaust gas, it is expected to prove useful in the design and development of new types of combustion chambers for gas turbines and jet engines.

Fuel burned in jet combustion chambers releases energy which is converted either to thrust, to shaft horsepower, or to both, depending on the type of installation. The efficiency of the combustion process thus has a direct bearing on the over-all efficiency of the engine. While combustion efficiency can be calculated from observations of the temperatures and rates of flow of air, exhaust gas, and fuel, it is often difficult or impossible to make sufficiently accurate measurements of these quantities. The common methods of gas analysis have also proved unsatisfactory for this purpose because the fuel is burned with so much excess air that the concentration of the products of combustion is very low. To provide a more effective means for studying jet combustion efficiency, NBS therefore undertook to develop a reliable method of exhaust gas analysis. Since analysis by weight gives precise results for small quantities, gravimetric methods were applied to the problem.

The NBS method aims primarily to determine the efficiency of the combustion process rather than to identify all constituents. Essentially, it involves, first, the determination of the products of complete combustion, namely water and carbon dioxide, initially present in the sample, and second, determination of water and carbon dioxide obtained by oxidizing any combustibles remaining in the sample. All of the water and carbon dioxide initially present in the partially burned exhaust gas are first removed separately by absorption on solid reagents. The combustibles remaining in the gas are then burned completely in a quartz combustion tube, and the water and carbon dioxide thus formed are selectively absorbed as before. From the weights of carbon dioxide and water collected before and after complete combustion, the combustion efficiency of the jet engine can be calculated.

The sample of exhaust gas is first passed through a cold trap kept at −78° C., then through two absorption bottles containing drierite and ascarite, respectively, where water and carbon dioxide are absorbed. Hydrocarbons, which would otherwise be absorbed on the surface of the reagents used to absorb water and carbon dioxide, are condensed and remain in the cold trap. The remaining gases enter a quartz combustion tube containing copper oxide at 1000° C. Here combustibles

[1] For further details, see "Gravimetric Analysis of Exhaust Gas from Gas Turbine Combustion Chambers," by Fillmer W. Ruegg and Carl Halpern, *J. Research NBS*, Vol. 45, p. 113 (1950), RP 2117.

such as carbon monoxide, hydrogen, and methane are oxidized to water and carbon dioxide, which are collected in absorption bottles containing anhydrone and ascarite. The condensate in the cold trap is then volatilized by gentle heating and flushed into the combustion tube by a stream of dry, carbon dioxide-free air. After complete combustion of these fuels, the resulting water and carbon dioxide are collected as before. The weights of water and carbon dioxide collected both before and after the combustion are obtained separately. In addition, a small portion of the sample is analyzed for its carbon monoxide content by use of the NBS Carbon Monoxide Indicator.[2]

The combustion efficiency is computed from the equation

$$\eta_b = 1 - \frac{W_1 + 1.50\ W_2}{W_3 + 1.50\ W_4},$$

where η_b is the combustion efficiency, W_1 is the weight of carbon dioxide determined by combustion of the combustibles in the exhaust, W_2 is the weight of water obtained from the unburned material, W_3 is the sum of the weights of carbon dioxide originally in the sample and that obtained from the combustibles, and W_4 is the weight of water originally in the sample plus the weight of water from the unburned material. While W_1, W_2, and W_3 are experimental values, W_4 is calculated from the total weight of carbon dioxide collected in the absorption bottles. Before substitution in the equation, W_1 is corrected for the carbon monoxide found to be present in the sample.

In studies of the method at NBS, several samples of known composition, containing substances typical of actual exhaust gas, were prepared and analyzed. Agreement between combustion efficiency calculated from the known composition and from the analytical data was excellent. In fact, in one large series of analyses, the combustion efficiency calculated from the analytical data agreed within one per cent with that obtained from heat and flow measurements of the actual combustion chamber.

[2] *NBS Technical News Bulletin No. 354*, p. 73 (October 1946).

THE FRANKLIN INSTITUTE

MUSEUM

One of the difficulties in arranging an aviation section in a technical museum is the problem of space. Unless one has an area comparable in extent to a flying field there can be no hope of displaying many actual machines. Representation has to be highly selective, as it is in our Museum. But the story of flight can be told adequately in a collection of models, and we have been exceedingly fortunate to obtain the co-operation of enthusiastic amateur model makers in forming a creditable array to illustrate this story. Attention is drawn to this collection because of a discouraging story from Britain that an exhibition of models and drawings of Sir George Cayley has failed to attract much interest in that country. Those familiar with aeronautical history recognize Cayley as "the Father of Flight." One French historian has called him the "greatest genius in aviation." Sir George did not devise a machine that would get into the air and sustain itself for any length of time because he worked in an age before the discovery of any practical form of combustion engine. His articles on "Aerial Navigation," published in 1809–10, constitute the first truly scientific discussion of the principles of mechanical flight. In 1843 he published a design of a helicopter with twin rotors. Yet by a strange freak of circumstance this pioneer's name is known only to a few specialists.

The problem of flight came late to America but it was approached with all the enthusiasm and energy characteristic of the New World and appropriate to a new subject. Nor was there any discouragement by the negative feeling due to persistent failures which prevailed in Europe. The names of the Wright Brothers are never likely to slip into oblivion, but there are some other names that have appeared in the progress of flying which deserve more prominence than they have received. The investigations of Octave Chanute definitely transferred the ascendancy in flight from Europe to America. He began his gliding in 1896, the same year that S. P. Langley, of the Smithsonian Institution, made his experiments with models. This double event marks the opening of the period which produced human flight. J. J. Montgomery, of Santa Clara College, appears to have been the first to practice gliding in this country, but without marked success. He was experimenting with ornithopters as early as 1883.

These gliding experiments formed the basis of practical mechanical flight. The danger of applying the means of propulsion to an air structure whose behavior was unknown was thus avoided. The first study had to be of aerodynamics and the second the application of power. The Wright Brothers earned the honor of combining the two in a practical airplane. Thereafter progress was rapid in this country, France, Germany, and Britain. So manifold were the improvements that a complete record would be tedious to all but the specialist. Yet in the collection of models displayed in the Aviation Section, no historically important step in the rapid development of flying has been overlooked. The visitor is presented with a comprehensive view of the salient features of all those machines which have made flying history.

Those whose interest is not specifically flying are also encouraged to examine the collection of airplane models for they furnish in small compass the proof of one of man's greatest urges. The idea which inspired the development of those devices is paramount—the will to fly was the will to conquer, to overcome all obstacles in the effort to gain control over natural conditions of environment, and it has pervaded the mind of man from the earliest civilizations.

MEMBERSHIP

ACTIVE MEMBERS ELECTED AT THE MEETING OF THE BOARD OF MANAGERS

September 19, 1951

ACTIVE FAMILY

D. J. Alexander
William G. Bush
Samuel Edelson
Erwin Faller
Robert C. Gebhardt, Sr.
Herman Hassinger
F. W. Hecker
Edmond F. Hurlong
A. Moyer Kulp
Charles H. McBurney, Ph.D.

ACTIVE

Richard F. Alley
John T. Barron
Daniel S. Bernheim
J. Leonard Blayney
Charles A. Bott
Roscoe H. Bowers
Alfred Boyles
T. A. Brandolini
Spencer L. Bunting
James L. Cherry
M. C. Cameron Chisholm, Jr.
A. C. Class
Eugene L. Cohen, D.Sc.
Ralph Cornell
Clarence M. Cox
Walter P. Crockett
Edward K. Crothers, Jr.
Bruce F. Denman
Leon L. Douglas
Robert B. Eaves
Alfred C. Elsasser
Gordon A. Field
William F. S. Fluck
John H. Geyer
Richard M. Golub
James E. Griffith
Stanley E. Haigh
Albert Hepworth
George W. Hoft
Thomas M. Hyndman
Clarence L. Johnson
Mrs. Charles Kehan
Leonard Kissileff
Robert Kunin, Ph.D.
Thomas A. Landis
Jack Leefson
Philip J. Lo Presti
James L. Lohrke, Jr.
Victor S. Markovitz
Alexander A. Marks
Robert E. McLaughlin
Stephen E. McLoughlin, Jr.
Charles D. Mertz
William B. Moore
Charles F. Nahill
Edwin E. Ochs
Henry T. Paiste, Jr.
John A. Petroskas
Harold Polis
Norman E. Polster
James W. Reid, Jr.
Raymond Roth
Reuben W. Schackerman
Howell Lewis Shay
Harold Sherman
Runcie L. Tatnall
Charles F. Teller
W. A. Thawley
David A. Toy
Edwin G. Uhl
Charles A. W. Uhle, M.D.
R. S. Uzzell
Albert E. Waters
James L. Wilkins
E. Leonard Williams

ACTIVE NON-RESIDENT

Robert A. Barbera
Jean A. Ruthven
R. Tom Sawyer
J. Lee Tracy
Robert Walker Zimmerer

NECROLOGY

Brooke M. Anspach, M.D. '42
G. Frederic Bauer '44
Mrs. Richard L. Binder '36
Louis Bless '47
William B. Brendlinger '42
Howard H. Bristol '40
John Burt '42
Joseph F. Chabot '36
Daniel Eppelsheimer '94
William Gaertner '30
F. Lynwood Garrison '15
Edward F. Harvey '44
Alex Hicks '45
Charles F. Jenkins '36
Andrew King '40
Cornelius C. Mershon '44
P. A. Rebok '46
Herman W. Stehfest '36
Frederick Thomas '38
Joseph H. Towle '37

JOURNAL OF THE FRANKLIN INSTITUTE

The following papers will appear in the JOURNAL within the next few months:

ATKINSON, RALPH B. AND STEVEN G. ELLIS: Ferrography.
SYMONDS, P. S.: Recent Progress in the Plastic Methods of Structural Analysis.
SPENCER, DOMINA EBERLE AND CYNTHIA SANBORN: Interflections and Color.
KRZYWOBLOCKI, M. Z.: On the Foundations of Certain Theories of Turbulence.
COULSON, THOMAS: Centenary of the Foucault Pendulum.
BUSH, V. AND J. E. JACKSON: Correction of Spherical Error of a Pendulum.
GEORGE, E. F.: Light—Inadequacy of the Ultraviolet Theory of Ionization in the E-Layer.
ARCHIBALD, FRANK R.: The Step Shaped Film Applied to a Journal Bearing.
GOLOMB, MICHAEL AND EUGENE USDIN: A Theory of Multidimensional Servomechanisms.
AYRE, ROBERT S.: Transient Vibration of Linear Multi-Degree-of-Freedom Systems by the Phase-Plane Method.
MCCLESKY, CHARLES S., JR.: Resistance of Plates with Small Electrodes.

LIBRARY

The Committee on Library desires to add to the collections any technical works that members may wish to contribute. Contributions will be gratefully acknowledged and placed in the library. Duplicates received will be transferred to other libraries as gifts of the donor.

Photostat Service. Photostat prints of any material in the collections can be supplied on request.

The Library and reading room are open on Mondays, Tuesdays, Fridays and Saturdays from 9 A.M. until 5 P.M.; Wednesdays and Thursdays from 2 P.M. until 10 P.M.

RECENT ADDITIONS

AGRICULTURE

KELLEY, W. P. Alkali Soils. 1951.

ARCHITECTURE AND BUILDING

HOLMES, RICHARD E. Air Conditioning in Summer and Winter. Ed. 2. 1951.

ASTRONOMY

DOLMAGE, CECIL G. Astronomy of To-Day. Ed. 4. 1919.

BIBLIOGRAPHY

LODGE, SIR OLIVER JOSEPH. A Bibliography of Sir Oliver Lodge, F. R. S. 1935.
PROVENZAL, GUILIO. Profili Bio-Bibliografica de Chimici Italiani Sec. XV-Sec. XIX. 1950.
Refractories Bibliography 1928–1947. 1950.

BIOGRAPHY

BACHE, RICHARD MEADE. Franklin's Grave. 1897.
INSTITUTION OF ELECTRICAL ENGINEERS, LONDON. The Heaviside Centenary Volume. 1950.
KELLY, FRED CHARLES. Miracle at Kitty Hawk: The Letters of Wilbur and Orville Wright. 1951.
RUSH, BENJAMIN. Letters of Benjamin Rush. Vol. 1–2. 1951.

CHEMISTRY AND CHEMICAL TECHNOLOGY

ALLEN, CHARLES FRANCIS HITCHCOCK. Six-Membered Heterocyclic Nitrogen Compounds. 1951.
ASTON, FRANCIS WILLIAM. Isotope. 1923.
BRADBURY, ROBERT HART. First Book in Chemistry. Ed. 3. 1934.
CHARLOT, GASTON. Méthodes Modernes D'Analyse Quantitative Minérale. Ed. 2. 1949.

GOOSTRAY, STELLA AND KARR, WALTER. Applied Chemistry for Nurses. Ed. 2. 1928.
GRAETZ, LEO. Atomtheorie. Ed. 5. 1925.
KNOEVENAGEL, HEINRICH EMIL ALBERT. Praktikum des Anorganischen Chemikers. Ed. 2. 1909.
HOLMES, HARRY NICHOLLS. General Chemistry. 1922.
KENDALL, JAMES. Intermediate Chemistry Companion. 1925.
KÜSTER, F. W. Logarithmische Rechentafeln. Ed. 23. 1920.
LEA, CAREY. Kolloides Silber und die Photohaloide. 1908.
LIEBIG, JUSTUS VON. Chemische Briefe. 1913.
LINCOLN, AZARIAH T. Textbook of Physical Chemistry. 1918.
LINDE, O. Anleitung zur Chemischen Untersuchung des Wassers. Ed. 2. 1906.
LOWY, ALEXANDER AND HARROW, BENJAMIN. An Introduction to Organic Chemistry. Ed. 3. 1932.
NEWELL, LYMAN CHURCHILL. Descriptive Chemistry. 1911.
NOYES, ARTHUR AMOS. A Course of Instruction in the Qualitative Chemical Analysis of Inorganic Substances. Ed. 7. 1918.
MEIGEN, W. Übungsbeispiele zur Quantitativen Analyse. 1910.
PECHMANN, HANS VON. Volhard's Anleitung zur Qualitativen Chemischen Analyse. Ed. 13. 1912.
PLATT, CHARLES. A Manual of Qualitative Analysis and of Clinical Medical Chemistry. Ed. 3. 1900.
PÖSCHL, VIKTOR. Einführung in die Kolloid-Chemie. Ed. 5. 1919.
RICHTER, VICTOR VON. Textbook of Inorganic Chemistry. Ed. 2. 1885.
ROSCOE, H. E. Chemie. Ed. 7. 1903.
RÜDORFF, FRIEDRICH. Anleitung zur Chemischen Analyse. 1905.
STAUDINGER, HERMANN. Organische Kolloidchemie. Ed. 3. 1950.
RÜST, C. Anleitung zur Darstellung Anorganischer Präparate. 1903.
VALENTIN, WILLIAM GEORGE. Twenty Lessons in Inorganic Chemistry. 1879.
WITTHAUS, RUDOLPH AUGUST. Medical Student's Manual of Chemistry. Ed. 4. 1893.
YOUMANS, EDWARD LIVINGSTON. Classbook of Chemistry. 1863.

CIVIL ENGINEERING

RUBEY, HARRY. Route Surveys. 1951.

DICTIONARIES

GEORGES, KARL ERNST. Kleines Lateinisch-Deutsches Handwörterbuch. Ed. 8. 1902.

ELECTRICITY AND ELECTRICAL ENGINEERING

ADKINS, B. AND GIBBS, W. J. Polyphase Commutator Machines. 1951.
HERRMANN, G. AND WAGENER, S. The Oxide-Coated Cathode. Vol. 1. 1951.
HERRMANN, J. Elektrotechnik. Ed. 4. Vol. 1–4. 1922–1925.
MOSES, GRAHAM LEE. Electrical Insulation, its Application to Shipboard Electrical Equipment. 1951.
PETERSON, HAROLD A. Transients in Power Systems. 1951.
TIMBIE, WILLIAM H. AND BUSH, VANNEVAR. Principles of Electrical Engineering. Ed. 4. 1951.

ELECTRONICS

GEPPERT, DONOVAN N. Basic Electron Tubes. 1951.

ENGINEERING

GARWOOD, M. F. AND OTHERS. Interpretation of Tests and Correlation with Service. 1951.

GEOLOGY

KUENEN, PH. H. Marine Geology. 1950.

MANUFACTURE

BAILEY, ALTON EDWARD. Industrial Oil and Fat Products. Ed. 2. 1951.
DREAPER, W. P. The Chemistry and Physics of Dyeing. 1906.
HESS, MANFRED. Paint Film Defects. 1951.
TRESSLER, DONALD K. AND LEMON, JAMES McW. Marine Products of Commerce. Ed. 2. 1951.

MATHEMATICS

CELL, JOHN W. Analytical Geometry. Ed. 2. 1951.
CROCKETT, C. W. Elements of Plane and Spherical Trigonometry. 1896.
GAUSZ, F. G. Fünfstellige Vollständige Logarithmische und Trigonometrische Tafeln. Ed. 95. 1907.
GRANVILLE, WILLIAM ANTHONY. Elements of Differential and Integral Calculus. c1911.
LÜBSEN, HEINRICH BORCHERT. Ausführliches Lehrbuch der Ebenen und Sphärischen Trigonometrie. Ed. 20. 1917.
SMITH, DAVID EUGENE. The Teaching of Elementary Mathematics. 1906.

MECHANICAL ENGINEERING

BRYANT, LELAND A. AND DICKINSON, THOMAS A. Jigs and Fixtures for Mass Production. 1947.
LICHTY, LESTER CLYDE. Internal-Combustion Engines. Ed. 6. 1951.

OPTICS

LÖWE, CARL FRIEDRICH. Optische Messungen des Chemikers und des Mediziners. 1925.
ROHR, MORITZ VON. Optischen Instrumente. Ed. 2. 1911.
ZEISS, CARL. Mikrophotographische Apparate und Zubohör. 1926.
ZEISS, CARL. Gebrauchsanweisung für die Projektion Optischer Versuche. n.d.

PHOTOGRAPHY

ABEL, CHARLES AND TYDINGS, KENNETH S. The Bolsey Guide. c1951.
EDER, JOSEF MARIA. Die Photographischen Copirverfahren Mittels Mangan, -Cobalt, -Zinn-Salzen und Asphalt. Ed. 2. 1899.
MORTENSEN, WILLIAM. Outdoor Portraiture. Ed. 2. 1951.

PHYSICS

BEER, HERMANN AND OTHERS. Beiträge zur Angewandten Mechanik. 1950.
CHURCH, AUSTIN H. Elementary Mechanical Vibrations. 1948.
DUSHMAN, SAUL. Fundamentals of Atomic Physics. 1951.
EDSER, EDWIN. Light. 1921.
EINSTEIN, ALBERT. Über die Spezielle und die Allgemein Relativitätstheorie. Ed. 6. 1920.
ELENBAAS, W. The High Pressure Mercury Vapour Discharge. 1951.
INGLIS, CHARLES. Applied Mechanics for Engineers. 1951.
INGLIS, DAVID RITTENHOUSE. Dynamic Principles of Mechanics. 1949.
JELLETT, JOHN HEWITT. A Treatise on Theory of Friction. 1872.
JOCHMANN, EMIL CARL GUSTAV G. Grundriss der Experimentalphysik und Elemente der Chemie. Ed. 15. 1903.
JOHANNESON, P. Physikalische Mechanik. 1900.
LÜPKE, ROBERT. Grundzüge der Elektrochemie. Ed. 5. 1907.
JOOS, JAKOB CHRISTOF GEORG. Theoretical Physics. Ed. 2. 1951.
NEHLS, CHR. Über Graphische Integration und ihre Anwendung in der Graphischen Statik. 1877.
NORRIS, P. W. AND LEGGE, W. SEYMOUR. Mechanics via Calculus. Ed. 3. 1950.
PADELLETTI, DINO. Lezioni in Meccanica Rationalle. Vol. 1–2. 1880.
PLETTA, DAN HENRY. Engineering Statics and Dynamics. 1951.

SKILLING, HUGH HILDRETH. Electric Transmission Lines. 1951.
THOMSON, JOSEPH JOHN. Notes on Recent Researches in Electricity and Magnetism. 1893.
THORNTON, D. LAUGHARNE. Mechanics Applied to Vibrations and Balancing. Ed. 2. 1951.
VENEMA, G. A. Over de Balans en het Wegen. 1848.
WHITEHEAD, S. Dielectric Breakdown of Solids. 1951.

PLASTICS

BAKELITE CORPORATION. Vinylite Resins for Surface Coatings. 1942.
ERDMANN, H. Spektraltafeln. 1913.

RADIO

EDITORS AND ENGINEERS LIMITED. The Radio Handbook. Ed. 13. c1951.

SCIENCE

HURLEY, C. H. Allgemeine Einführung in die Naturwissenschaften. Ed. 4. 1902.
STOKLEY, JAMES. Science Marches On. 1951.

SUGAR

MCGINNIS, R. A. Beet-Sugar Technology. 1951.

NOTES FROM THE BIOCHEMICAL RESEARCH FOUNDATION

ELLICE McDONALD, DIRECTOR

Abstract of **Roentgen Irradiation of Desoxyribonucleic Acid. III. The Relation of Dose to Degree of Depolymerization *in Vivo* and the Influence of Oxygen Tension.**—GEORGE LIMPEROS (*Cancer Research*, 11, 325 (1951)). The degree of depolymerization of desoxyribonucleic acid (DNA) extracted from rat thymus 24 hours after roentgen irradiation *in vivo*, as measured by the structural viscosity and streaming birefringence of the solutions, was found to be directly proportional to doses of 250 r to 1000 r.

A reduced oxygen tension (10 per cent) was found to inhibit the depolymerization of DNA, whereas an increased oxygen tension (100 per cent) was found to be relatively ineffective in increasing the depolymerization.

A 10 per cent oxygen tension was found to be less effective than thiourea in preventing the involution of rat thymus tissue induced by roentgen irradiation.

These results are regarded as further evidence for the indirect mechanism of the action of roentgen irradiation *in vivo*.

Abstract of **The Dilution of Blood Plasma by Calcium-Combining Anticoagulants.**—A. R. ADAMS AND W. A. MOSHER (*Blood, J. Hematol.*, 6, 661 (1951)). When used in equimolar concentrations, five different calcium-combining anticoagulants produced uniform dilution of a given blood sample.

The potassium anticoagulants seem to exert a hemolytic effect on the erythrocytes.

The plasma dilution caused by a given concentration of the calcium-combining anticoagulants ranged from 8 to 20 per cent in the bloods examined. This shows the importance of using serum or unoxalated plasma for comparing the plasma protein concentrations of individual blood samples.

Abstract of **Dexoxyribonucleic Acid Content of Rat Liver Nuclei Influenced by Diet.**—J. O. ELY AND M. H. ROSS (*Science*, 114, 70 (1951)). In order to study the influence of diet on the desoxyribonucleic acid (DNA) content of liver nuclei, 3 different diets (A) Fox Food Blox (Allied Mills) which contained a minimum of 26 per cent protein, (B) a semisynthetic diet containing 12 per cent casein, and (C) a protein-free diet, were fed to groups of rats. The DNA content of a known

number of nuclei was determined chemically. It was found that the average DNA value per nucleus with diet C was 18 per cent greater (with diet B, 15 per cent greater) than that with diet A, although the average nuclear volume with diet C was 35 per cent smaller (with diet B, 13.6 per cent smaller) than that with diet A.

The DNA content of the hepatic nuclei, compared photometrically was 50 per cent greater in the rats fed the protein-free diet than in those fed the Fox Food Blox diet although the nuclei in the latter were approximately 14 per cent larger than in the other 2 groups which were equal in size. The DNA content of the hepatic nuclei from the rats of the group fed the 12 per cent casein diet was also greater (33 per cent) than that of the Fox Food Blox fed group.

The results do not support the contention that all diploid cells of an animal and the species contain identical amounts of DNA.

BOOK REVIEWS

LINEAR COMPUTATIONS, by Paul S. Dwyer. 344 pages, 15 × 23 cm. New York, John Wiley & Sons, Inc., 1951. Price, $6.50.

"Linear computations" as used by Professor Dwyer applies to the computations involved in the solution of simultaneous linear equations and such allied problems as the evaluation of determinants, the calculation of the adjoint and the inverse of a matrix, and the solution of problems involving the characteristic equation.

Methods presented are ideal for use by operators of modern desk-type calculating machines. The method of computing square root on such machines is mentioned briefly. Considerable attention is given to computation with approximate numbers, and the associated errors. The subjects of determinants and matrices are introduced as needed; previous familiarity with these subjects is not required. The book is concluded with chapters entitled "Application to Statistics" and "Application to Non-Linear Problems."

The third chapter, "The Principles of Computational Design," stresses the need for computational methods that provide for the control of errors, minimize the recording and resetting, and are fast and easy. Professor Dwyer's methods of solving linear equations live up to his own standards. Provision is made for row checking wherever possible. The methods have been perfected through their repeated use with desk calculators, through being taught at the University of Michigan, and through Professor Dwyer's published articles on the subject.

Professor Dwyer is thoroughly familiar with the modern calculating machine and his courses in mathematical statistics are well received. Students in such courses at the University of Michigan perform their homework problems in a laboratory equipped with desk calculators. His methods have been tried and proved, and though used today in several aircraft companies and the country's leading laboratories, they deserve the wider publicity made possible by publication in book form.

The book is of text book style, amply fortified with examples, exercises, and references. It should be required reading for any desk calculating machine operator, as familiarity with it will pay dividends in accurate work and time saved. It is a must for supervisors of computer groups. Though no more than high school algebra is needed, the book would make a fine text for a course for college seniors majoring in mathematics at universities equipped with calculating machines.

Some of the machine salesmen who, in trying to peddle their brand, consistently demonstrate accounting methods to computing groups, would do well to brush up on the latest techniques presented in Professor Dwyer's *Linear Computations*.

DONALD B. HOUGHTON

SIMPLIFIED MECHANICS AND STRENGTH OF MATERIALS, by Harry Parker. 275 pages, illustrations, 13 × 20 cm. New York, John Wiley & Sons, Inc., 1951. Price, $4.00.

Within this volume is found all the necessary material for the avid engineering draftsman to solve the problems encountered in the designing and detailing of ordinary structures. Only a few principles of mechanics are discussed in the introductory chapters, but the material is adequate. In the first four chapters forces and moments are defined and illustrated by planar force systems together with the conditions required for equilibrium. The topics following this elementary material have been selected from the point of view of greatest practical utility. Thus the chapters following are dealing extensively with the subjects of stresses and deformations, properties of sections, shearing stresses and bending moments in beams and the stability of columns and struts.

There is a chapter on the elements of reinforced concrete design, simple beams and columns, and the final chapter brings a short, but excellent treatment of dams and retaining walls under various conditions of loading and earth pressure.

The large number of illustrative problems is well chosen, the explanations simple and precise, the mathematics elementary and the minimum necessary. It contains enough material for the design of structural members and connections for a variety of building construction. It is highly recommended for self-instruction as well as reference, and may well serve as a model for publications of similar scope.

R. FRIESINGER

RADIOISOTOPES, INDUSTRIAL APPLICATIONS, by G. H. Guest. 185 pages, illustrations, 15 × 24 cm. New York, Pitman Publishing Corp., 1951. Price, $4.50.

In this concise and effectively written book, the title subject is covered authoritatively but simply. The book was written for the interested layman as well as the scientist, but it would seem that full value could not be derived without more background than the short course in chemistry provided in the first three chapters. (It behooves the reviewer to question, at this point, the justification for the 30-minute courses in nuclear physics, physical chemistry, etc., found in the introductions of so many contemporary scientific books, ostensibly inserted to enable a layman to fully comprehend the technical material to follow.)

In the twelve chapters devoted to industrial applications, there are covered numerous subjects of interest to the industrialist and commercial scientist. Each chapter considers a specific branch of industry—for example, iron and steel production, petroleum, glass, and ceramics—and specifies, with probably a too brief description, the existing applications of radioactive tracers to the solution of problems in these fields. A worthwhile feature of each chapter is a listing of potential and suggested uses of tracers in solving problems in the field in question.

Several chapters at the end of the book are given over to the physical requirements of radioisotopic laboratories and precautions to be observed in the handling of these tracers.

A book of this type should provide an important stimulus to the use of tracers in the smaller chemical corporations and research institutes which have not yet adopted this invaluable method of research.

A. L. MYERSON

AIRCRAFT JET POWERPLANTS, by Franklin P. Durham. 326 pages, illustrations, drawings, tables, 15 × 22 cm. New York, Prentice-Hall, Inc., 1951. Price, $5.00.

In *Aircraft Jet Powerplants*, Mr. Durham has drawn on his experience in teaching to produce a text book well-suited for use in undergraduate aeronautical engineering courses.

Starting with a general description of the various types of jet powerplants and the necessary definitions and symbols, he has developed the principles involved, making frequent use of numerical examples, and closing each chapter with a list of pertinent problems.

The development proceeds in easy stages so that a student with a background in elementary thermodynamics and fluid mechanics should have little difficulty in following the steps.

As is proper in such a work, attention has been focussed on principles rather than design details.

R. S. BARNABY

THE NATURE OF POLYPHASE INDUCTION MACHINES, by Philip L. Alger. 397 pages, illustrations, 15 × 24 cm. New York, John Wiley & Sons, Inc., 1951. Price, $7.50.

The treatise by P. L. Alger on induction machines is of particular value to all engineers interested in rotating electrical machinery. While the latter part of the book is devoted to the induction motor including its design and performance characteristics, the first part includes the basic theory common to all a-c. machines. As for the induction motor itself, it is not only the "work horse of industry" but it is the technical acme of a-c. machinery.

The author combines, in a unique way, an authoritative and matured discussion of fundamental electromagnetic theory, along with a useful design aspect. The induction motor is frequently relegated to an equivalent circuit or an expanded transformer. Actually, it requires a basic understanding of electromagnetic field theory. The author develops the theory of revolving fields and m.m.f.'s and shows the space-phase relations of the interaction of current

loading of the stator and the magnetic field component of the rotor, for the mutual torque reaction between stator and rotor, together with corresponding power relations. The analysis extends to complex wave forms and the method of harmonic separation into wave trains, including the flux distribution in the core and teeth.

Chapters I to V cover basic theory common to all a-c. electrical machines, as well as circuit analysis including special features such as the treatment of Kelvin's law, the calculation of torque by differentiating the gap energy with respect to the displacement between rotor and stator fields, and in the use of the Null unit function for transient circuit relations. The author discusses over-all characteristics, including torque-current *vs.* speed relations, the circle diagram and power losses, as well as performance calculations at start, power-factor determination and dynamic braking.

Chapters from VI on are more concerned with detail of particular value to the designer. The author discusses saturation conditions at teeth, slip, core and friction-windage losses with a careful presentation of reactance calculations for slots, including zero phase sequence and the zigzag reactance. The theory of belt and end coil leakage is included, together with the Rüdenberg flux distribution equations in the core. A thorough discussion of speed torque relations covers basic limitations in starting as heat losses proportional to torque times slip with high starting currents, and means for reducing these losses through rotor resistance and the design of deep and idle bar rotors. Squirrel cage rotors, pole changing and concatenation methods are discussed. The remaining chapters cover unique matters on crawling and locking phenomena, noise and voltage ripples and on the general subject of ratings.

The book is a fundamental contribution of permanent value to the field of electrical machinery, both from a theoretical and a design point of view.

RUPEN EKSERGIAN

ULTRASONICS, by P. Vigoureux. 163 pages, illustrations, 16 × 25 cm. New York, John Wiley & Sons, Inc., 1951. Price, $4.00.

Although numerous papers dealing with various aspects of ultrasonics are to be found in scientific journals, very few books devoted to the subject have appeared since the publication of Bergmann's standard work in 1937. Dr. Vigoureux, recognizing the need for such a work, has in this book provided an up-to-date treatment of the general principles of the propagation of ultrasonics in fluids.

Two chapters are devoted to apparatus and experimental methods. In these chapters, one on generation and one on observation, the author stresses the general principles involved, rather than presenting very detailed descriptions of equipment and procedure for particular applications.

The rest of the book deals with the theory of propagation, and the application of the theory to some of the empirical results obtained by various workers in studies of liquids and gases. The theoretical treatment is kept as simple as possible, consistent with what is required for the explanations of phenomena here presented. Results which have still not been adequately accounted for by theory are also pointed out in the discussions on liquids and gases.

An excellent bibliography of ultrasonics publications from 1939 to 1950 is included at the end of the book. The subject and name indices, also to be found at the back of the book, further enhance its value as a reference volume.

Both as an introduction to the field for students and new workers, and as an historical review of accomplishments since 1939, *Ultrasonics* represents a much-needed and valuable contribution to one of the most rapidly advancing areas of science today.

JEAN A. MINKIN

WORDS INTO TYPE, by Marjorie E. Skillin, Robert M. Gay, and others. 585 pages, 16 × 24 cm. New York, Appleton-Century-Crofts, Inc., 1948. Price, $5.00.

As a reference work, *Words Into Type* is a "must" for editors, proofreaders, authors and printers. A 12-page table of contents and a 27-page index make it easy to find answers to the innumerable questions which arise daily in the printing business—questions involving

when to hyphenate words, how to use quotation marks, when to split an infinitive (yes, it has to be done occasionally), how much paper to order for printing a book, what type faces to use for particular effects, and even why "widows" should be avoided!

The book is divided into six parts: Manuscript, Techniques for Copy and Proof, Typography and Illustration, Printing Style, Grammar, and Use of Words. Part I covers in detail the preparation of the manuscript, including the legal responsibilities of the author; Part II, aimed at editors and proofreaders, is a short, but very clear, summary of their duties and responsibilities; Part III is devoted to the mechanics of printing, typesetting, computation of copy, typographical style, paging and illustrations; Part IV, the largest section of the book, gives accepted styles for the use of abbreviations, italics, punctuation, compounding and division of words, and foreign language material, with numerous well-chosen examples of each; Part V answers just about any question on grammar that can arise, through rules and "right" and "wrong" examples; and Part VI, to help authors and editors avoid redundancy, tautology, trite expressions and misuse of words, lists many examples of these violations of good usage and contains a 30-page "dictionary" of colloquial, slang and provincial terms, a 15-page list of words with their correct accompanying prepositions, and a 28-page list of definitions of pairs of words which are often confused (for example, "credible" and "creditable"). An appendix contains a glossary of grammatical terms, one of printing terms, a list of book publishers and a list of foreign words and phrases.

Coverage of the many phases of the printing industry is so complete and so detailed that the book would be practically useless if it were not for the excellent index (there are 99 entries under "Capitalization," for example) and the informative table of contents. The authors and the publisher are to be highly complimented on this practical, thorough treatment of a complex subject.

NANCY S. GLENN

TRANSATLANTIC PADDLE STEAMERS, by H. Philip Spratt. 69 pages, plates, 15 × 22 cm. Glasgow, Brown, Son & Ferguson, Ltd., 1951. Price, 7s. 6d.

Anyone who needs a scholarly account of steam navigation and marine engines turns naturally to those handbooks on the subjects issued by the Science Museum of London. The author of these books, Mr. H. Philip Spratt, has now furnished us with a more detailed supplementary chapter to the story of steam on the ocean. The paddle steamers that ploughed and lurched their way across the Atlantic before Parsons and Diesel showed how the voyage could be made more expeditiously and comfortably are worthy of fuller treatment than they have previously received. The book is divided into three parts which deal with the spasmodic pioneer attempts where steam was auxiliary to sails; the sustained steam power rendered possible by the invention of the condenser; and the days of the Atlantic paddle ferry. In all, 32 vessels are described. Valuable appendices provide handy reference data on details of construction and machinery, and the index is adequate.

Nowhere have we been able to find such a comprehensive picture of the early days of steam on the Atlantic. Mr. Spratt's research has been of unusual diligence and the fruits are of considerable worth. For the first time he gives adequate accounts of such little known vessels as the "Caroline" and the "Curaçao," which have been little more than ghost ships to most students of the steamboat. His book will serve as the reference authority on the subject.

T. C.

ALTERNATING-CURRENT MACHINERY, by Benjamin F. Bailey and James S. Gault. 421 pages, photographs, diagrams, drawings, 16 × 24 cm. New York, McGraw-Hill Book Co., Inc., 1951. Price, $6.00.

Whenever a new textbook on an old subject appears, one is likely to ask whether it can possibly contribute anything new. This may not be a fair or relevant question because the purpose of many textbooks is that of teaching. All teachers know the varying degrees of success with which different authors present a technical subject. Therefore, it is more correct to ask of this text that it do a creditable job of its intended task.

Furthermore, one cannot assume that any large technical subject over becomes a closed book and ceases to develop. On the contrary, developments in various allied fields usually provide new techniques which have applications to the subject considered, and it is necessary to revise the texts to pick up these developments from time to time. All will recognize the obsolescence of a book on electrical measurements published a decade or so ago. Older books on a-c. machinery, for example, do not specifically discuss selsyn devices, servomotors and numerous new applications of a-c. machine principles.

The teaching level of this book is appropriate for the sophomore year of the undergraduate E.E. course. The mathematics used in the analyses involves vector diagrams, algebra of complex quantities and elementary calculus. Material on transformers, and every practical type of a-c. motor is clearly presented with worked-out numerical illustrations. Each chapter is accompanied by a group of problems in which an attempt has been made to include some aspects of engineering as well as theory. Owing to the inclusion of a large amount of detail pertaining to the construction, design principles and performance of machines the students of this book should derive considerable useful knowledge of a-c. equipment. Sufficient diagrams and curves are used so that the student will learn how to make a creditable presentation of an engineering problem upon which he might be asked to report in a professional capacity.

When a professor of electrical engineering has taught a subject for many years, as have the authors of this book, it is to be expected that his own understanding of its ramifications will become more thorough and his explanations more lucid. The teaching experience of the authors has supplied the wisdom for choosing the material for a first course in a-c. machinery. The volume appears to be up-to-date as well as basically sound. It should be a pleasure to use this book for the instruction purposes for which it is intended although there will perhaps be little demand by those desiring a complete reference on the engineering aspects of a-c. machinery.

C. W. HARGENS

AN INTRODUCTION TO THE THEORY OF CONTROL, by R. H. Macmillan. 195 pages, illustrations, plates, 29 × 37 cm. New York, Cambridge University Press, 1951. Price, $6.00.

This book is an introductory account of the theory of control. It deals with problems that arise in mechanical engineering in a way that can be read and understood by those who have no extensive knowledge of servomechanism theory.

The first chapters of this book are devoted to an explanation of the basic principles of control systems and the characteristics of various types of regulators which may be employed. Elements which comprise the control system are described briefly. Included among those elements are hydraulic transmissions, both flow and valve controlled, and electric drive including data in field and armature control and amplidyne and metodyne generators. The author also discusses hydraulic components, measuring elements and data-transmission links and power amplifiers. Power amplifiers are illustrated for pneumatic, hydraulic, and mechanical operation.

Simple servo systems are considered and typical examples of a practical nature are discussed and illustrated to show the principles involved. The analysis of idealized servo systems is approached from the standpoint of static and dynamic errors, transient and frequency response, and stability of the system. The effect of damping ratio and the incorporation of derivative and integral control upon transient and frequency response are discussed.

A general approach to control theory covers the concepts of transfer functions, block diagrams and analytical methods by which the equation describing the dynamics of the system may be more readily solved. Among these analytical approaches are the use of complex numbers and Laplace transforms. These approaches lead to simplification of the procedure for determining transient and frequency response. It is shown that the amount of computation may be reduced by graphical solution for the roots of characteristic equations and that other graphical solutions can be used in designing a system to meet specific needs and to check the stability of that system. These graphical procedures are illustrated by the solution of a problem involving a hydraulic position control.

The engineer who has not had previous background in servo theory will find this book helpful as an introduction to the analysis and synthesis of control systems.

R. H. MARVIN

AN INTRODUCTION TO ELECTRON OPTICS, by L. Jacob. 150 pages, illustrations, 11 × 17 cm. Methuen's Monographs on Physical Subjects. London, Methuen & Co., Ltd., 1951. Distributed by John Wiley & Sons, Inc. Price, $2.00.

ELECTROMAGNETIC PROBLEMS OF MICROWAVE THEORY, by H. Motz. 184 pages, illustrations 11 × 17 cm. Methuen's Monographs on Physical Subjects. London, Methuen & Co., Ltd., 1951. Distributed by John Wiley & Sons, Inc. Price, $2.00.

These two books are grouped together here since they are two more of the Methuen Monographs on Physical Subjects, and because they represent a contrast in the technique of the monograph.

In a statement printed on the dust jackets of these books, the publisher sets forth the intent of the series as being "to supply readers of average scientific attainment with a compact statement of the modern position in each subject. The student and the research worker in other branches of physics, those engaged on work in related sciences, and those who are no longer in contact with active scientific work. . . ." The present reviewer is one of the targets at which these books are aimed.

Jacob's book, perhaps because of its compactness, proved disappointing. Electron optics is not a science requiring extremely difficult and abstruse physical principles. Its difficulties lie in the impossibility of an exact straightforward mathematical analysis of the attainable and useful fields, so that recourse must be had to ingenious approximate methods of numerical calculation, graphical analysis or analog methods, such as the electrolytic tank and rubber membrane.

One would expect, then, that this monograph would present several of these methods in considerable detail. However, Jacob has chosen to give merely brief statements with literature references. The result is hardly more than a bibliographic list. Throughout the reader is required to have a considerable background in electromagnetic theory, mathematical techniques, and in "optical" optics. As an introduction to the subject the more expansive tests of Cosslett, Pierce, or Zworykin, Heller *et al.*, are to be preferred.

In contrast, Motz' book is far more satisfactory, giving well organized and coherent discussions of klystron theory, mode selection in cavity magnetrons and wave guide fields, including discontinuities in wave guides and the impedance of probes or antennas in wave guides. A useful description of field calculation by the relaxation method is included. While it makes no pretense of rivaling the more complete texts such as Slater's *Microwave Electrons*, it should prove a useful introduction for those "readers of average scientific attainment" who do not wish to attempt the larger books.

ALAN C. BYERS

HANDBOOK OF EXPERIMENTAL PSYCHOLOGY, edited by S. S. Stevens. 1436 pages, illustrations, diagrams, 17 × 24 cm. New York, John Wiley & Sons, Inc., 1951. Price, $15.00.

This volume performs a valuable service in the reference shelf of engineers and scientists who are engaged in the design of equipment for human use. Although much of the *Handbook* is of direct professional interest more or less exclusively to the experimental psychologist, several large and well written sections pertain to the designer of equipment. The attributes of the processes of seeing and hearing are of obvious interest in equipment design, and these sensory processes are discussed with great competence in this volume. The mechanical properties of the ear comprise a well written and fascinating chapter and could commendably serve to acquaint the non-psychologist with the methods and results of good psycho-physiological research.

Other chapters of interest to the designer of gadgets for human use deal with human learning and speech and language. A section in itself is devoted to human performance and discusses the selection and training of personnel, work and motor performance, and engineering

psychology and equipment design. Engineering psychology, or as it is sometimes called, human engineering, attempts to solve the many problems which arise in optimizing the output of man-machine combinations. The performance of man-machine combinations is of critical importance when their output determines life or death, as in a fire control system. Thus one can see why this study was generated during the scientific mobilization of the last war.

On page 1329 the fact that for simple sinusoidal visual inputs up to 3 or 4 cycles per second, the human output does not contain exogeneous frequencies does not seem to allow the conclusion that from 0 to 3 or 4 cps. the human operator is either a linear or a linear time invariant system. The point that must be considered is—knowing the human response to simple sinusoids—can the response to a complex input be synthesized by a Fourier summation?

Professor S. S. Stevens is to be congratulated for having so successfully undertaken the collection and editing of the papers comprising this volume, as well as for selecting so eminent a group of chapter authors. All in all, this *Handbook* is a massive contribution to those working in the technical fields in which experimental psychology is of interest.

EZRA KRENDEL

FOURIER TRANSFORMS, by Ian N. Sneddon. 542 pages, diagrams, 16 × 24 cm. New York, McGraw-Hill Book Co., Inc., 1951. Price, $10.00.

Many books have been written on the application of integral transforms to the solution of physical problems. The vast majority of these books deal with the theory and application of a special transform such as that of Laplace or Mellin. Unlike the aforementioned volumes, *Fourier Transforms* includes three chapters on basic theory which deal with the common properties of Fourier, Mellin, Laplace and Hankel transforms. Furthermore, finite transforms, dual integral equations, the Wiener-Hopf procedure, and the properties of the Dirac delta function are considered in some detail.

Though theoretical throughout, this book presents the above theory in a form suitable for use by both students and research workers concerned with the solution of boundary value problems of physics and engineering. There is no attempt to establish the foundations of the theory in their most general form as is done in the classical treatises of Tichtmarsh and Widder. This fact enables the book to encompass a wider group of readers and permits the author to devote the bulk of the book to applications. The final seven chapters are devoted to illustration of the use of the theory in the solution of problems in the fields of the theory of vibrations, conduction of heat, slowing down of neutrons, hydrodynamics, atomic and nuclear physics, and elasticity. The combination of unified transform theory with numerous applications makes the book both stimulating and useful.

M. R. AARON

BOOK NOTES

WELTSYSTEM, WELTÄTHER UND DIE RELATIVITÄTSTHEORIE, by Karl Jellinek. 450 pages, illustrations, 16 × 24 cm. Basel, Wepf & Co., 1949. Price, S. Fr. 45.

The author has attempted to bridge the gap from theoretical physics to experimental science and present the theory of relativity in a manner understandable to the experimental scientist. The book covers the fundamental concepts of nonrelativistic physics, special theory and its modifications on pre-relativistic physics, Einstein's theory of gravitation and his general theory of relativity, the cosmological theory, and the expanding universe. The book is well written and would serve as a text.

THE STRUCTURE AND MECHANICAL PROPERTIES OF METALS, by Bruce Chalmers. 132 pages, illustrations, 14 × 22 cm. New York, John Wiley & Sons, Inc., 1951. Price, $3.50.

The object of this book is to provide the simplest possible picture of the structure of metals and alloys and its relation to the mechanical properties. Since it is aimed at readers who have only an elementary background in physics and chemistry, the book has been stripped of mathematics. The result is an oversimplification which may not be of interest to the serious student of metals, but should prove helpful to those just beginning this subject. There is no bibliography.

TABLES RELATING TO MATHIEU FUNCTIONS, prepared by The Computation Laboratory of the National Applied Mathematics Laboratories, National Bureau of Standards. xliii plus 278 pages, 21 × 27 cm. New York, Columbia University Press, 1951. No price.

The present volume is one of a series of tables compiled by the Computation Laboratory of the National Bureau of Standards. An excellent introduction enables the reader to use the tables intelligently and to understand their construction. The main part of the book is comprised of: tables of the characteristic values $be_r(s)$ and $bo_r(s)$; tables of coefficients $De_k(s)$ and $Do_k(s)$; a table of joining factors; values of $E_2(p)$ and $F_2(p)$, $p = [0(.001)1; 7D]$; values of $\frac{1}{2}p(1 - p)$; sines and cosines $0(1°)90°$; and multiples of $\frac{1}{2}\pi$. The work is an outgrowth of the program begun under the auspices of the Applied Mathematics Panel, NDRC, to provide more adequate tables of the elliptic cylinder functions, and will be enthusiastically received.

INTRODUCTION TO HEAT TRANSFER, by Aubrey Brown and Salvatore M. Marco. Second edition, 267 pages, diagrams, 16 × 24 cm. New York, McGraw-Hill Book Co., Inc., 1951. Price, $4.50.

The second edition of this text retains the same approach to the subject which proved so successful in the first edition—emphasis on fundamental principles and the development of the most common mathematical expressions for heat transfer, with a minimum of complicated mathematics. Changes in the second edition include: revisions in the nomenclature to conform to current practice; revisions in the treatment of the mapping method of estimating heat conduction; new material on conduction and radiation, particularly on insulating materials and solar radiation; and expansion of the material on fluid flow. In addition, a table of conversion factors has been included and the number of problems has been more than doubled. In its revised form, this text should be in continued demand for undergraduate work.

ADSORPTION, by C. L. Mantell. Second edition, 634 pages, illustrations, 15 × 24 cm. New York, McGraw-Hill Book Co., Inc., 1951, Price, $9.00.

This second edition is a revision of the original text covering the practical, commercial and engineering aspects of industrial adsorption. New sections include fractionation of liquids, gases and ions and their applications such as refining of waxes; fractionation of rare earths, fission products; refining of sugar; water treatment; and medicine and pharmacy.

VERSTÄNDLICHE ELEMENTE DER WELLENMECHANIK, by Karl Jellinek. Vol. 1, 304 pages, illustrations, 16 × 24 cm. Basel, Wepf & Co., 1950. Price, S. Fr. 34.

Author's aim is to present wave mechanics in a form understandable to chemists and physicists. Jellinek has developed an interpretation of wave mechanical formulation in contradiction with present accepted interpretations. The other parts of the book, involving mathematical treatment of harmonic oscillator, etc., are sound. Could not be used as a text.

AN INTRODUCTION TO THE CHEMISTRY OF THE SILICONES, by Eugene G. Rochow. Second edition, 213 pages, diagrams, illustrations, 15 × 24 cm. New York, John Wiley & Sons, Inc., 1951. Price, $5.00.

With the increasing use of silicones in industry, the author sets forth a survey of the silicon and organosilicon derivatives for the use of chemists, engineers. The new chapters of the book include "The Carbon-Silicon Bond," "Synthesis of Organosilicon Compounds," "Physical Chemistry of Silicones," and enlarged tables of Physical Properties of Organosilicon Compounds. The material is presented in such a manner that the reader can obtain a sound knowledge of the properties and uses of the silicones.

ELECTRIC CIRCUITS FOR ENGINEERS, by Edward K. Kraybill. 212 pages, diagrams, 16 × 24 cm. New York, The Macmillan Co., 1951. Price, $3.85.

The author has presented a broad picture of steady-state electric circuit theory by combination of alternating-current and direct-current relationships. A definite effort has been made to correlate electric phenomena with related phenomena in general scientific field, practical problems included to cover certain general engineering information. It is an unusually clear presentation of material relating to electric circuits.

CURRENT TOPICS

Geochemistry Offers New Aid to Mineral Prospectors.—New techniques devised by research scientists of the Geological Survey are offering novel aid to mineral prospectors in locating ore that would otherwise be missed by those searching for visible signs of deposits at the surface, Secretary of Interior Oscar L. Chapman disclosed recently.

These new discovery methods involve close teamwork between two major divisions of science, geology and chemistry, whereby extremely sensitive chemical tests are made in the field for traces of cobalt, copper, nickel, lead, silver, tungsten, molybdenum, zinc and other elements to guide geologists in prospecting. Chemical prospecting is possible in some areas where bedrock deposits are hidden beneath several hundred feet of soil or glacial debris.

"It does not seem premature to predict a very useful future for this new field of 'geochemical prospecting,' " Secretary Chapman said. "It is especially welcome at a time in our history when the demand for metals for both industrial and national defense uses is higher than ever. Geologists have informed us that probably most of the major deposits outcropping at the surface have been discovered already and have been largely exploited. To locate the portion of our wealth that is hidden will require an even higher degree of skill and greater technical knowledge."

While analysis for minor traces of elements has been developed to a high degree of perfection by workers in agricultural and biological sciences, such methods are lengthy and expensive. All techniques developed by the Geological Survey are for specific problems met in geochemical prospecting. Some are relatively simple modifications of standard procedures used in chemical analysis. Others are sufficiently novel to be called "new."

Both conventional colorimetric and chromographic (spot) tests are used. In conventional colorimetric methods, colored solutions are obtained in which the intensity of the color provides a means of measuring the amount of the metal present. The chromographic spot test, on the other hand, yields colored spots of definite size, and again the intensity of the final color is the means of measuring the amount of metal present.

For making chromographic tests Survey chemists, Rollin E. Stevens and Hubert W. Lakin, have designed a new instrument called the "chromograph" which enables an analyst to produce colored spots confined to a definite area on a strip of filter paper. These spots are then compared with standard spots made with known amounts of metal. By these comparisons it is possible to detect with the unaided eye, minute amounts of metals occurring in soils, rocks, and plant tissues. The further disclosure of exactly how much of a particular element is present through color intensity, allows the "geochemical prospector" to follow a "hot" trail and pinpoint an ore deposit in much the same manner as a bloodhound pursuing its quarry.

All equipment and chemicals used are inexpensive and easily transported. The processes are devised for speed, sensitivity and simplicity, so that relatively inexperienced workers can be trained to map rapidly the surface distribution of

valuable metals present in any given area. Unlike assaying, these analyses avoid time-consuming shipments of samples to centralized but usually distant laboratories with attendant delays in processing samples and rendering reports. Success in prospecting frequently requires that results of soil or rock analyses be available immediately, not days after the prospector has left the area.

The chromograph has proved useful thus far for making quantitative spot tests for cobalt, copper, nickel, and silver in soils and rocks, and for determining nickel in vegetation. With this device a field technician is now able to make copper or nickel tests for geologists anywhere and provide the analyses within a few hours' time. The equipment needed is a "pocket type" gasoline stove, the chromograph, and a reagent box—these can be packed in two boxes the size of small suitcases.

A summary report entitled "Compilation of field tests used in geochemical prospecting by the Geological Survey" has recently been released in open file for public inspection. Written by Messrs. Lakin, Almond, and Ward, it gives the field chemical techniques and procedures that have been developed to date by the Geochemical Prospecting Section. Copies may be examined at Room 1033 (Geological Survey Library) General Services Building, Washington 25, D. C., and at Geological Survey offices at South 157 Howard Street, Spokane, Washington, and at the Denver Federal Center, Denver, Colorado.

The compilation contains field methods for the determination of heavy metals in water or in soil, and specific methods for determining cobalt, copper, lead, molybdenum, nickel, silver, tungsten, and zinc in rocks and soils. It also includes methods for determining readily soluble copper, zinc, and lead in soils and rocks, and for total zinc, nickel, and molybdenum in plants. Descriptions are given of special apparatus to facilitate the adoption of trace analysis to field use.

Fire Prevention.—Glance at your watch or look at the nearest clock. Before you can read for one minute—48 seconds, to be exact—a destructive fire will have broken out somewhere in the United States. Chances are it will cause loss of life in addition to destroying valuable possessions.

Fire attacks an American home every minute and a half around the clock. It attacks a store every 11 minutes, a factory or place of business every 14 minutes, a school every three hours, and a hospital every six hours. The money wasted through these American fire losses in 1950 would have built 764 jet-powered B-36 heavy bombing planes for the U. S. Air Force or 830 jet-powered bombers for the U. S. Navy.

American home owners and American industry suffered financial losses of $688,460,000 from fire in 1950, and these same fires caused the loss of almost 25 million man-hours of work. This was an increase of $36,926,000 over total property losses by fire in the United States in 1949.

If your house or place of business has already been built, you may be startled to know that there is very little that you can do to improve its basic fire safety. It is true that you can eliminate many of the causes and breeding grounds of fire, and this of course should be done regularly. But regardless of how clean and free from inflammable waste and accumulation the structure may be, your present safety is dependent to a very large extent upon your judgment when you selected the building materials. Here, better than any-

where else, the old axiom about an ounce of prevention being worth a pound of cure applies. The ounce of prevention is firesafe construction.

According to the National Bureau of Standards, firesafe construction is "a type of construction designed to withstand a complete burn-out of the contents for which the structure was intended without impairment of structural integrity." This is just another way of saying that a really firesafe structure is one that is well planned and wisely built of materials that will not burn.

Requirements for firesafety need not be complicated. When walls and floors are of concrete, and the roof is constructed of a non-burning material such as asbestos-cement shingles or concrete tile, a structure will have maximum safety from structural damage due to fire. Most important is a concrete first floor. A first floor built of concrete gives dependable protection from fire which originates in the basement. The concrete floor acts as a barrier to these basement flames and prevents the rapid upward spread of the blaze.

The cause of about 22 per cent of fires in city homes can be traced to electricity. In concrete floors, conduits for electric wires are embedded in the concrete or pass through precast concrete units. Similarly, boxed-in openings for heating ducts and pipes are installed in the concrete floors, thus minimizing danger of fire from faulty heating plants, which cause about 15 per cent of the fires in city homes.

The roof of a structure, in addition to being exposed to the normal wear-and-tear of the elements, is highly vulnerable to fire. Sparks landing on combustible roofs account for about seven per cent of home fires each year, both in town and on the farm. A roof covered with firesafe asbestos-cement shingles or concrete tile protects a home from this type of fire destruction.

Concrete masonry now accounts for about 65 per cent of total volume of new masonry wall construction in the United States. Severe fire tests conducted by the Underwriters' Laboratories in Chicago showed that concrete masonry walls are effective fire barriers for three, four and even five hours. In these exacting tests, walls of seven different commercially manufactured concrete masonry units (blocks) were given impartial but highly competitive tests. Even when subjected to temperatures above 2200 degrees F., concrete masonry walls continued to serve as effective fire barriers and supported loads with a high margin of safety.

At the conclusion of each of the fire tests, the walls while still under compression were subjected to a stream of water from a fire hose, without any significant damage or reduction in load-carrying ability.

Although fire tests have brought about important developments in the design and construction of firesafe buildings during the last decade, 300,000 homes are still leveled in the United States each year by fire and about 11,000 persons die annually in domestic and industrial fires. All should have been fires that never started. The only way to lick this destroyer of human life and property is to make every week Fire Prevention Week—and to remember the ounce of prevention is the use of firesafe construction.

Battery Charger Designed for Shelf Mounting.—A new motor-generator type battery charger, designed to permit mounting on balconies or shelves to save vital floor space, has been announced by General Electric's Small and Medium Motor Divisions.

For charging batteries in driver-lead and small driver-ride industrial lift trucks, the new unit accommodates lead-acid batteries of 6–19 cells and nickel-iron-alkaline batteries of 10–30 cells. It is about the size of a tank type vacuum cleaner with a control box mounted on its side, weighs only 190 lb., and can be installed on a shelf measuring $6\frac{3}{4} \times 8\frac{1}{4}$ in.

The unit is fully automatic and easy to operate, according to G-E engineers. It is only necessary to plug it in and set the timer; automatic controls do the rest. Voltage (based on number of battery cells) and current (based on ampere-hour battery ratings) are adjustable.

Protection from external damage to the charger is provided by completely enclosed construction, and maintenance, when necessary, is simplified by the easy accessibility of control parts, commutator, and brushes. Mounting feet are integrally cast with the intermediate frame—no special foundation is required. Permanent bearing alignment, established by factory assembly, cannot be disturbed during mounting.

Incorporated in the design of the new unit are many features recommended by the Industrial Truck Association. Included are: automatic disconnection of charger from power line and opening of charging circuit in case of power interruption, automatic restart of charger upon resumption of power supply following an interruption, automatic control of charging rate under the Modified Constant Voltage Charging System, and automatic cut-off of battery and shutdown of charger when battery is fully charged.

The single-circuit equipment operates on 3-phase, 60-cycle, a-c power, and has generator-overload and motor-overload protection to guard against excessive currents.

Photoangulator.—A simple device that shows all the angles—on photographs—has passed operational tests at Fort Belvoir's Engineer Research and Development Laboratories.

It is the photoangulator which accurately gives true horizontal directions from oblique aerial photographs.

Military aerial photographs used in the production of most aeronautical charts and small scale mapping, a prime source of reliable intelligence, are made with three cameras that simultaneously shoot one vertical and two oblique photographs, thus covering a wide area.

With the aid of the photoangulator, a network of intermediate horizontal control is established from the oblique photographs to which the map is compiled.

There are three principal parts to the photoangulator: a depression angle assembly for adjustment to the depression angle of the aerial camera at the instant of exposure; a transparent photo arm under which intermediate control points are intersected on the photo; a templet arm that juts over the map manuscript gives the true horizontal directions.

A specially designed plastic slide rule calculator enables the operator to obtain quickly the correct photo arm setting. The entire outfit can be securely carried in a weatherproof, hardwood case with dimensions of $25\frac{1}{2}$ by $8\frac{1}{2}$ by $3\frac{1}{2}$ inches. The total weight with case is $14\frac{1}{2}$ lbs.

Horizontal directions may be produced from 6i-inch focal length photography with camera tilts ranging from 40 to 72 degrees. The equipment can be satisfactorily used with a minimum of operator training. It is not affected

by wide temperature changes and the materials are normally resistant to tropical conditions.

The basic instrument was invented by James G. Lewis of the U. S. Geological Survey, and the original model was built in June 1942. It was modified after extensive tests over a five year period. ERDL project engineers incorporated an improved locking assembly, secured positioning pins with spring clamps, provided a longer non-corrosive templet arm, designed a means of determining the correct photo arm setting and redesigned the depression angle adjustment mechanism. The instrument was standardized for issue to Engineer topographic troops.

The photoangulator differs from the present Corps of Engineers angulator and the Air Force rectoblique plotter both of which present a geometrical solution in determining horizontal direction of points on the oblique photographs, in that the photoangulator affords a trigonometical solution. The weight and bulk have been greatly reduced.

Glowing Crystals.—The secret to an old chemical mystery—crystals that glow in the dark when heated—has been solved by University of Wisconsin scientists. The discovery has opened up entirely new fields of research and application in chemistry, geology, mineral prospecting, and in the development of a practical radiation dosimeter—the type of gadget that can be used as a dog tag to measure the amount of radiation to which individuals are exposed during an atomic bomb blast. The study of crystals that glow was conducted by Farrington Daniels, UW professor of chemistry, Donald F. Saunders, project assistant, and other Wisconsin scientists, under an Atomic Energy commission grant.

The UW scientists found that the glow given off by certain mineral crystals when heated is caused by electrons escaping from "traps" in the lattice-like structure of the crystal. The electrons are driven into the traps by radioactivity either from very small amounts of natural radioactive substances or by man-made radiation in the laboratory. When the chemical crystal is heated slightly, the electrons escape the traps and fall back to their normal positions, emitting light in the process.

The scientists have found that the phenomenon is much more common than had previously been realized. Practically all limestone and granites will emit light when heated—as anyone can learn by grinding a small piece of limestone into powder, placing it in a frying pan, and heating almost red hot in the dark. A few prospectors have known for years that some minerals will glow for a moment when heated, but it was not known that small amounts of uranium and thorium furnished the radioactivity necessary for the trick. Because of the small amounts of these elements present in most minerals, centuries are required for the trapping of enough electrons to give a few seconds' glow. During an atomic bomb blast, however, the radioactivity would be so intense that crystals of lithium fluoride, for example, would trap sufficient electrons in a few seconds to glow when heated. The amount of radiation to which a lithium fluoride dog tag was exposed would determine the intensity of the glow. The UW scientists have designed a thermoluminescent apparatus to heat the crystals and record the amount of light emitted. Use of such a device could enable authorities to quickly divide a population exposed to radiation into groups of individuals requiring similar medical treatment.

After thermoluminescent crystals have been heated once, the ability to glow is destroyed, but it can be restored by exposure to radiation. Each mineral has its individual "glow" pattern. When heated at a rate of one degree a second, the intensity of the light varies noticeably with the type of mineral and its geologic history. And each type has peaks and dips in brightness which are characteristic of the type.

The UW chemists, working with UW Geologists E. J. Zeller and J. M. Parks, found that it is possible in some cases to estimate the age of limestone and fluorite deposits by use of the thermoluminescent apparatus. There is hope that dating of material by the new method may be extended to other types of rocks and even to some archaeological materials. "The realization that the thermoluminescence of rocks is due to the presence of uranium and thorium led in turn to field explorations in Northwestern Canada and to a new theory for the geo-chemical concentration of uranium in granites and to the use of the method as a stratigraphic tool," the scientists report.

Working with UW Geologist R. C. Emmons, an expert on the history of granite formations, the scientists hit upon a theory of uranium concentration which may be of value in geo-prospecting for the vital metal. By studying the glow produced by various uranium-bearing ores when heated, the UW scientists found that the uranium was apparently concentrated in granite formations known as lamprophyre dikes, and that these dikes, or cracks, were formed late in the history of the cooling of the granite formations.

Another use for the thermoluminescent capacity of minerals may be found in the field of oil exploration. The samples of limestone taken from various depths of one drilling, for example, can be compared with samples from other wells to aid in predicting whether or not the same oil-bearing strata are present.

THE FRANKLIN INSTITUTE

exists today because of the faith and generosity of the men and women who for 127 years have given time and money to its support.

The Institute welcomes financial gifts and bequests and hopes that all those who desire to perpetuate its work will make the The Institute one of their beneficiaries.

FORM OF BEQUEST

*I give and bequeath to The Franklin Institute of the State of Pennsylvania for the Promotion of the Mechanic Arts, the sum of*_____

_____